MOLECULAR IDENTIFICATION

OF

CYTOTOXIC COMPOUNDS FROM A MARINE ORGANISM

Thesis submitted by

Antonius R B Ola, S.Si (Gadjah Mada University)

for the degree of Master of Science

in the Department of Chemistry

James Cook University of North Queensland

STATEMENT OF ACCESS

I, the undersigned, author of this work, understand that James Cook University will make this thesis available for use within the University Library and, via the Australian Digital Theses network, for use elsewhere.

I understand that, as an unpublished work, a thesis has significant protection under the Copyright Act and;

I do not wish to place any further restriction on access to this work.

Antonius R B Ola December 2009

STATEMENT REGARDING THE ELECTRONIC COPY

I, the undersigned and author of this work, declare that the electronic copy provided to the James Cook University Library is an accurate copy of the printed thesis submitted, within the limits of technology available.

Antonius R B Ola December 2009

STATEMENT OF SOURCES

DECLARATION

I declare that this thesis is my own work and has not been submitted in any form for another degree or diploma at any university or other institution of tertiary education. Information derived from the published or unpublished work of others has been acknowledged in the text and a list of references is given.

Antonius R B Ola December 2009

STATEMENT OF THE CONTRIBUTION OF OTHERS

I, the undersigned of this work, acknowledge the contribution of others to this work. Substantial supervision was provided Assoc. Prof. Bruce Bowden (School of Pharmacy and Molecular Sciences, JCU). Editorial assistance in the preparation of this thesis was provided by Assoc. Prof. Bruce Bowden. Ms Cherrie Moti at the Australian Institute of Marine Sciences, Townsville, performed mass spectrometry (ESI-MS) on samples. Dr Anna-Marie Babey (School of Biomedical Sciences, JCU) performed cytotoxic assay.

Antonius R B Ola December 2009

DECLARATION OF ETHICS

I, the undersigned and author of this work, declare that the research presented and reported in this thesis was conducted within the guidelines for research ethics outlined in the *James Cook University Policy on Experimentation Ethics*, *Standard Practices and Guidelines on Research Practice (2001)*, and the *James Cook University Statement and Guidelines on Research Practice (2001)*. Research involving the use of animals followed the Australian code of Practice for the Care and Use of Animals for Scientific Purposes and the Queensland Animal Care and Protection Act 2001.

Antonius R B Ola December 2009

ACKNOWLEGEMENTS

Firstly, I wish to thank AUSAID for the postgraduate studies scholarships (APS).

I wish to thank my supervisor Bruce Bowden for his patient, guidance and support over the years, especially for my *Chondria armata* project. I am also grateful to Dr. Anna Marie-Babey for conducting the cytotoxicity assays.

I am also thankful to my wife for her understanding and support during the hardest time in my study. I am really grateful to all the staff of School of Pharmacy and Molecular Sciences for the knowledge contribution.

I DEDICATE THIS WORK TO MY WIFE,

Ms. MARIA RENNY PRAPTIWI AND MY DAUGHTER GRACE

MICHELLE AUSSIOLA

ABSTRACT

The marine world has become an important source of anticancer lead drugs with novel mechanisms of action. Many of these are in active phase I or phase II clinical trials while Yondelis in 2007 was approved for clinical use for the treatment of advanced sarcoma. This study aims to identify the molecular structure of pharmacologically active metabolites from tropical marine organisms.

The study of pharmacological activity was focused on discovering novel cytotoxic compounds with potential as anticancer agents. Cytotoxicity was assessed *in vitro* using the P388D1 mouse lymphoma cell line. The structural elucidation was done via 1D and 2D NMR. From the marine red alga *Chondria armata*, seven new halogenated triterpene polycylic ethers, armatols G-J and aplysiols C-E were isolated. The absolute stereochemistry of armatol G was determined through an X-ray structure while the stereochemistry of armatol H was proposed from acetylation of armatol G which indicated the same absolute configuration as was present in armatol G. The relative stereochemistry of armatol I and J were established via nOe experiments and by using Chem 3D and its MM2 energy minimization program to predict the lowest energy conformations. The relative stereochemistry of aplysiols C-E was determined by comparison with the very closely related structure of aplysiol B and from gradient selective NOESY experiments. Armatol J showed potent cytotoxic activity with an IC_{50} value of 5 μg/mL while armatol I and aplysiol C had moderate cytotoxic effects with IC_{50} value of 18 and 25 μg/mL respectively.

Seven known compounds were also isolated from the alga included 3 halogenated C_{15} acetogenins, two diterpenes [(-) angasiol and (-) angasiol acetate], a triterpene, intricatetraol and a diketopiperazine (dihydrodisamide C). (-) Angasiol acetate is the enantiomer of the diterpene reported from the sea hare *Aplysia juliana* and (-) pinnatifidenyne is the enantiomer of the C_{15} acetogenin produced by the marine red alga *Laurencia pinnatifida* from Canary Island. (-) Angasiol and (-) angasiol acetate were found to be inactive while intricatetraol and C_{15} acetogenins showed weak activity. Dihydrodisamide C was among the most potent of all the purified metabolites tested with an IC_{50} value of 5 μg/mL. It is probable that the collection of *Chondria armata* may have been contaminated by the sponge *Dysidea herbacea* from the substrate on which the alga was growing, or that the dihydrodysamide C was exuded by *D.herbacea* and absorbed into the alga.

TABLE OF CONTENTS

LIST OF TABLES

LIST OF FIGURES

LIST OF ABBREVIATIONS

1D	one dimensional
2D	two dimensional
br d	broad doublet
C_6D_6	deuterated benzene
$CDCl_3$	deuterated chloroform
CH_2Cl_2	dichloromethane
$CHCl_3$	chloroform
COSY	Correlated Spectroscopy
d	doublet
dd	doublet of doublets
ddd	doublet of doublet of doublets
dddd	doublet of doublet of doublet of doublets
ddq	doublet of doublet of quartets
ESI-MS	Electrospray Ionisation Mass Spectrometry
EtOAc	ethyl acetate
FCS	foetal calf serum
HMBC	Heteronuclear Multiple-Bond Coherence
HSQC	Heteronuclear Single-Quantum Coherence
HPLC	High-performance Liquid Chromatography
i.d.	internal diameter
IR	Infrared
m	multiplet
MeOH	methanol
m.p.	melting point
NCI	National Cancer Institute, Washington DC
NMR	Nuclear Magnetic Resonance
nOe	Nuclear Overhauser Effect
NOESY	Nuclear Overhauser Effect Spectroscopy
PDA	photodiode-array
ROESY	Rotational Overhauser Effect Spectroscopy
S	singlet

sp.	species (singular)
spp.	species (plural)
SRB	sulforhodamine B
TCA	trichloroacetic acid
t	triplet
Tris	tris(hydroxymethyl)aminomethane
UV	Ultraviolet
Vis	Visible Light

CHAPTER 1

Introduction-

Literature review of genera from which metabolites have been isolated

1.1 General Introduction

Cancer is the second leading cause of death world wide and the total number of cases globally is increasing. The use of anticancer drugs has significantly reduced the mortality rate. Many of these drugs were derived from natural products. For example vincristine, a plant alkaloid from the Madagascar periwinkle has been used in the treatment of several types of leukaemia for nearly thirty years (Roberge et al., 2000). Paclitaxel, the trade name of taxol (also an N-containing metabolite), from the pacific yew (*Taxus brevifolia*), is an antimitotic agent that has been used successfully in the treatment of breast, ovarian, and lung carcinomas (Roberge et al., 2000). However, these drugs have severe side effects, especially myelosupression (bone marow toxicity) and neurotoxicity. More importantly, many cancers become resistant to these drugs during the treatment (Rowinsky, 1997). Clearly, there would be an advantage to patients if new, nontoxic drugs could be developed against which the cancers are not resistant.

Unlike the long-standing historical medical uses of terrestrial plants, marine organisms have a shorter history of utilization in the treatment and/or prevention of human disease. The leading works of Bergmann (Bergmann and Feeney, 1951; Bergmann and Burke 1955; and Bergmann and Feeney, 1950) have provided the lead compounds for the development of the therapeutically used Ara-C **(**unusual arabinosyl nucleoside, spongothymidine, spongosine and sponguridine from the sponge *Cryptotethya crypta*) for treatment of leukemia. However, until the mid-1960s, investigation of natural products from marine organisms was essentially non-existent.

The first generation of drugs isolated from marine organisms that have successfully advanced to the late stages of clinical trials for the treatment of cancer are ecteinascidin 743 (yondelis™, trabectedin™, trabectin™), aplidine/dehydrodidemnin (aplidine™), bryostatin and kahalalide F (Simmon et al., 2005). Prialt, a cone snail toxin is the first drug that was obtained directly from a sea entity to become a licensed pharmaceutical for pain relief (Newman and Cragg, 2007). The list of marine natural products in anticancer preclinical or clinical trials have been well reviewed by Simmon et al (2005) and Newman and Cragg (2004).

Anticancer agents can be isolated from various marine organisms, mainly from invertebrates (molluscs, ascidians/tunicates, sponges, bryozoans, soft corals and echinoderms), and algae. Only squalamine, an aminosteroid has been isolated from a vertebrate, a dog fish shark. Ecteinascidin 743 (ET-743/yondelis/trabectedin) and aplidine/dehydrodidemnin were isolated from tunicates. Ecteinascidin 743 was isolated from the Caribbean marine tunicate *Ecteinascidia turbinata* while aplidine/dehydrodidemnin has been isolated from the tunicate *Aplidium albicans* (family *Polyclinidae*). These cytotoxic agents, however, differ in their

chemical classes and mechanisms of action. Ecteinascidin 743 is a tetrahydroisoquinoline alkaloid and targets DNA by binding in the minor groove in GC-rich sequences, alkylating the 2-amino group of guanine, whereas aplidine is a cyclic depsipeptide that targets ornithine decarboxylase. Kahalalide F is also a cyclic depsipeptide derived from the sea slug *Elysia rufescens* and originating from the green alga *Bryopsis sp***.** Bryostatins are a group of macro cyclic polyether lactones isolated from the bryozoan *Bugula neritina*.

It is noteworthy that marine drug candidates such as ET-743, aplidine, bryostatin and kahalalide F are selected against certain cancers and are less toxic. In phase II trials, ET-743 was most effective, with acceptable toxicity, in patients with refractory soft tissue sarcoma, ovarian, and breast cancer. Although difficulties in establishing the drug's efficacy in soft tissue sarcomas prevented its approval in 2003, yondelis was in 2007 approved for clinical use for the treatment of advanced sarcoma (www.medicalnewstoday.com/articles). In addition, the European Union's Committee for Proprietary Medicinal Products has granted ET-743 orphan drug status for the treatment of refractory ovarian cancer. Aplidine was more selective towards leukemia and lymphoma cells than towards normal cells and well below the toxic level. Moreover, the activity of aplidine was found to be independent of other anticancer drugs commonly used in treatment of leukemia and lymphoma, which suggests that it may be effective in cases that have proved unresponsive to other agents. Kahalalide F is selected against liver carcinoma (www.pharmamar.es). Bryostatins are extremely potent against P-388 mouse leukemia and human ovarian sarcoma *in vivo* (Pettit et al., 1982).

1.2 Literature Review of C_{15} Acetogenins and Terpenes from *Laurencia* and *Chondria*

Algae belonging to the genus *Laurencia* are extremely widespread and have been well documented to produce diverse, unique secondary metabolites. The characteristic secondary metabolites from *Laurencia* can be classified into two groups based on their biogenetic pathway: terpenoid and C_{15} acetogenins. The first bulk group of metabolites isolated from these algae are sesquiterpenoids while reports of diterpenoids and triterpenoids are few. The vast majority of non terpenoids are C_{15} acetogenins, which are based on a linear C_{15} chain cyclised by ether rings of different sizes with a terminal enyne or allenic side chain derived from the metabolism of a fatty acid (Fernandez et al., 2000). In addition, C_{15} acetogenins of marine origin are mainly produced from members of the marine algae genus *Laurencia*. It is also interesting to note that several *Laurencia* halogenated C_{15} acetogenins (Findlay and Li, 2002; McPhail et al., 2005; and Manzo et al., 2005) and terpenoids (Petitt et al., 1978 and Atta-ur-Rahman et al., 1991) have also been found from opistobranch molluscs that feed upon these algae and from the sponge *Mycale rotalis* (Giordano et al., 1990 and Notaro et al., 1992).

An abundant supply of C_{15} acetogenins and terpenes has been found from marine red algae, genus *Laurencia*. In contrast, the occurrence of C_{15} acetogenins and terpenes from the genus *Chondria*, algae of the same family as *Laurencia*, is very limited. Metabolites from the red algae of the genus *Chondria* are known for their antimicrobial, antibiotic, neurotoxic and cytotoxic (Agrawal and Bowden, 2007) activities. The *Chondria* compounds responsible for these activities are polysulfides, amino acid derivatives and polycyclic ethers. This review will cover marine C_{15} acetogenins and terpenoids from *Laurencia* and *Chondria armata*.

1.2.1 C_{15} Acetogenins from *Laurencia* and Related Marine Organisms

Laurencia is unique in producing C_{15} halogenated acetogenins. Obtusenyne (**1**) was first reported from *Laurencia obtusa* (King et al., 1979), and the two diastereomers, 3*Z*- and 3*E*-obtusenyne (**1, 2**) were subsequently also reported from *Laurencia pinnatifida* (Norte et al., 1991). 3*E*- and 3*Z*- pinnatifidenyne (**3,4**), 12-epi-obtusenyne (**5**) and brasilenyne (**6**), a known acetogenin that had previously been reported from the sea hare *Aplysia brasiliana* along with *cis*-dihydrorhodophytin (**7**) (Kinnel et al., 1979), were isolated from *Laurencia pinnatifida* (Gonzalez et al., 1982 and Norte et al., 1991). *trans*-Dihydrorhodophytin (**8**) was also reported as a metabolite of *Laurencia pinnatifida* (Norte et al., 1989). (3*Z*)-13-epi-Pinnatifidenyne (**9**) was found in *Laurencia claviformis* (San-Martin et al., 1997). The 3*E*-isomer (**10**) was obtained from *Laurencia obtusa* (Iliopoulou et al., 2002). The *Laurencia obtusa* sample that afforded (**10**) also afforded (3Z)- and (3*E*)-13-epilaurencienyne (**12,13**), (3*E*,6*S**,7*R**,9*S**,10*S**,12*R**)-9-chloro-13-bromo-6:12-epoxy-7,10-diacetoxypentadec-3-en-1-yne (**14**), as well as (3*Z*,6*S**,7*R**,9*S**,10*S**,12*R**)-9-chloro-13-bromo-6:12-epoxy-7,10-diacetoxypentadec-3-en-1-yne (**15**) (Iliopoulou et al., 2002). It is noteworthy that the enantiomer of 3*E*-13-epi-pinnatifidenyne (**11**) has also subsequently been reported from the anaspidean mollusc *Aplysia dactylomela* (Manzo et al., 2005).

A study of *Laurencia* from Hawai revealed that *L. majuscula* is a source of lauroxolane (**16**) containing a 2,2'-bis-tetrahydrofuran substructure (Kim et al., 1989). Its stereochemistry was determined by using spectroscopic techniques. Three similar structures (**17-19**) also containing a tetrahydrofuran ring were isolated from *L. obtusa* collected from waters near the Canary Islands (Norte et al., 1989b). Moreover, L. *nipponica* from Hokkaido was reported to produce laureoxolane (**20**), a brominated C_{15} acetogenin with one tetrahydrofuran ring as well (Fukuzawa et al., 1989).

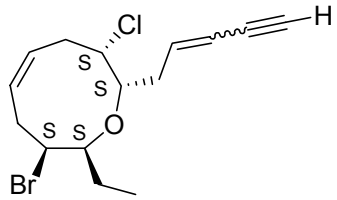

(3*Z*)-obtusenyne (**1**)

(3*E*)-obtusenyne (**2**)

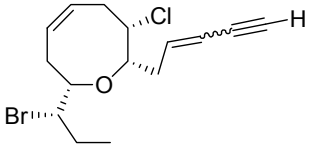

(+)-(3*E*)-pinnatifidenyne (**3**)

(+)-(3*Z*)-pinnatifidenyne (**4**)

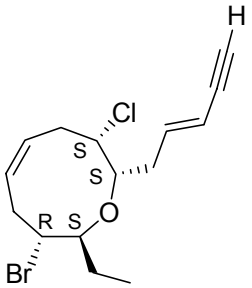

12-*epi*-3*E*-obtusenyne (**5**)

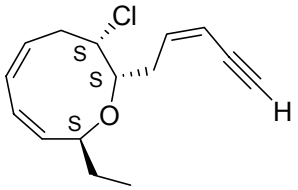

brasilenyne (**6**)

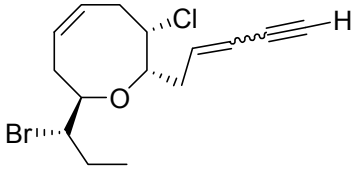

cis-dihydrorhodophytin (**7**)

trans-dihydrorhodophytin (**8**)

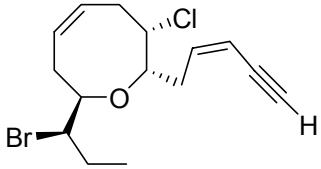

(+)-(3*Z*,12*R*,13*R*)-pinnatifidenyne (**9**)

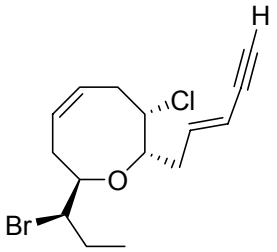

(+)-(3*E*,12*R*,13*R*)-pinnatifidenyne (**10**)

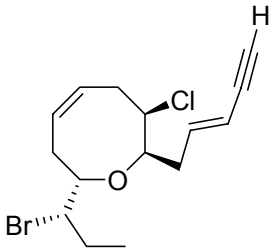

(-)-(3*E*,12*R*,13*R*)-pinnatifidenyne (**11**)

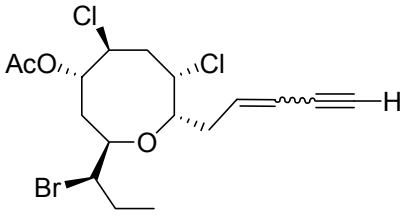

(3*Z*)-13-epilaurencienyne (**12**)

(3*E*)-13-epilaurencienyne (**13**)

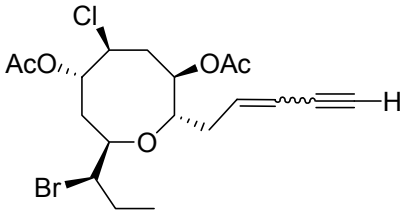

(3*E*,6S*,7*R**,9*S**,10*S**,12*R**)-9-chloro-13-bromo-6:12-epoxy-7,10-diacetoxypentadec-3-en-1-yne (**14**)

(3*Z*,6*S**,7*R**,9*S**,10*S**,12*R**)-9-chloro-13-bromo-6:12-epoxy-7,10-diacetoxypentadec-3-en-1-yne (**15**)

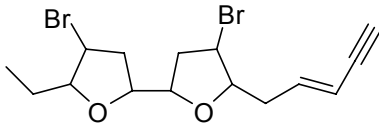

lauroxolane (**16**)

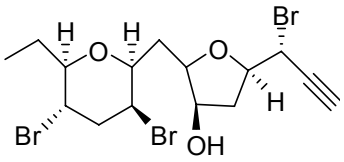

(**17**)

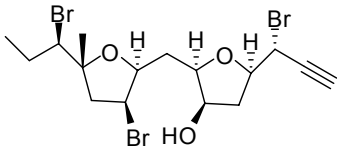

(**18**)

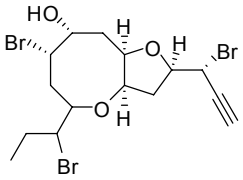

(**19**)

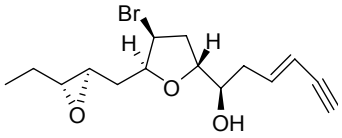

(**20**)

Laurencienyne (**21**) was reported from a *Laurencia obtusa* sample collected in the Mediterranean (Caccamese et al., 1980). A halogenated acetogenin with a ketonic moiety at C-7, scanlonenyne (**22**), was also isolated from *Laurencia obtusa* collected in Irish waters (Suzuki et al., 1997). Another *Laurencia obtusa* sample collected from Turkish waters contained laurencienyne (**21**), and (3*E*)-dactomelyne (**23**) (Aydomus et al., 2004). Compound (**18**) and 12-epi-obtusenyne (**5**) were previously reported from the sea hare, *Aplysia dactylomela,* collected from the Bahamas (Gopichand et al., 1981). The Turkish collection of *Laurencia obtusa* also contained (**24**) (Aydomus et al., 2004), a stereoisomer of neoisoprelaurofucin (**25**), which had previously been reported from *Laurencia nipponica* that had been collected in Japanese waters (Suzuki et al., 1996).

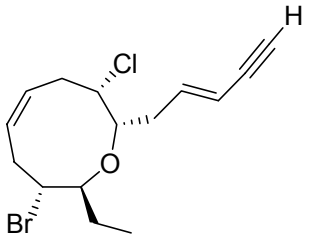

laurencienyne (**21**)

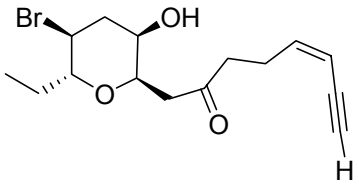

scanlonenyne (**22**)

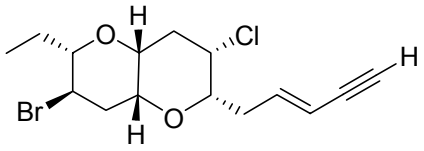

dactomelyne (**23**)

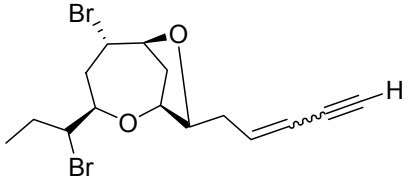

3*E*-neoisoprelaurofucin (**24**)

3*Z*-neoisoprelaurofucin (**25**)

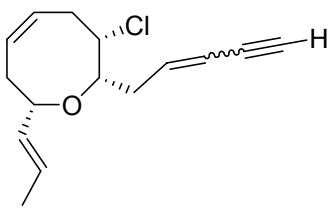

(+)-(3*Z*)-laurenyne (**26**)

(+)-(3*E*)-laurenyne (**29**)

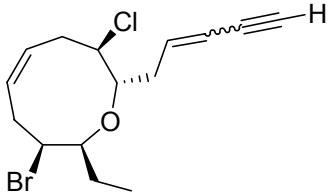

(+)-(3*Z*,6*R*,7*R*)-obtusenyne (**27**)

(+)-(3*E*,6*R*,7*R*)-obtusenyne (**28**)

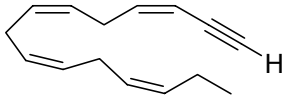

laurencenyne (**30**)

(+)-(3*E*)-pinnatifidenyne (**3**), (+)-(3*Z*)-laurenyne (**26**), (+)-(3*Z*,6*R*,7*R*)-obtusenyne (**27**), and (+)-(3*E*,6*R*,*7R)*-obtusenyne (**28**) were also isolated from the sea hare *Aplysia dactylomela* (Manzo et al., 2005). 3*Z*-Laurenyne has also been reported from a new *Laurencia* species, L. *yonaguniensis* (Takahashi et al., 2002). Moreover, the (3*E*)-isomer (**29**) had previously been found in *Laurencia obtusa* (Falshaw et al., 1980), and was also isolated from the Italian Sea hare *Aplysia punctata* (Findlay and Li, 2005). A C_{15} acetogenin hydrocarbon, laurencenyne (**30**), was also isolated from this sea hare. Laurencenyne had previously been isolated from the red alga *Laurencia okamurai* and might be a precursor for various nonterpenoid C_{15} compounds in Laurencia and related red algae (Kigoshi et al., 1981).

Laurencia is also a prolific source of C_{15} acetogenins that consist of an eight member ring fused with a tetrahydrofuran ring. A new C_{15} acetogenin, (3*Z*)-bromofucin (**31**) was recently reported from the South African sea hare *Aplysia parvula* (McPhail and Davies-Coleman, 2005) while (3*E*)–bromofucin (**32**) was previously found from the Australian red alga *Laurencia implicata* (Coll and Wright, 1989). C_{15} acetogenins **33-34** and chlorofucin (**35**) were also reported in the Australian alga. Moreover, 3*E*- and 3*Z*- chlorofucin (**35,36**) were isolated from a Malaysian sample of *Laurencia pannosa* (Suzuki et al., 2001). Compound **36** had previously been isolated from a Vietnamese collection of *Laurencia pannosa* (Suzuki et al., 1996) and from *Laurencia snyderae* collected from La Jolla (Howard et al., 1980).

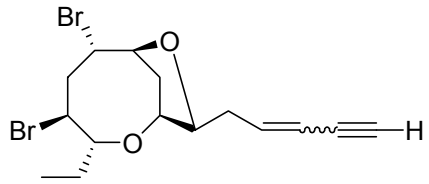

(3*Z*)-bromofucin (**31**)

(3*E*)-bromofucin (**32**)

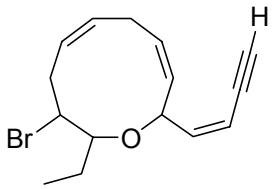

(**33**)

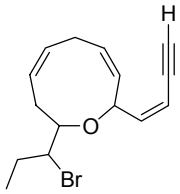

(**34**)

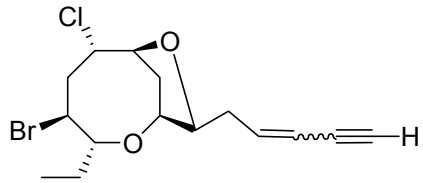

(3*E*)-chlorofucin (**35**)

(3*Z*)-chlorofucin (**36**)

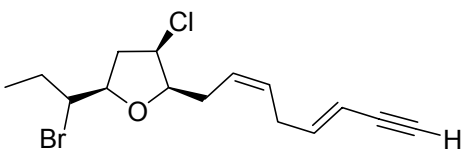

bisezakyne-A (**37**)

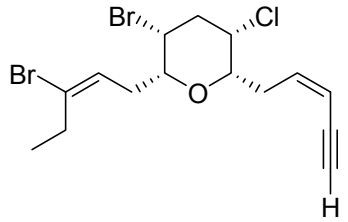

bisezakyne-B (**38**)

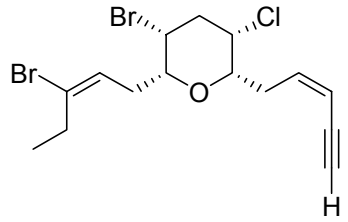

dactylyne (**39**)

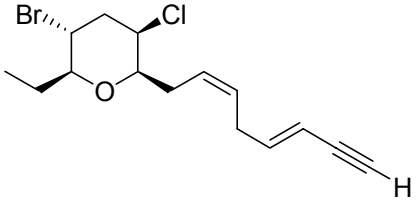

srilankenyne (**40**)

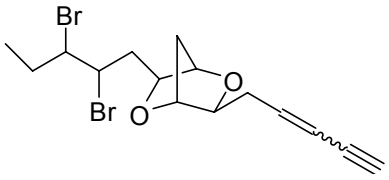

ocellenyne E (**41**)

ocellenyne Z (**42**)

Sea hares generally store typical algal halogenated metabolites. Three C_{15} acetogenins, named bisezakyne-A (**37**) and –B (**38**) and dactylyne (**39**) were isolated from an undescribed red algal species from the genus *Laurencia* collected from Japan (Suzuki et al., 1999). Dactylyne (**39**) had previously been isolated from the sea hare *Aplysia dactylomela* (McDonald et al., 1975) while an isomer of dactylyne was also reported from another collection of the same sea hare (Vanderah and Schmitz, 1976). This is another example where the sea hare may accumulate a compound from consumption of a *Laurencia* species. In addition, an isomer of bisezakyne-A, srilankenyne (**40**) had been reported from the sea hare *Aplysia oculifera* (de Silva et al., 1983). The sea hare *Aplysia oculifera* collected on Oahu (Schulte et al., 1983) was also known to afford E and Z- ocellenyne (**41**, **42**).

Japanese *Laurencia* species have been well known to produce C_{15} acetogenins. *Laurencia nipponica* Yamada (Kikuchi et al., 1991) displayed a marked variation in C_{15} acetogenins: laurencin (**43**), laureatin (**44**), isolaureatin (**45**), epilaurallene (**46**), kumausallene (**47**), trans-kumausyne (**48**), (3*Z*)-isoprelaurefucin (**49**, (3*Z*)-laurefucin (**50**) and notoryne (**51**). Lyakhova et al., (2006) reported two new brominated allenes, nipponallene (**52** and neonipponallene (**53** from the Japanese red alga *Laurencia nipponica.* Laurencin (**43**), a bromo compound was initially reported from *Laurencia glandulifera* Kützing (Irie et al., 1968). *Laurencia japonensis* has been reported to afford two new C_{15} acetogenins, japonenynes-A and -B (**54, 55**) (Takahashi et al., 1999).

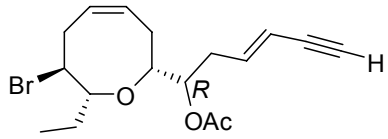

laurencin (**43**)

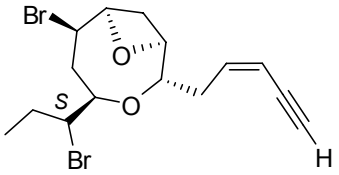

laureatin (**44**)

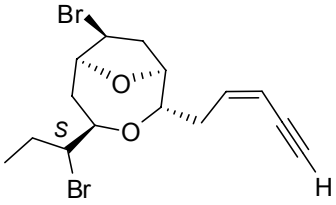

isolaureatin (**45**)

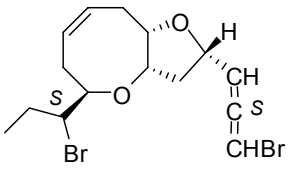

epilaurallene (**46**)

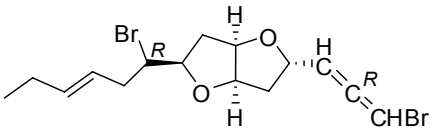

kumausallene (**47**)

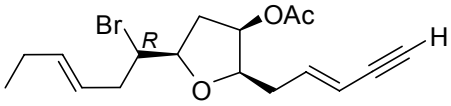

trans-kumausyne (**48**)

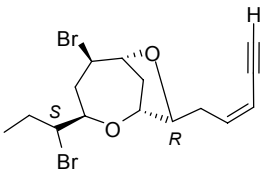

isoprelaurefucin (**49**)

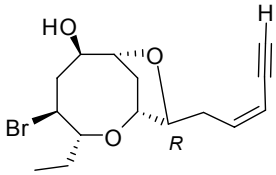

3*Z*-laurefucin (**50**)

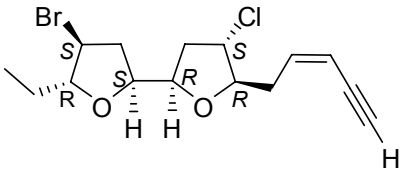

notoryne (**51**)

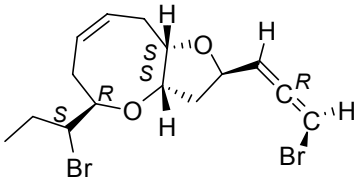

nipponallene (**52**)

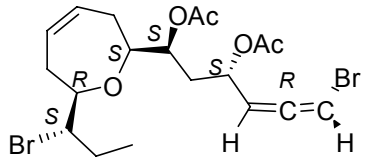

neonipponallene (**53**)

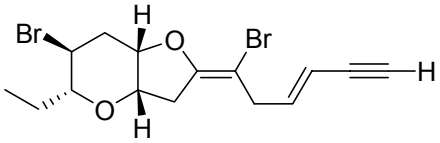

japonenyne-A (**54**)

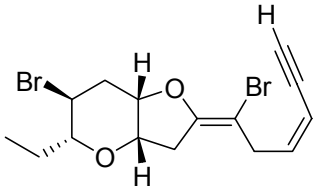

japonenyne-B (**55**)

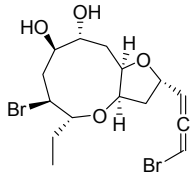

laurendecumallene A (**56**)

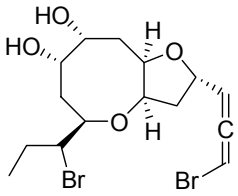

laurendecumallene B (**57**)

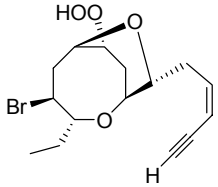

laurendecumenyne A (**58**)

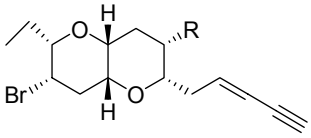

laurendecumenyne B: R=Cl (**59**)

elatenyne : R = Br (**60**)

Laurencia is also a producer of bromoallene acetogenins. Four new unusual C_{15} bromoallene and enyne acetogenins, laurendecumallene A (**56**), laurendecumallene B (**57**), laurendecumenyne A **(58)**, laurendecumenyne B (**59**) and one known halogenated C_{15} acetogenin elatenyne (**60**) (Hall and Reiss, 1986) were recently isolated from *Laurencia decumbens* (Ji et al., 2007a). In addition, a new C_{15} acetogenin, (12*E*)-lembyne-A (**61**), was reported from *Laurencia marinannensis* (Vairappan et al., 2001a). Moreover, two new halogenated metabolites, named 12*Z* lembyne-A (**62**) and lembyne-B (**63**), were isolated from an unrecorded *Laurencia* species collected in algal habitats in Malaysian coastal waters (Vairappan et al., 2001b).

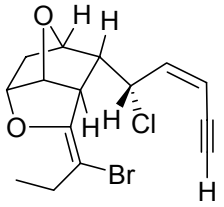

12*E*-lembyne-A (**61**)

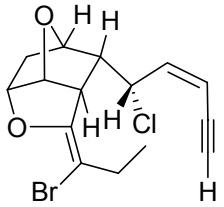

12*Z*-lembyne-A (**62**)

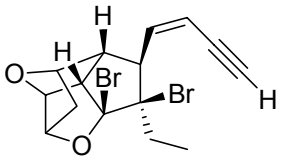

lembyne-B (**63**)

It is also interesting to note that three polybrominated C_{15} acetogenins (**64-66**) have been isolated from an encrusting sponge, *Mycale rotalis* (Giordano et al., 1990 and Notaro et al., 1992).

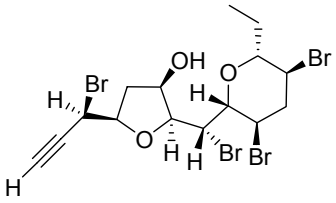

(**64**)

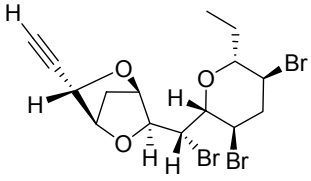

(**65**)

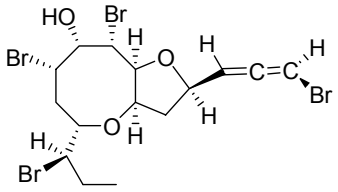

(**66**)

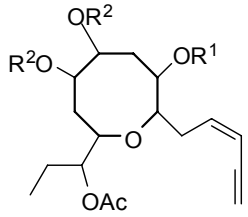

doliculol A (**67**, $R^1 = R^2 = H$)

doliculol B (**68**, $R^1 = Ac$, $R^2 = H$)

Although a number of halogenated C_{15} acetogenins have been isolated from both the red algae of the genus *Laurencia* as well as from the sea hares that feed upon them, reports on non-halogenated C_{15} acetogenins are very limited. Doliculols A and B (**67**, **68**) are the only example of non-halogenated C_{15} acetogenins isolated from the sea hare *Dolabela auricularia* collected from Japanese coasts (Ojika et al., 1993).

Biological Activity of C_{15} Acetogenins

C_{15} acetogenin metabolites exhibit some interesting biological activities such as anti feeding, toxicity, antibacterial and cytotoxic activities. Several C_{15} acetogenins such as (-) 3*E*,6*R*,7*R*-pinnatifidenyne (**11**), *E*-laurenyne (**29**), brasilenyne (**6**) and *cis*-dihydrorhodophytin (**7)** showed anti feeding activities**.** (-)-3*E*,6*R*,7*R*-Pinnatifidenyne (**11**) and *E*-laurenyne (**29**) demonstrate anti-feeding activity towards goldfish, *Carassius auratus*, at a concentration of 50 mg/cm^2 (Manzo et al., 2005). Brasilenyne (**6**) and *cis*-dihydrorhodophytin (**7**) were found to have strong anti-feeding activity for swordtail fish (*Xiphophorus helleri*) at 0.1 and 0.3 μg respectively (applied to small beetle larvae, average weight 0.8 mg). (3*Z*)-laurenyne (**26**) showed low toxicity toward brine shrimp with an LC_{50} value of 467.0 μM (Takahashi et al., 2002).

The unusual C_{15} bromoallenes and enynes, laurendecumallene A (**56**), laurendecumallene B (**57)**, laurendecumenyne A **(59)**, laurendecumenyne B (**60**) and elatenyne (**61**) from *Laurencia decumbens* showed weak activity against A549, human lung adenocarcinoma tumor cell line with IC_{50} values >10 μg/mL (Ji et al., 2007a). In addition, for the *cis* C_{15} acetogenins (**12**) and (**14**) from *L. obtusa*, strong ant toxicity was observed, with knockdown of *Pheidole pallidula* ants on the first day, while the *trans*-isomers (**9**), (**13**) and (**14**) showed a gradual toxicity (1.5 mg/disk) with 70% mortality after 4 days (Iliopoulou et al., 2002). (12*E*)-lembyne-A (**61**), isolated from *Laurencia marinannensis* showed antibacterial activity against marine bacteria *Alcaligenes aquamarinus, Azomonas agilis, Erwinia amylovora* and *Escherichia coli* with the minimum inhibitory concentration (MIC) values between 20 and 30 mg/disc (Vairappan et al., 2001a). Moreover, lembyne-A (**62**) also showed weak antibacterial activity with MIC values in the range of 20–60 mg/disc against *Clostridium cellobioparum*, *Chromobacterium violaceum, Flavobacterium helmiphilum, Proteus mirabilis* and *Vibrio parahaemolyticus* (Vairappan et al., 2001b). (3*Z*)-Chlorofucin (**36**) showed antibacterial activity against *Chromobacterium violaceum* with an MIC value 100 μg/disk (Suzuki et al., 2001).

1.2.2 Terpenes from *Laurencia* and Related Marine Organisms

Red algae of the genus *Laurencia* are known as prolific sources of halogenated terpenes. Although diterpenes and triterpenes have also been found, sesquiterpenes are the most abundant members in the terpenoid groups isolated from these algae. In addition, sesquiterpene with chamigrene type skeleton have been isolated in high number and great diversity, while other

sesquiterpenes with bisabolane and farnesane type skeletons are less common. Diterpenes and triterpenes are an interesting group of marine natural products due to their chemical structure with various ring sizes and biological activities.

1.2.2.1 Diterpenes

Halogenated diterpenes account for an important part of *Laurencia* metabolites with many unique skeletons (Ji et al., 2007b; Howard and Fenical, 1978; Kuniyoshi et al., 2005 and Iliopoulou et al., 2003b) and interesting biological activities (Iliopolou et al., 2003b and Mohammed et al., 2004). The skeleton of diterpenoids isolated from *Laurencia* varies for each species. The most common skeleton type is labdane diterpene. However, the possibility of discovering a novel skeleton is still high, as this genus has been known to produce an astonishing variety of secondary metabolites.

The first labdane type diterpene, aplysin-20 (**69**) was isolated from the sea hare *Aplysia kurodai* (Yammamura and Hirata, 1971). Concinndiol (**70**) was found two years later from *Laurencia concinna* (Sims et al., 1973) collected from the coast of New South Wales, Australia. This may suggest that the source of (**69**) was a *Laurencia* species. Several labdane type diterpenes have been isolated from other *Laurencia* spp: isoconcinndiol (**71**) from *L. snyderae* var. *guadalupensis* (Howard et al., 1980), pinnatols A, B, C, and D (**72-75**) from *L. pinnata* (Fukuzawa et al., 1985), venustanol (**76**) from *L. venusta* (Suzuki et al., 1988) and paniculatol (**77**) from *L. paniculata* (Briand et al., 1997). An Okinawan unidentified species of *Laurencia* was also reported to produce two novel brominated labdane type diterpenoids (**78** and **79**). The structure and absolute stereochemistry of (**78** and **79**) were determined using both spectroscopic data and X-ray crystallographic data (Suzuki et al., 2002). The following year, two labdane brominated diterpenes (**80** and **81**) were reported from *L. obtusa* (Iliopoulou et al., 2003a) from Greek waters.

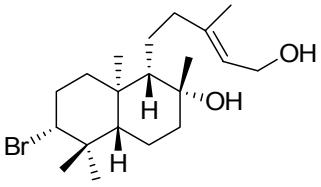

(**69**) aplysin 20

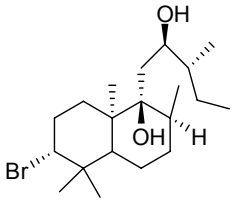

concinndiol (**70**)

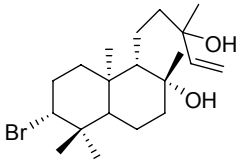

isoconcinndiol (**71**)

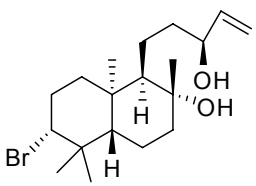

pinnatol A (72)

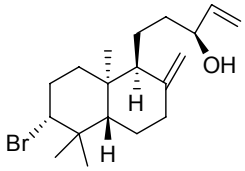

pinnatol B (73)

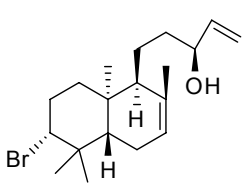

pinnatol C (74)

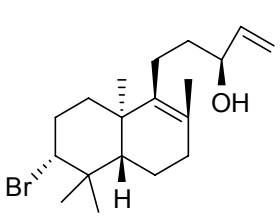

pinnatol D (75)

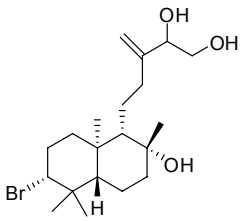

venustanol (**76**)

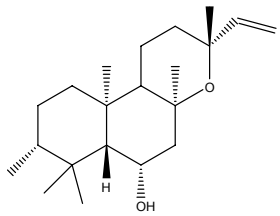

paniculatol (**77**)

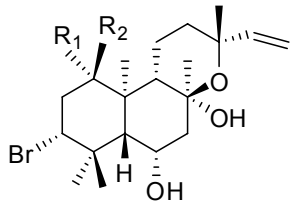

(**78**) R_1 = OAc R_2 = H)
(**79**) R_1 = R_2 = O)

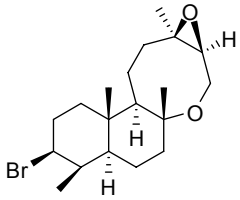

(**80**)

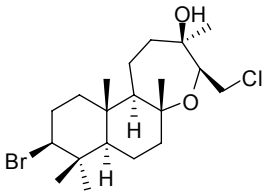

(**81**)

Unusual skeletal bromoditerpenoids, irieol A (**82**) and iriediol (**83**) were isolated from *Laurencia irieii* collected from the Gulf of California, Mexico (Howard and Fenical, 1978). It is interesting to note that diterpenoids with the irieol type skeleton, angasiol (**84**) and angasiol acetate (**85**) have also been found from an East Australian sea hare *Aplysia angasi* (Petit et al., 1978) and *Aplysia juliana* (Atta-ur-Rahman et al., 1991) collected in Pakistan. Since (**84**) and (**85**) were found from sea hare, it would be an interesting to search for algal sources of these metabolites.

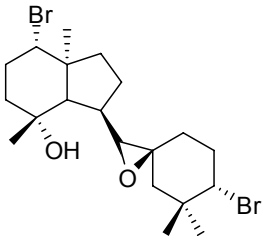

(**82**)

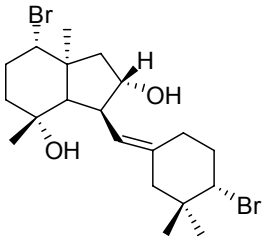

(**83**)

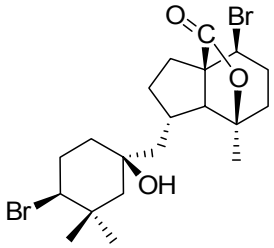

(**84**)

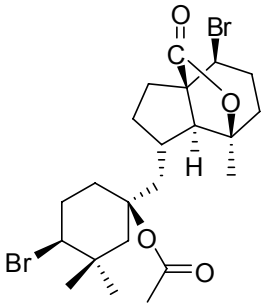

(**85**)

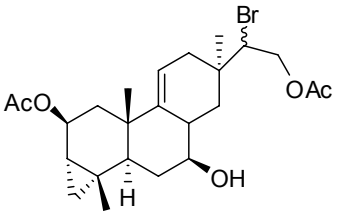

(**86**)

Laurencia obtusa is well known to produce halogenated diterpenes. 15-Bromo-2,6-diacetoxy-7-hydroxy-9(11)-parguarene (**86**) had been found from *L. obtusa* collected at Dorset (Higgs and

Faulkner, 1982). Parguarane (**87**), a bromoditerpene with the same carbon skeleton was previously isolated from the sea hare *Aplysia datylomela* collected at La Parguera, Puerto Rico (Schmitz et al., 1981). Closely related to this carbon skeleton, five pargueranes (**88-92**) were later reported to be produced from Australian *L. filiformis* (Rochfort and Capon, 1996). In addition, another Greek collection of *L. obtusa* at Preveza was the source of five new bromoditerpenes, prevesol B-E (**93-96**), neorogioldiol B (**97**) and the known bromoditerpenes neorogioldiol (**98**) and *O*-11,15-cyclo-14-bromo-14,15-dihydrorogiol-3,11-diol (Iliopolou et al., 2003b). It is noteworthy that prevesols B and E possess two new carbon skeleton types.

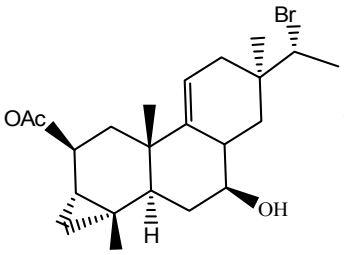

(**87**)

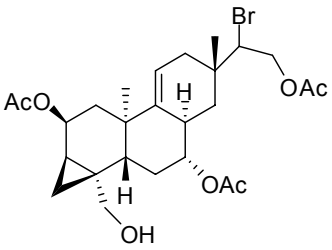

(**88**)

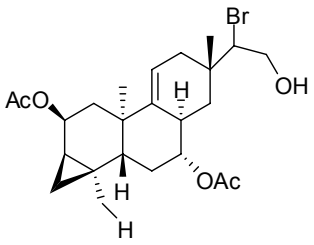

(89)

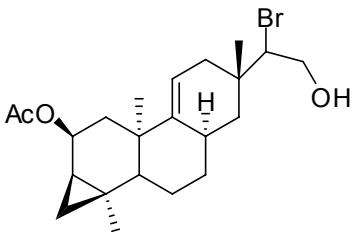

(**90**)

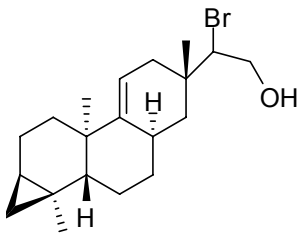

(**91**)

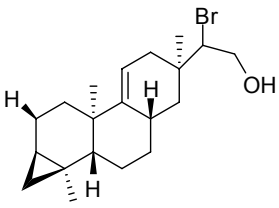

(**92**)

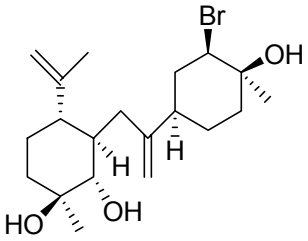

(**93**)

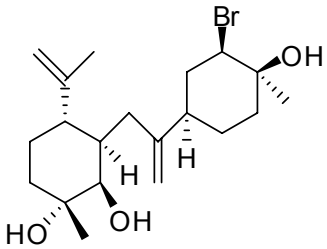

(**94**)

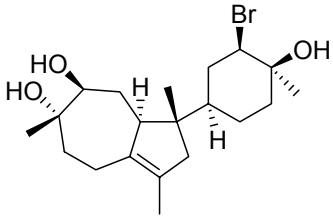

(**95**)

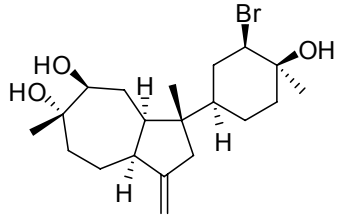

(**96**)

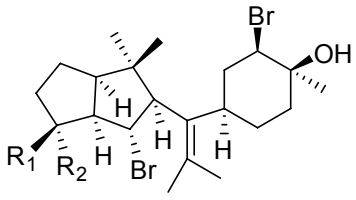

(**97**) R_1 = OH, R_2 = CH_3

(**98**) R_1 = CH_3, R_2 = OH

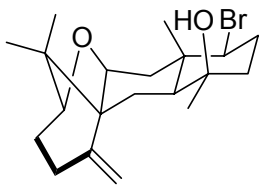

(**99**)

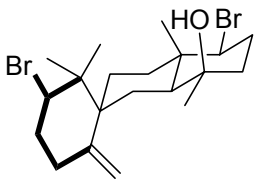

(**100**)

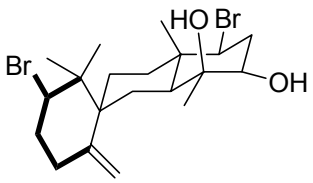

(**101**)

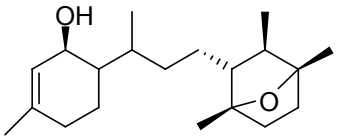

(**102**)

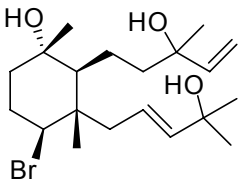

(**103**)

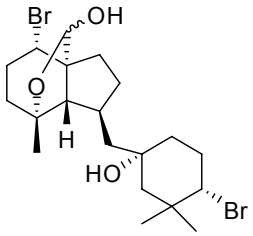

(**104**)

Hawaian *Laurencia majuscula* elaborated a new type of diterpene, kahukuenes A (**99**) and B (**100**) with an isoprene unit extension of the basic chamigrane sesquiterpene skeleton (Brennan et al., 1993). The Hawaiian species is unique in its secondary metabolites compared to the same species from Japanese, Australian and Mediterranean algae. The Hawaiian *L. majuscula* only produces lauroxolane (**16**) and other diterpenoids but no sesquiterpenoids.
10-Hydroxykahukuene B (**101**) has also been recently isolated from Chinese *L. marianennensis* (Ji et al., 2007b).

Laurencia intricata and *L. decumbens* have also been reported as producers of diterpenes recently. Laurenditerpenol (**102**) was isolated from tropical *L. intricata* collected at Jamaica (Mohammed et al., 2004) based on bioassay-guided fractionation. It is interesting to note that this is the first example of non brominated diterpene among *Laurencia* metabolites. Another species, *L. decumbens* collected from Chinese waters has been also reported to elaborate two new brominated terpenes, namely, laurendecumtriol (**103**) and 11-*O*-deacetylpinnaterpene C (**104**) (Ji et al., 2007c and 2007d).

Biological activity of *Laurencia* Diterpenes

Some biological activities of diterpenes from *Laurencia* have been reported. Metabolites (**93-97**) have been tested for cytotoxic activity towards MCF7 (mammary adenocarcinoma), HeLa (cervix adenocarcinoma), PC3 (prostate adenocarcinoma), A431 (epidermoidcarcinoma) and K562 (a chronic myelogenous leukemia cell line) cancer cell lines (Iliopolou et al., 2003b). Compounds (**94**) and (**96**) were shown to be potent as cytotoxic agents with an inhibitory activity at doses lower than 100 μM. Compound (**96**) seemed to be selective against PC3 and

HeLa cell lines with IC_{50} 50.8 and 34.4 μM and lower activities against A431 and K562 while compound (**94**) showed greater activity toward A431 and K562 cell lines. Structure activity relationship analysis reveals that the relative stereochemistry of the diol structural motif is responsible for the cytotoxic activity for (**94**), as it had double the activity of the stereoisomer (**93)** for PC3 and K562 cell lines.

Laurenditerpenol (**102**), a non halogenated diterpene, is the first marine diterpene that selectively and potently inhibits physiological hypoaxia-induced HIF-1 activation in tumor cells without affecting normoxic cell growth. It has been shown to inhibit hypoxia-induced HIF-1 with an IC_{50} 0.4μM in T47D breast tumor cells (Mohammed et al., 2004). Studies have revealed that Inhibition of HIF-1 production/function significantly reduces tumor growth. Therefore, specific HIF-1 inhibitors may represent potential anticancer drug leads targeting tumor hypoxia.

To date, only two papers report the antibacterial activity of marine halogenated diterpenes. The metabolite 10-hydroxykahukuene B (**101**) exhibited weak activity toward *Escherichia coli* with an inhibition diameter of 6.5 mm. Moreover, it had no antifungal activity (Ji et al., 2007b). Another study showed that two labdane type diterpenes (**78** and **79**) were also inactive against several pathogenic bacteria using the paper disk diffusion method (Suzuki et al., 2002).

1.2.2.2 Triterpenes

One of the most interesting groups of marine natural products is formed by polyether triterpene compounds due to their chemical structure and biological acitivies. All known polyether triterpenes isolated from red algae are squalene-derived and usually consist of two or more separate ring systems with 5-7 membered rings. Several polyethers have also been reported from molluscs (Suenaga et al., 1998 and Manzo et al., 2007). Studies of the biological activity of these compounds have focused mainly on their potent cytotoxic effects (Suzuki et al., 1987; Suenaga et al., 1998; Norte et al., 1996 and Fernandez et al., 2000).

Squalene-derived polyether triterpenoids possessing a dioxabicyclo decane ring system represent a very interesting secondary metabolite group from *Laurencia* red algae.The first examples of this group, thyrsiferol (**105**) and thyrsiferyl 18-acetate (**106**), were isolated from *L. thyrsifera* collected at the coast of New Zealand (Blunt et al., 1978). However, the absolute stereochemistry of thyrsiferol was not fully determined. The structure of thyrsiferyl 18-acetate was determined by X-ray crystallography. Biological testing of the crude sample indicated that thyrsiferol and thyrsiferyl 18-acetate were inactive against several pathogenic bacteria. The

second example of squalene-derived polyethers, dehydrothyrsiferol (**107**), was reported from *L. pinnatifida* collected in the Canary Islands six years later. The chemical transformation into thyrsiferol confirmed it structure (Gonzales et al., 1984).

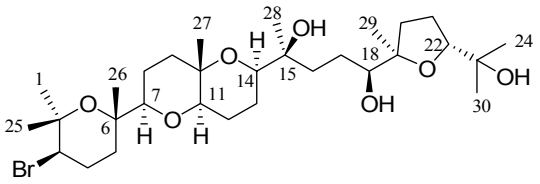

thyrsiferol ((**105**, R = H)

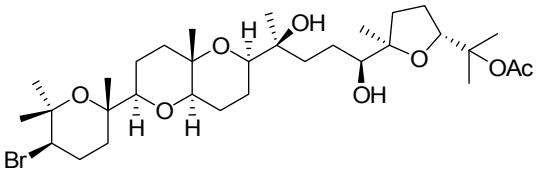

thyrsiferyl 18-acetate (**106,** R = Ac)

thyrsiferyl 23-acetate (**108**)

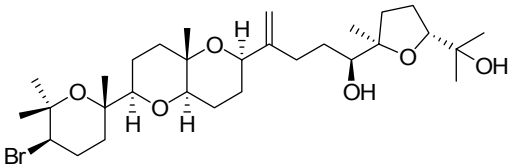

dehyrothyrsiferol (**107**)

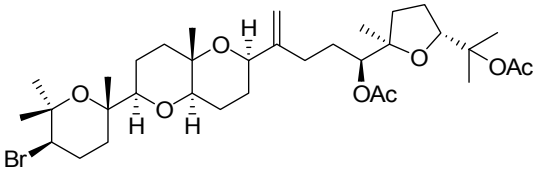

15(28)-anhydro-thyrsiferyl diacetate (**109**)

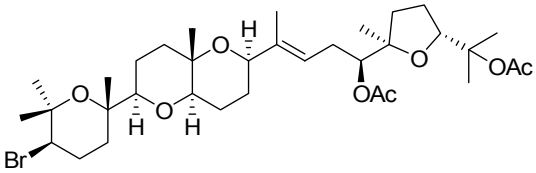

15- anhydrothyrsiferyl diacetate (**110**)

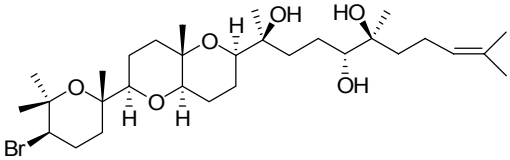

magireol A (**111**)

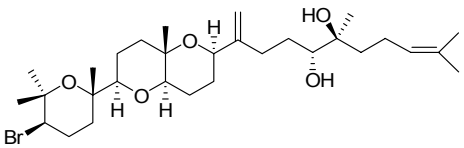

magireol B (**112**)

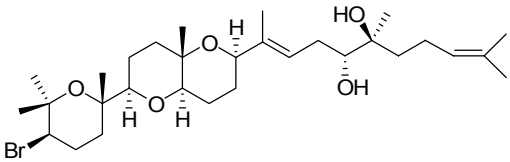

magireol C (**113**)

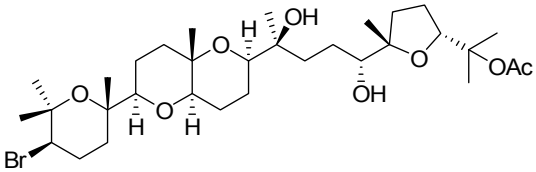

venustatriol (**114**)

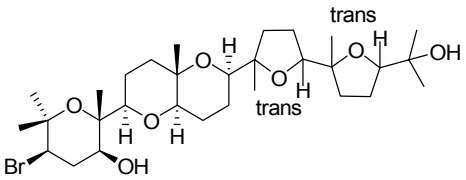

callicladol (**115**)

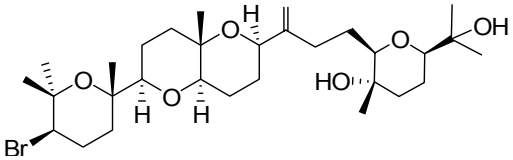

isodehydrothyrsiferol (**116**)

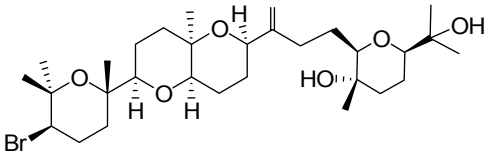

10-epi-Isodehydrothyrsiferol (**117**)

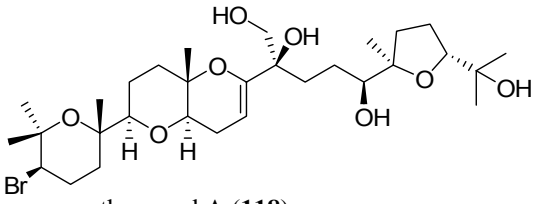

thyrsenol A (**118**)

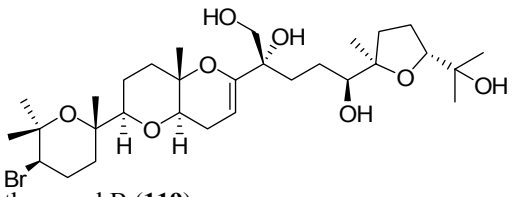

thyrsenol B (**119**)

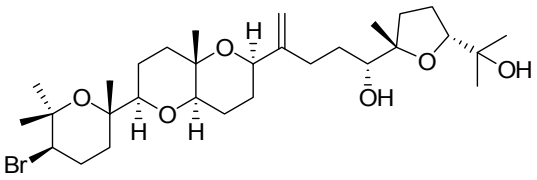

dehydrovenustatriol (**120**)

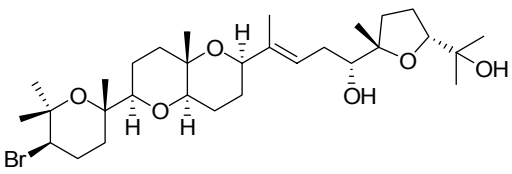

15,16-dehydrovenustatriol (**121**)

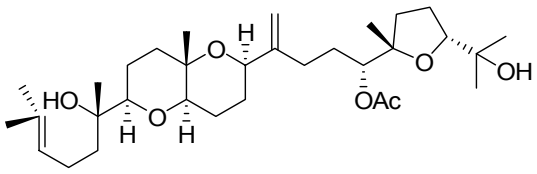

predehydrovenustatriol acetate (**122**)

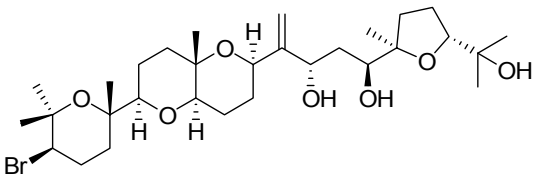

16-hydroxydehydrothyrsiferol (**123**)

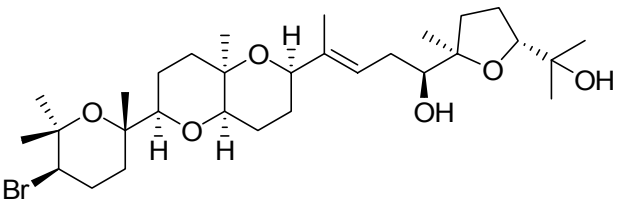

10-epi-15,16-dehydrothyrsiferol (**124**)

A Japanese *L. obtusa* elaborated the novel cyclic ether, thyrsiferyl 23-acetate (**108**) (Suzuki et al., 1985). Its structure was confirmed by spectral data and chemical transformation which yielded thyrsiferol. This compound is a potent cytotoxic agent with ED_{50} = 0.3 ng/mL against P388 cell line. A recollection of the Japanese *L. obtusa* (Hudson) Lamouroux afforded five cytotoxic polyether triterpenes: 15(28)-anhydro-thyrsiferyl diacetate (**109**), 15-anhydrothyrsiferyl diacetate (**110**), magireol A (**111**), magireol B (**112**) and magireol C (**113**) (Suzuki et al., 1987). Confirmation of the structures was undertaken using spectroscopic data and chemical methods. All of these compounds exhibited remarkable cytotoxic activity against a P388 cell line (appox. 30 ng/ml).

Venustatriol (**114**), a compound isolated from *Laurencia venusta* exhibited significant activity against the vesicular stomatitis virus (VSV) and Herpes simplex type 1 (HSV-1). The structure and absolute configuration was determined from X-ray data (Sakemi et al., 1986).

Callicladol (**115**), a pentacyclic compound, was isolated from *Laurencia calliclada* Masuda sp. ined., a Vietnamese species of the red algal genus *Laurencia* (Suzuki et al., 1995). The relative stereochemistry was determined using spectroscopic data and chemical methods. Its structure is

similar to that of thyrsiferol (**105**) except for a β-secondary hydroxyl group at C-5. Calicllado l showed a significant cytotoxic effect against P388 murine leukemia cells with IC_{50} of 1.75 μg/mL.

Laurencia viridis is well known to produce polyether triterpenes with a squalene carbon skeleton. Isodehydrothyrsiferol (**116**) and 10-epidehydrothyrsiferol (**117**) were isolated from this species collected in the Canary Island (Norte et al., 1996). These compounds were isolated from acetone extracts. Isodehydrothyrsiferol (**118**) displayed a selective and strong cytotoxic activity against P388 cell lines with IC_{50} of 0.01 μg/mL. Two new polyether squalene derivatives possessing an unusual enol-ether moiety, thyrsenols A (**118**) and B (**119**) were also reported from *Laurencia viridis* a year later (Norte et al., 1997a). Both of these compounds have significant antitumoral activity against P388 cells. It is an interesting point to note that thyrsenol A (**118**), dehydrothyrsiferol (**107**) and isodehydrothyrsiferol (**116**) exhibited similar cytotoxic activity against P388 cells with an IC_{50} of 0.01 μg/mL. Therefore, a study of the structure activity relationship can be undertaken. Another study on the constituents of *L. viridis* by the same authors revealed five novel triterpene polyethers: dehydrovenustatriol (**120**), 15,16-dehydrovenustatriol (**121**), predehydrovenustatriol acetate (**122**), 16-hydroxydehydrothyrsiferol (**123**) and 10-*epi*-15,16-dehydrothyrsiferol (**124**) (Norte et al., 1997b).

The first example of a symmetric polyether triterpene, teurilene (**125**), was isolated from *L. obtusa* collected from Teuri Island. Teurilene (**125**) consists of three linked tetrahydrofuran units in the centre of the molecule with eight chiral centres and C_s symmetry (Suzuki et al., 1985). The structure and absolute stereochemistry was determined using spectral data and X-ray methods. It is interesting to note that teurilene is an example of a non halogenated triterpene. Pure teurilene was inactive against P388 cells.

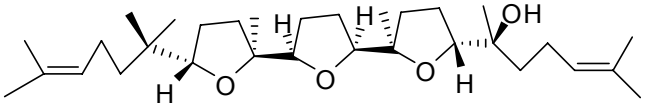

teurilene (**125**)

Laurencia intricata collected from the Japanese coast was shown to produce intricatetraol (**126**), a novel structure that contains chlorine and C_2 symmetry (Suzuki et al., 1993). It is the first example of a halogenated polyether triterpene possessing chlorine atom from the genus *Laurencia*. Its absolute stereochemistry was determined by using chemical synthesis (Yoshiki et al., 2007a) due to the difficulties of acyclic portions that include stereogenic quaternary carbon centres. Although crude extracts that contained intricatetraol as the major component exhibited weak cytotoxic activity (IC_{50} 12.5 μg/mL), the pure compound showed no cytotoxic activity against P388 cell lines.

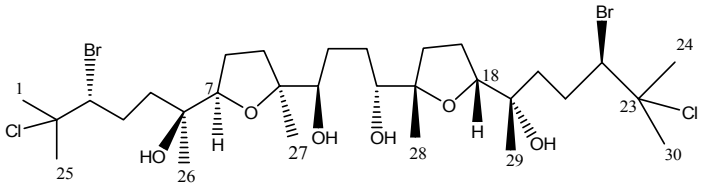

intricatetraol (**126**)

Enshuol (**127**) was the first example of a new class of triterpene with a dioxabicyclo (5.4.0) undecane ring system. Its structure is composed of a 2,8-dioxabicyclo[5.4.0]undecane ring (A-B ring) and three tetrahydrofuran rings (C-D-E rings). It was isolated from *L. omaezakiana* Masuda (Matsuo et al., 1995). Although the planar structure and partial configuration of enshuol were elucidated by spectroscopic and chemical analysis, the absolute stereochemistry was determined by chemical synthesis (Yoshiki et al., 2007b).

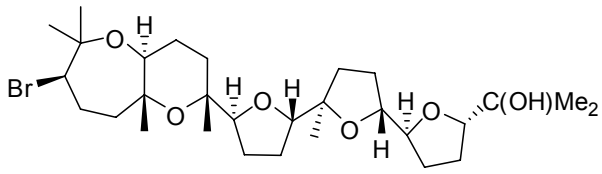

enshuol (**127**)

aurilol (**128)**

Polyether triterpenes have also been reported from molluscs. Aurilol (**128**) was isolated from the Japanese sea hare *Dolabella auricularia* (Suenaga et al., 1998). It is another example of a polyether with a dioxabicyclo (5.4.0) undecane ring system. It is suggested that aurilol is derived from the sea hare diet, as its structure was closely related to enshuol, a *Laurencia* metabolite. Aurilol displayed cytotoxic activity against HeLa S3 cells, with an IC_{50} of 4.3 μg /mL. More recently, aplysiols A (**129**) and B (**130**) have been reported from the the anaspidean mollusc *Aplysia dactylomela* (Manzo et al., 2007). Aplysiol A (**129**) and aplysiol **B** (**130**) are structurally related to thyrsiferol (**105**).

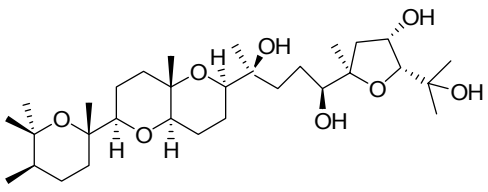

aplysiol A (**129**)

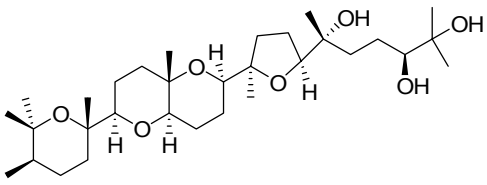

aplysiol B (**130**)

1.2.3 C_{15} Acetogenins and Terpenes from Red Algae of the Genus *Chondria*

1.2.3.1 C_{15} acetogenins

There is only one example of the isolation of a halogenated C_{15} acetogenin from a red alga of the genus *Chondria*. Chondriol (**131**) was isolated from *Chondria oppositiclada* (Fenical and Sims, 1973). It is interesting to point out that chondriol contains both Br and Cl. Its structure was elucidated from spectral data mainly NMR spectra. The absolute configuration was determined two years later using X-ray crystallography. Chondriol displayed a moderate and selective antimicrobial activity against gram positive bacteria (Sims et al., 1975).

1.2.3.2. Terpenes

Terpenes have been isolated from three species of the genus *Chondria* namely *Chondria oppositiclada*, *C. tenussima* and *C. armata* with each species affording metabolites that represent one of the terpene groups (sesquiterpene, diterpene and triterpene).
Cycloeudesmol (**132**), an antibiotic sesquiterpene, was reported from *Chondria oppositiclada* (Fenical and Sim, 1974). It showed strong antibacterial activity against gram negative bacteria (Sims et al., 1975). The diterpene, ent-13-epiconcinndiol (**133**) was produced by *C. tenussima* (Oztunc et al., 1989). This *Chondria* diterpene is closely related to other groups of labdane type bromoditerpenes that include concinndiol, aplysin-20 and isoconcinndiol isolated from red algae from the genus *Laurencia* and sea hares. On the other hand, triterpenes produced *by C. armata* have a different carbon skeleton from those groups isolated from *Laurencia*.

The bromotriterpene polyethers include bromotriterpene polyethers armatol A-F (**134-139**) isolated from the Indian Ocean *Chondria armata* (Ciavatta et al., 2001) and two further armatols isolated from an Australian specimen (Agrawal and Bowden, 2007). Although the absolute stereochemistry for one centre of armatol A was obtained using Mosher methodology, no evidence is presented in that report to correlate the relative stereochemistry for one ring system with the others and the stereochemistry of the tertiary centre on the uncyclised portion remained undetermined. The crude extract that contained armatols A-F showed antiviral, antibacterial and antifungal activity. Cytotoxic activity from *Chondria* polyethers was first reported for armatols (**140**) and (**141**). They have shown moderate cytotoxic effect against the mouse lymphoma cell line, P388D1, with IC_{50} values of 6.3 and 5.8 μg /mL respectively.

The stereochemistries postulated for these latter two armatols were only relative stereochemistry, determined by NMR from NOESY correlations; the absolute stereochemistries remained undetermined.

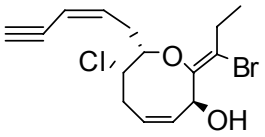

chondriol (**131**)

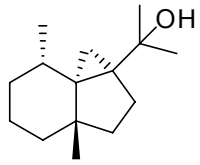

cycloeudesmol (**132**)

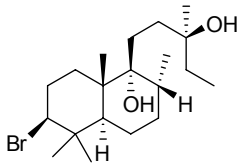

ent-13-epiconcinndiol (**133**)

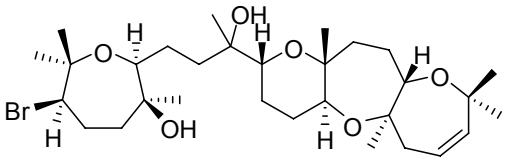

armatol A **(134)**

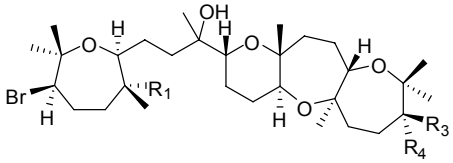

armatol B (**135**) R_1=Me, R_2= OH, R_3=H, R_4=Br

armatol C (**136**) R_1=OH, R_2=Me, R_3=H, R_4=Br

armatol D (**137**) R_1=Me, R_2=OH, R_3=Br, R_4=H

armatol E (**138**) R_1=OH, R_2=Me, R_3=Br, R_4=H

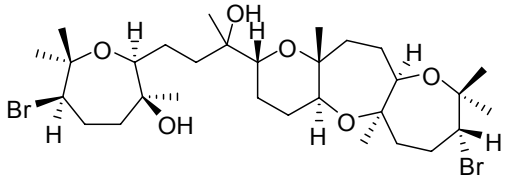

armatol F (**139**)

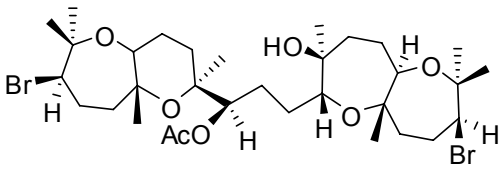

(**140**)

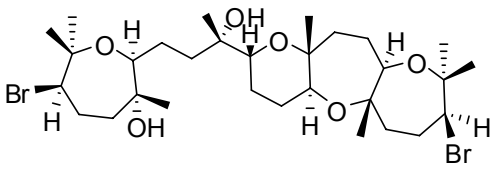

(**141**)

CHAPTER 2

Results and Discussion

2.1 Results and discussion of metabolites isolated from the red alga *Chondria armata*

2.1.1 C_{15} ACETOGENINS

2.1.1.1 (-) (Z) Pinnatifidenyne (142)

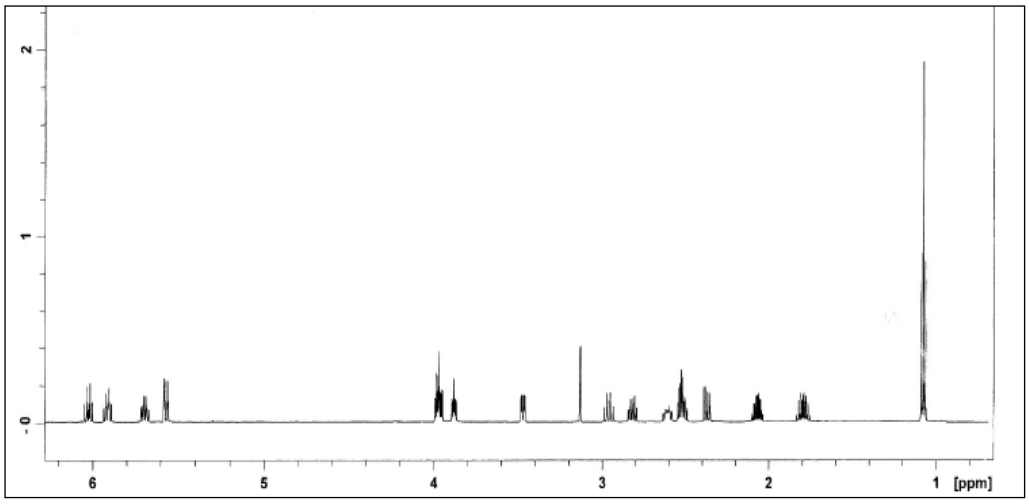

Figure 1. ^{1}H NMR spectrum of (-) (*Z*)-pinnatifidenyne (**142**) at 600 MHz in $CDCl_3$

A C_{15} acetogenin was purified through HPLC separation and was isolated as a colourless oil. This compound was identified as (-) (*Z*)-pinnatifidenyne by comparison of its ^{1}H and ^{13}C NMR spectra with previously reported data (Gonzales et al., 1982 and Norte et al., 1991) as well as by 2D NMR techniques (HSQC, HMBC and COSY). The ^{1}H NMR spectrum (Figure 1) exhibited signals for a terminal methyl group (δ 1.08, 3H, t, J = 7.3 Hz, H_3-15), four olefinic protons (δ 5.57, 5.69, 5.91 and 6.02), an acetylenic proton (δ 3.13, d, J = 2.3 Hz), two protons on oxygenated carbons (δ 3.47 and 3.88), two protons on halogenated carbons (δ 3.97 and 3.98) and four methylenes (δ 1.79-2.96, 8H).

The ^{13}C NMR spectrum exhibited 15 carbon signals attributed to one methyl, four methylenes, one quaternary carbon and nine methine carbons. All the protonated carbons were assigned using an HSQC experiment. Two olefinic proton signals that appeared at δ 5.69 (ddd J =12.1, 10.2, 6.5, 1.8 Hz) and δ 5.91 (dddd J = 10.2, 8.3, 7.2, 1.1 Hz) corresponded to the double bond carbon signals at 128.8 (C-9) and 130.9 (C-10) ppm respectively. Another pair of olefinic protons observed at δ 5.57 (H-3) and 6.02 (H-4) were assigned to another pair of double bond carbon at 111.0 (C-3) and 140.9 (C-4) ppm respectively. Carbon signals at 61.0 and 64.9 ppm were assigned to a bromomethine carbon and a chloromethine carbon which corresponded to the two methine proton signals at δ 3.98 (ddd J = 6.6 5.4, 3.0 Hz) and 3.97 (ddd J = 10.4, 5.1,

2.6 Hz) respectively. The methine signals at 79.7 and 83.4 ppm established the ether linkage between carbons C-6 and C-12 and the presence of an oxocane ring in the molecule was supported by long range HMBC correlations between H-6 (δ 3.88) and C-12 (83.4 ppm) and in turn between H-12 (δ 3.47) and C-6 (79.7 ppm). The assignments of these methine groups are in agreement with literature data for C_{15} acetogenins (Gonzales et al., 1982 and Norte et al., 1991).

The presence of a terminal conjugated enyne group was suggested by long-range $^{1}H–^{13}C$ (HMBC) correlation from the acetylenic proton at δ 3.13 (82.5 ppm, C-1) to the quaternary carbon C-2 (79.9 ppm) and C-3 (111.0 ppm). These correlations together with the correlations from the methylene protons (H-5) to the carbon signals at 111.0 and 140.9 ppm confirmed the locations C-3 and C-4 respectively. The magnitude of the coupling constant 10.8 Hz ($J_{3,4}$) and the chemical shifts of the two olefinic protons (δ 5.57 and 6.02) for H-3 and H-4 as well as the chemical shift value (δ 3.13) of the acetylenic proton indicated the geometry of the double bond at C-3 to be *Z* (Gonzales et al., 1982 and San-Martin et al., 1997). All data are in accordance with data for a C_{15} acetogenin *Z*-pinnatifidenyne and other related compounds (Gonzales et al., 1982 and Norte et al., 1991).

(-) Pinnatifidenyne (**142**)				
Position	δ C	δ H	Multiplicities (*J* in Hz)	HMBC
1	82.5	3.13	d (2.3)	C2,C3
2	79.9			
3	111	5.57	dd (10.8, 2.3)	C5
4	140.9	6.02	dt (10.8, 7.5)	
5a	34.9	2.83	dt (14.2, 7.9)	C3, C4, C7
5b		2.51	ddd (14.2, 7.6, 6.2)	C3, C4,C6
6	79.7	3.88	ddd (8.2, 5.7, 2.5)	C5, C12
7	64.9	3.97	ddd (10.4, 5.1, 2.6)	
8α	34.4	2.52	ddd (12.1, 4.2, 1.1)	C7, C9
8		2.96	ddd (12.7, 10.1, 1.1)	C10
9	128.8	5.69	dddd (12.1, 10.2, 6.5, 1.8)	C8, C11
10	130.9	5.91	dddd (10.3, 8.3, 7.2, 1.1)	C8, C11
11α	30.1	2.37	ddd (13.9, 8.4, 1.1)	C10, C12
11β		2.61	ddd (14.0, 10.2, 0.2)	C10, C12
12	83.4	3.47	ddd (10.2, 4.1, 3.0)	C6
13	61.0	3.98	ddd (6.6, 5.4, 3.0)	C12
14a	27.1	1.79	ddq (14.5, 10.1, 7.2)	C13
14b		2.07	ddq (14.5, 7.2, 3.4)	
15	12.8	1.08	t (7.3)	C13, C14

Table 1.^{1}H and ^{13}C NMR assignment for (-) *Z*-pinnatifidenyne (**142**) at 600 (^{1}H) MHz and 75 MHz (^{13}C) in $CDCl_3$

The NMR data of compound **142** (Table 1) were identical with those of *Z*-pinnatifidenyne isolated from *Laurencia pinnatifida* (Gonzales et al., 1982 and Norte et al., 1991) while the sign of the $[\alpha]_D$ value was opposite, suggesting that **142** should be the enantiomer of the literature compound. It is noteworthy that the (+) *Z*-pinnatifidenyne was isolated from a red alga in the Atlantic Ocean (Tenerife) while its enantiomer, (-) *Z*-pinnatifidenyne was produced by Australian red algae.

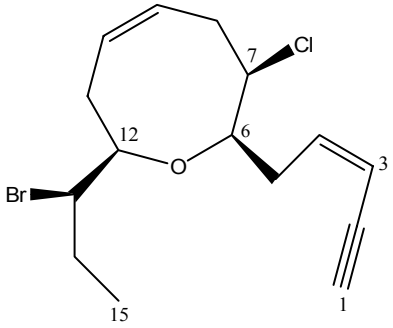

(-) Z-pinnatifydenyne (**142**)

2.1.1.2 (+) *Z*-laurenyne (**26**)

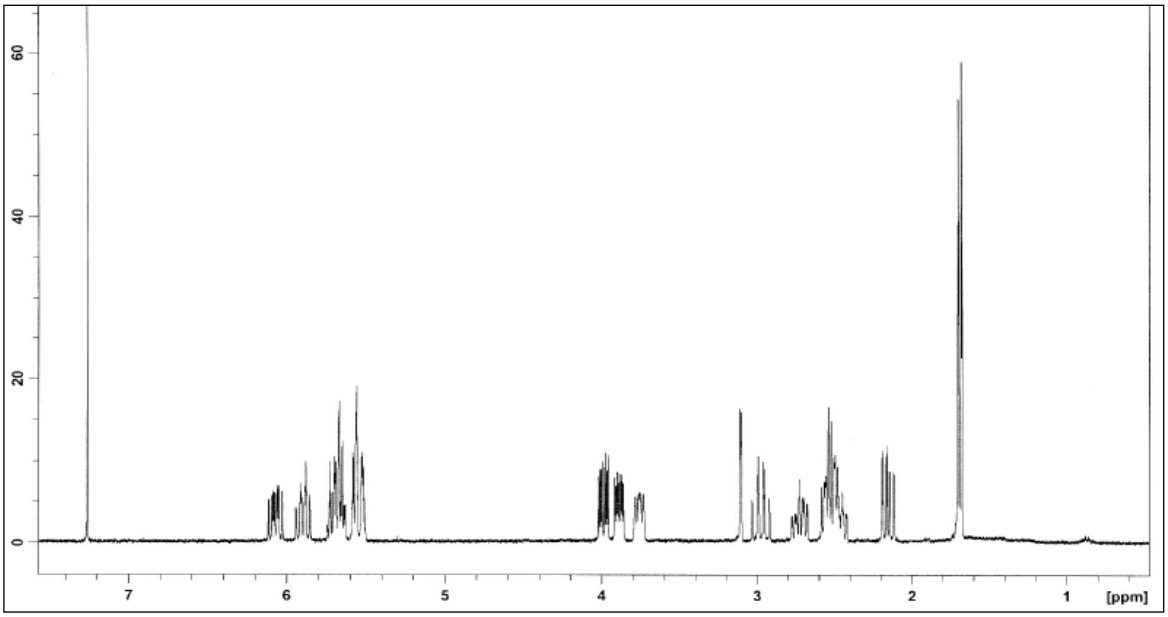

Figure 2. ^{1}H NMR spectrum of 3*Z*-laurenyne (**26**) at 600 MHz in $CDCl_3$

The second C_{15} acetogenin isolated was identified as (+) 3*Z*-laurenyne from the following spectral data. ^{1}H and ^{13}C NMR data suggest the presence of an 8-membered cyclic ether with α-propenyl and α'-pentenynyl side chains. The presence of an *E*-propenyl moiety was revealed by vinyl proton signals in the ^{1}H NMR spectrum (Figure 2) at δ 5.67 (1H, dqd, J = 15.3, 6.3, 1.2 Hz) and δ 5.55 (1H, ddq, J = 15.3, 6.2, 1.2 Hz) which were coupled to a methyl signal at δ 1.69 (3H, ddd, J = 6.3, 1.2, 1.0 Hz). The magnitude of coupling constant ($J_{13,14}$ = 15.3 Hz) between H-13 and H-14 indicated the geometry of the double bond at C-13 to be *E*. Moreover, the alkyne proton signal at δ 3.11 (1H, d, J = 2.2 Hz) and alkene methine proton signals at δ 5.54 (1H, m), and δ 6.07 (1H, dddd, J = 10.9, 8.7, 6.3, 0.9 Hz) provided evidence for the presence of 2-penten-4-ynyl side chain. The coupling constants ($J_{3,4}$=10.9 Hz) for H-3 and H-4 as well as the chemical shift value (δ 3.11) of the acetylenic proton were only compatible with a *Z* configuration for the double bond conjugated with the triple bond (Takahashi et al., 2002; San-Martin et al., 1997 and Gonzalez et al., 1982). Signals at δ 5.68 and δ 5.89 corresponded to an additional double bond between C- 9 and C-10.

The nature of a heteroatom substituent was readily recognized by correlating the assigned proton signals to the carbons chemical shifts in the HSQC experiment. Hence, the signal at δ 3.99 was from a proton attached to the carbon with chemical shift 65.2 ppm, so corresponded to a chloromethine proton. Furthermore, a correlation between the proton signal at δ 3.89 and

the carbon at 78.9 ppm and another correlation between the signal at δ 3.76 and the carbon with chemical shift 81.6 ppm indicated the presence of an ether bridge. These long range correlations confirmed the ether bridge between C-6 and C-12.

The comparison of spectral data of compound **26** with those reported by Takahashi et al 2002 for 3Z-laurenyne indicated that **26** had the same structure and stereochemistry. The assignments for C1 and C2 in the literature have been reversed (indicated by HSQC results) (Table 2).

Laurenyne (**26**)			
Position	δ C	δH	Multiplicities (J in Hz)
1	82.0*	3.11	d (2.2)
2	80.0*		
3	110.1	5.54	dddd (10.9, 2.2, 1.4, 1.0)
4	141.5	6.07	dddd (10.9, 8.7, 6.3, 0.9)
5a	35.2	2.72	dddd (14.4, 9.2, 6.2, 1.5)
5b		2.54	dddd (14.4, 8.7, 4.5, 0.9)
6	78.92	3.89	ddd (9.2, 4.4, 2.5)
7	65.2	3.99	ddd (11.4, 4.9, 2.5)
8α	34.4	2.97	dddd (12.5, 10.5, 10.2, 1.1)
8β		2.52	m
9	128.4	5.68	m
10	130.9	5.89	dddd (10.4, 8.3, 7.1, 0.9)
11α	34.7	2.47	dddd (14.1, 8.5, 7.1, 1.1)
11β		2.15	ddd (14.2, 8.5, 1.6)
12	81.6	3.76	br dd (8.9, 6.2)
13	131.9	5.55	ddq (15.3, 6.2, 1.2)
14	126.2	5.67	dqd (15.3, 6.3 ,1.2
15	17.6	1.69	ddd, (6.3, 1.2, 1.0)

Table 2. ^{1}H and ^{13}C NMR assignment for (**26**) (+) *Z*-laurenyne at 600 (^{1}H) MHz and 75MHz (^{13}C) in $CDCl_3$

* These assignments were reversed in the previous report (Takahashi et al., 2002)

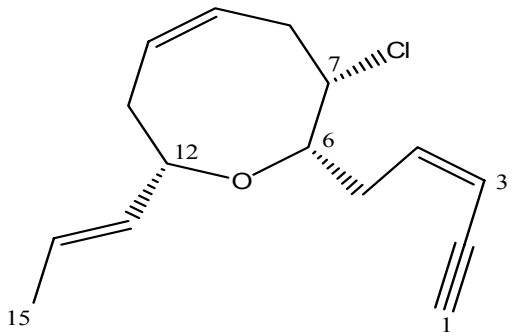

(+) Z-laurenyne (**26**)

2.1.1.3 (+)-3*Z*,6*R*,7*R*-obtusenyne (**27**)

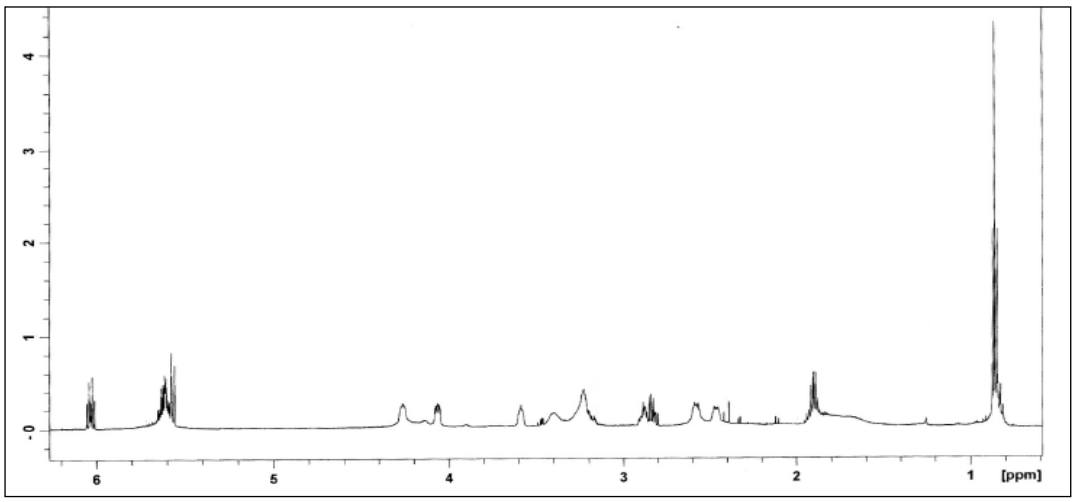

Figure 3. ^{1}H NMR spectrum of (+)-*3Z,6R,7R*-obtusenyne (**27**) 600 MHz in $CDCl_3$

The third C_{15} acetogenin isolated was identified as (+)-*3Z,6R,7R*-obtusenyne which was previously isolated from a South China Sea collection of the Opisthobranch *Aplysia dactylomela* Rang, 1828 (Manzo et al., 2005). It is interesting to note that this is the first isolation of (+)-*3Z,6R,7R*-obtusenyne from marine algae, which suggests that the mollusc may feed upon this or a similar alga.

Analysis of ^{1}H and ^{13}C NMR spectra confirmed the same enyne-containing side chain observed in **Z**-pinnatifidenyne and indicated the presence of a nine-membered cyclic ether skeleton. Comparison of the spectral data of compound **27** with those reported by Norte et al. (1991) and Manzo et al., (2005) for obtusenyne indicated that **27** had the same structure. However, neither of the previous reports identified the ^{13}C chemical shift of C-2. Based on the ^{13}C NMR spectrum we confirmed that C-2 has the chemical shift 79.8 ppm. The assignment was supported by HMBC long-range ^{1}H–^{13}C correlations from the alkyne proton H-1 (δ 3.16) and from methine protons H-3 (δ 5.56) and H-4 (δ 6.03) to a carbon with the chemical shift 79.8 ppm.

The other assignment difference was for the double bond carbons C-9 and C-10. Based on a long-range HMBC correlation between the H-12 proton at δ 4.25 and double bond carbon signal at 128.4 ppm, we suggest the assignment for C-10 should be 128.4 ppm. No correlation was observed from this methine proton (δ 4.25, H-12) to the other alkene carbon signal (129.9 ppm). This is also supported from the correlations observed between the H-8 methylene proton at δ 2.46 to the double bond carbon (129.9 ppm) and in turn from the methine proton (δ 5.62, H-

9) to C-8. Thus, we suggest that assignment for C-9 and C-10 should be 129.9 ppm and 128.4 ppm respectively. The two double bond carbons were reverse in both of the previous reports (Norte et al., 1991 and Takahashi et al., 2005).

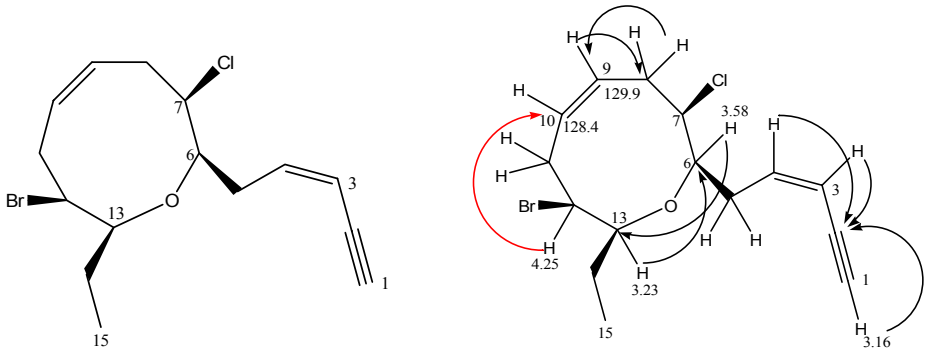

Figure 4. Structure and selected HMBC correlations of (+)-3*Z*,6*R*,7*R*-obtusenyne (**27**)

3*Z*,6*R*,7*R*-obtusenyne from *Chondria armata* has a (+) $[\alpha]_D$ value while the Tenerife alga, *Laurencia pinnatifida*, produced the acetogenin with the opposite value. It is noteworthy that this is the second example of metabolites produced by Atlantic Ocean *Laurencia* where the enantiomer now has been isolated from *Chondria armata* from the South Pacific Ocean.

Obtusenyne (**27**)				
Position	δ ^{13}C	δ ^{1}H	Multiplicities (J in Hz)	HMBC
1	82.2	3.16	d (2.8)	C2, C3
2	79.8			
3	111.2	5.56	dd (10.8)	C1,C2, C4, C5
4	140.1	6.03	dt (10.8, 7.1)	C2,C3,C5,C6
5a	34.5	2.83	m	C3, C6, C7
5b		2.87	m	C3, C4, C7
6	80.9	3.58	m	C5, C8,C13
7	62	4.06	ddd (10.4, 5.5, 3.3)	C8
8α	33.4	2.46	m	C7, C9, C 10
8β		3.25	m	
9	129.9	5.62	m	C8
10	128.4	5.61	m	
11α	34.2	2.58	m	C9, C10,C12
11β		3.40	m	
12	54.5	4.25	m	C11
13	83.5	3.23	m	
14	27.5	1.89	m	C6,C12,C13, C15
15	9.68	0.86	t (7.5)	C13, C14

Table 3. ^{1}H and ^{13}C NMR assignment for (+)-3*Z*,6*R*,7*R*-obtusenyne (**27**) at 600 (^{1}H) MHz and 75 MHz (^{13}C) in $CDCl_3$

2.1.2 Brominated Diterpenes

2.1.2.1 (-) Angasiol (143)

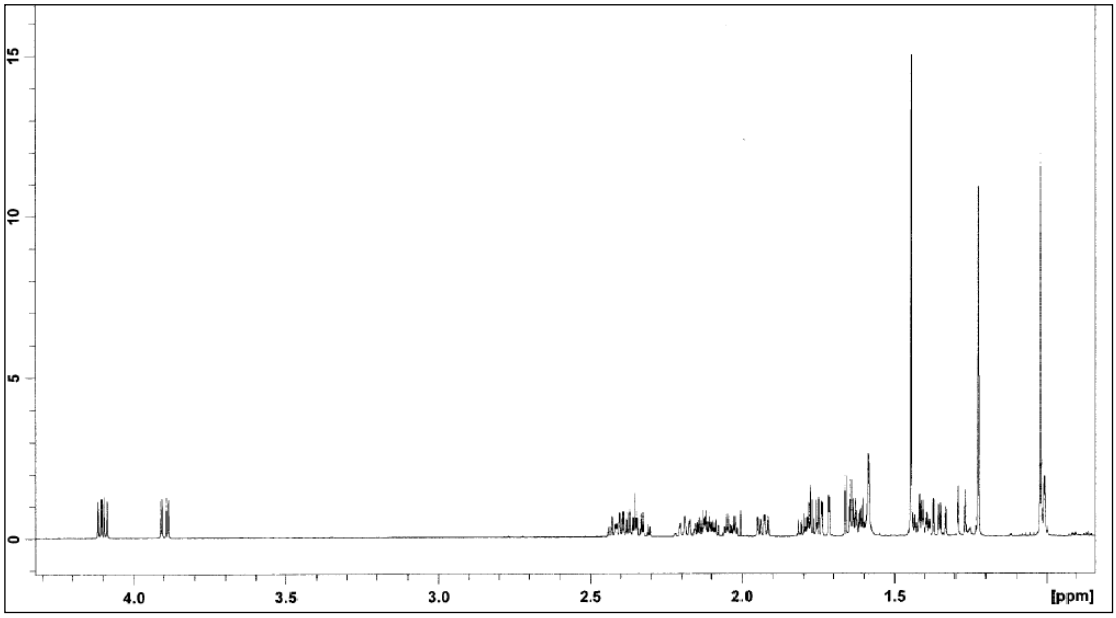

Figure 5. ^{1}H NMR spectrum of (-) angasiol (**143**) at 600 MHz in $CDCl_3$

Angasiol, mp 190-192, $[\alpha]_D^{22}$ -5.9°C (*c.* 0.24 in $CHCl_3$) was isolated as a white crystalline compound. The molecular formula of angasiol was established as $C_{20}H_{30}Br_2O_3$ on the basis of $[M+Na]^+$ and $[M - HBr + Na]^+$ ions in the ESI positive ion spectrum and also supported by its ^{13}C NMR data. The dibrominated nature of the compound was readily recognised from the $[M+Na]^+$ ion peaks, which showed intensities of 1:2:1. The presence of a hydroxyl group was evident from a hydroxyl stretch at 3501 cm^{-1} in the IR spectrum while the band at 1762 cm^{-1} in the IR spectrum indicated the presence of the ester carbonyl group. The ^{13}C NMR spectrum accounted for 20 carbons and the protonated carbons were all assigned using an HSQC experiment. The presence of an ester carbonyl was indicated by the signal at 176.7 ppm in the carbon spectrum. The carbon spectrum also showed that six carbons (with signals at 83.7, 72.6, 65.4, 63.5, 61.7 and 51.6 ppm) were bonded to electronegative heteroatoms or at bridgehead positions. Furthermore, the ^{1}H NMR spectrum showed two signals due to two bromomethine protons at δ 3.90 (1H dd 12.7, 3.8 Hz) and 4.10 (1H dd 11.9, 6.0 Hz), two methine proton at δ 1.65 (1H br d 9.7 Hz) and δ 2.19 (1H, ddddd 10.4, 9.7, 8.7, 8.6, 1.1 Hz) and eight methylene groups at δ 1.28-2.42 (16 H). Further analysis of the ^{1}H NMR spectrum revealed three tertiary methyl groups (singlets at δ 1.02, δ 1.23 and δ 1.45).

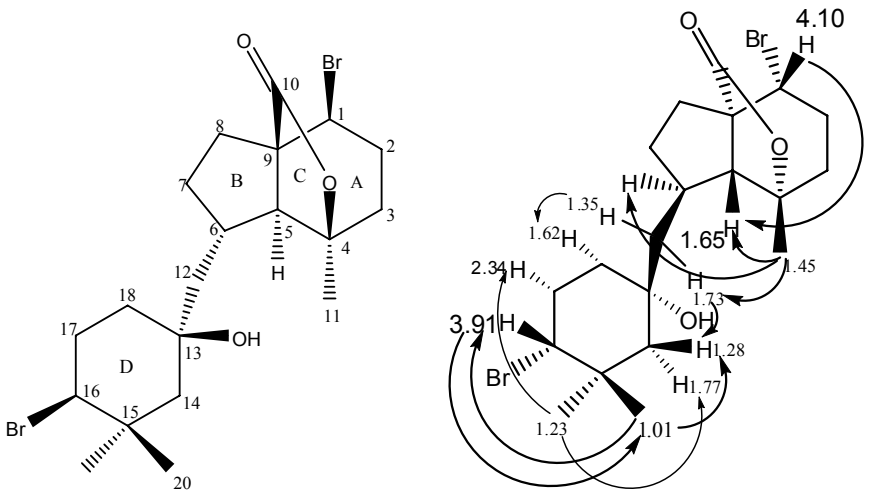

Figure 6. Structure of angasiol (**84**) and selected NOESY correlations of (-)-angasiol (**143**)

With an unsaturation degree of 5, in addition to the carbonyl group the structure contained four rings. Selective gradient TOCSY and COSY experiments on the two bromomethine protons (δ 3.90 and δ 4.11) allowed assignments for the protons on the two brominated rings. The bromomethine proton signal at δ 4.10 (H-1) was coupled to two methylene groups: H-2 protons (δ 2.42 and δ 2.10) and H-3 protons (δ 1.63 and δ 1.93). The sequence of this spin system was elucidated from a COSY experiment. In the COSY spectrum, the signal resonating at 4.10 (H-1) correlated with the methylene protons at δ 2.42 and 2.10 (H_2-2) which in turn was linked to another methylene signals at δ 1.63 and δ 1.93 (H_2-3).

In a selective gradient TOCSY experiment, the bromomethine proton signal at δ 3.90 (H-16) showed weak correlations with the H-14 protons (δ 1.77 and 1.28) in addition to correlation with the H_2-17 (δ 2.04 and δ 2.34) and H_2-18 (δ 1.62 and δ 1.42). The sequence was deduced from a COSY experiment. Thus, the signal at δ 3.90 (H-16) was coupled to the methylene signals at δ 2.34 and δ 2.04 which in turn showed correlations to another set of methylene signals at δ 1.62 and δ 1.42 (H_2-18). Another selective gradient TOCSY experiment showed that the methine proton signal at δ 2.19 (H-6) was in a spin system that contained the methine H-5 (δ 1.65), the methylene protons with signals at δ 1.41, 2.12 (H_2-7), 1.79, 2.37 (H_2-8) and also 1.73 and 1.35 (H_2-12). A COSY experiment was used to elucidate the sequence for these protons.

After proton signal were assigned to their respective carbon atoms by an HSQC experiment (table 3), the spin systems were connected through analysis of long-range $^{1}H{-}^{13}C$ couplings indicated by the HMBC spectrum. Strong long range correlations were observed from the methyl signal at δ 1.45 (H_3-11) to the oxygenated carbon at 83.7 ppm (C-4) and signals at 38.2 (C-3) and 63.5 (C-5) ppm. This indicated that the methyl group was attached to the quaternary

carbon C-4 which was in turns flanked by a methine (C-5) and a methylene group (C-3). The presence of ring A was established based on the HMBC correlations between the methine proton at δ 1.65 (H-5) to the carbons C-9 (61.7 ppm), C-1 (51.6 ppm), C-3 (38.2 ppm) and C-6 (35.9) ppm. The HMBC correlations to C-9 from H-7β (δ 2.12) and the H-8 protons together with the TOCSY-derived connectivities support the presence ring B. The location of the carbonyl carbon (C-10) was confirmed from the HMBC correlations from H-1, H-5 and H-8.

Ring D was established on the basis of HMBC correlations from H-14β (δ 1.77) to the oxygenated carbon C-13 (72.6 ppm) and C-18 (39.9 ppm) and correlations from H-14α to the quaternary carbon C-15 (36.7 ppm). The strong HMBC correlations between H_3-19 (δ 1.01) and H_3-20 (δ 1.23) to the quaternary carbon at 36.7 ppm indicated that these two methyls were attached to C-15. The mutual HMBC correlations observed between these two methyls and the long range correlations to the bromomethine carbon at 65.4 ppm (C-16) together with the TOCSY-derived connectivites completed the linkages required for ring D. Ring D connected to ring B through the methylene (H-12) based on the HMBC correlations from the methylene protons (H-12) to C-6, C-7, C-13, C-14 and C-18. The fourth ring would be provided if the carbonyl group was linked as an ester to either C-4 or C-13. A search of the literature revealed that linkage at C-4 would correspond with the structure of the known γ-lactone angasiol. Based on the very similar NMR spectral data the isolated diterpene was assumed to be identical with the reported angasiol (Petit et al., 1978) and NOESY experiments were carried out to confirm the stereochemistry.

The strong NOESY effect between H-1 (δ 4.11) and H-5 (δ 1.65) showed the axial orientation of these protons. Irradiation of H_3-11 (δ1.45) induced NOESY correlations to H-3β (δ 1.93), H-3α (δ 1.63), H-5 (δ 1.65), H-2α (δ 2.42), H-6 (δ 2.19) and H-12b (δ 1.73), which indicated the equatorial configuration for the H_3-11 methyl group on the brominated six-membered ring. Moreover, the NOESY correlation between H_3-11 (δ 1.45) and H-12b (1.73) suggested the likely orientation of the C-12 methylene bridge. The magnitude of coupling constant 9.7 Hz between H-6 and H-5 (δ 1.65) revealed the *trans* di-axial arrangement between H-5 and H-6.

The NOESY correlation between H-12b (δ 1.73) and H-14α (δ 1.28) together with the NOESY correlations from H-12a to H-18β (δ 1.62), H-5 (δ 1.65) and H-7β (δ 2.12) was used to orient the C-12 bridging methylene group with respect to the B and D rings. In addition, the observed mutual NOESY correlations between H-14α (δ 1.28) and H-16 (δ 3.90), H-14α and H_3-19 (δ 1.01) as well as between H_3-19 and H-16 (δ 3.90) indicate axial configuration of the these protons (the methyl at δ 1.01 is equatorial). Meanwhile, the NOESY effects between H-14β (δ

1.77) and H_3-20 (δ 1.23), H-17α (δ 2.34) and H_3-20 (δ 1.23) as well as between H-17α (δ 2.34) and H-18α (δ 1.62) distinguish the groups on the α and β faces of the ring.

These 1D NOESY and 1D ROESY correlations confirm that the relative stereochemistry for all chiral centres were the same as those reported for angasiol (Petit et al., 1978) and supported by an X-ray crystal structure, however, it should be noted that based on our 2D-NMR experiment (COSY, HSQC and HMBC), the reported NMR data of angasiol should be reassigned (see table 4).
No optical rotation was reported by Petit, but the absolute stereochemistry provided by an x-ray structure provided the same absolute stereochemical result as that subsequently reported for (+)-angasiol acetate (Atta-Ur-Rahman et al., 1991).

Because (-)-angasiol (**143**) and (-)-angasiol acetate (**144,** see discussion on following pages) produced from this *Chondria* both exhibit negative specific optical rotations and would be expected to have the same absolute stereochemistry, it is presumed that both the (-)-angasiol and the (-)-angasiol acetate isolated in this study are enantiomeric with angasiol and (+)-angasiol acetate previously reported.

2.1.2.2 (-)-**Angasiol acetate (144)**

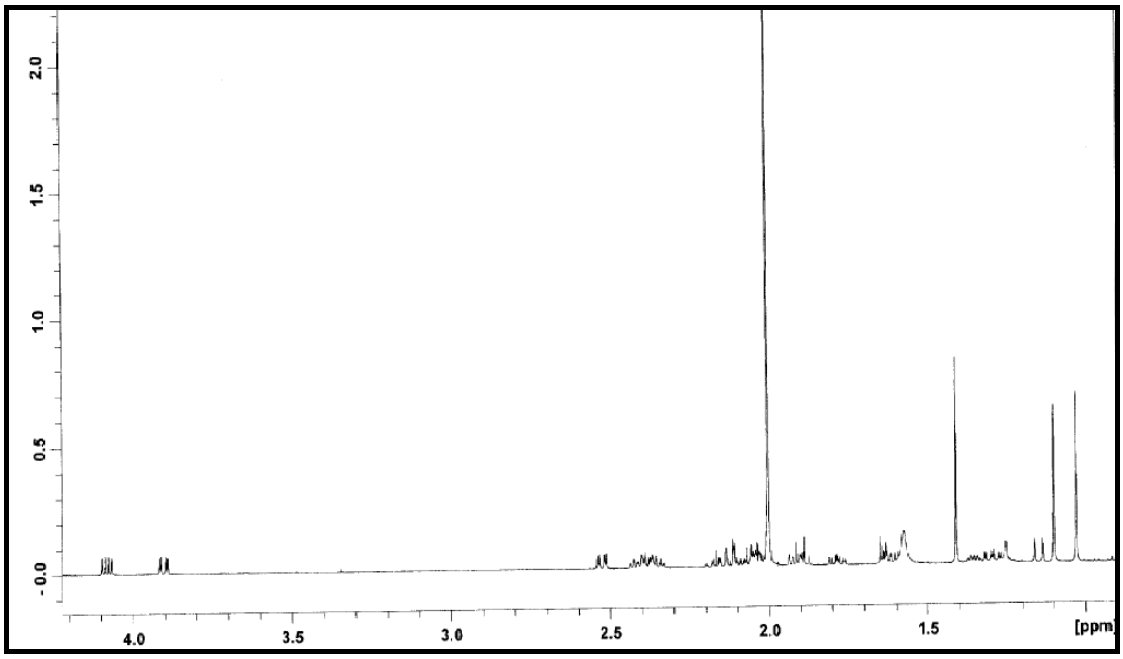

Figure 7. ^{1}H NMR spectrum of (-)-angasiol acetate **(144)** at 600 (^{1}H) MHz in $CDCl_3$

Angasiol acetate, $[\alpha]_D^{22}$ -2.5°C (*c.* 0.19 in $CHCl_3$), was obtained as a white crystalline solid. The opposite sign for the specific optical rotation of the isolated angasiol acetate to that reported by Atta-ur-Rahman et al., 1991 indicates that the isolated compound is the enantiomer, so its structure is *ent*-angasiol acetate (**143**). Both ^{13}C NMR data and ESI-MS measurement supported the molecular formula $C_{22}H_{32}Br_2O_4$, indicating six degree of unsaturation. The ESI-MS (positive mode) spectrum showed an ion cluster at *m/z* 541, 543 and 545 ($M+Na^+$) with the intensities 1:2:1, thus the presence of two bromine atoms in the molecule was indicated. The ^{1}H NMR spectrum displayed signals for two bromomethine protons at δ 3.90 (1H dd 12.6, 4.0 Hz) and 4.08 (1H dd 11.8, 5.9 Hz), two methine protons at δ 1.64 (1H br d), δ 2.05 (1H m), eight methylene groups between δ 1.14-2.52 (16 H), three quaternary methyl groups at δ 1.03, 1.10, 1.41 and an acetate methyl signal at δ 2.00. The ^{13}C NMR data and HSQC accounted for 22 carbon atoms: four methyl groups, four methines, eight methylenes, four quaternary carbons and two ester carbonyl groups.

Comparison of the spectral data of **144** with those of **143** revealed a great similarity in the structures of the two compounds and suggested an acetate derivative. Selective gradient TOCSY, COSY and HSQC experiments allowed assignments to identify spin systems of the

molecule. Selective gradient TOCSY experiments on two bromomethine protons, when combined with COSY data, enabled assignments to identify the spin systems at both six-membered brominated rings of angasiol acetate. H-1 (δ 4.08) was linked to a pair of methylene protons at H_2-2 (δ 2.10 and δ 2.41) and at H_2-3 (δ 1.62 and δ 1.92). The selective gradient TOCSY experiment on the other bromomethine proton (δ 3.90 H-16) indicated that it was part of a spin system that included three methylene groups (H_2-14: δ 1.14 and δ 2.52, H_2-17: δ 2.05 and δ 2.16, and H_2-18: δ 2.38 and δ 1.29). In the COSY spectrum, H-16 showed correlations with signals at δ 2.16 and δ 2.05 (H_2-17) which in turn were coupled to signals at δ 1.29 and 2.38 (H_2-18). The last spin system was identified by a selective gradient TOCSY experiment on the H-7β proton signal (δ 1.35). The H-7β (δ 1.35) was linked to H-7α (δ 2.04), two methine protons at δ 1. 64 (H-5) and δ 2.05 (H-6) and two methylene groups: H_2-8 (δ 1.78 and δ 2.35) and H_2-12 (δ 1.90 and δ 2.12).

The HMBC experiment allowed the spin systems to be connected with quaternary carbons bearing the methyl groups. Strong HMBC correlations from both H-8α (δ 2.35) and H-1 (δ 4.08) to the carbon resonating at 176.8 ppm confirmed the position of γ-lactone carbonyl at C-10. The other bromomethine proton (δ 3.90) was located at C-16 based on the strong HMBC correlations from the two tertiary methyl groups, H_3-20 (δ 1.10) and H_3-19 (δ 1.03) to the carbon resonating at 64.6 ppm (C-16). The HMBC correlations from H-2α (δ 2.41), H-3α (δ 1.92) and H_3-11 (δ 1.41) to the carbon at 83.6 ppm confirmed that this oxygenated carbon was positioned at C-4 and that the tertiary methyl group H_3-11 was attached to C-4. Since there was no OH group, an ester bridge should connect C-4 and C-10 as they were the only oxygenated carbon atoms located in the immediate vicinity of these two spin systems.

The stereochemical configuration of the chiral centres was resolved by a combination of NOESY data and analysis of coupling constants. Irradiation of bromomethine proton at δ 4.08 induced NOESY correlations to the H-3β (δ 1.62), H-5 and H-8β (δ 1.78) signals. This established the axial configuration of H-1, H-5 and H-3β. H-8β exerted NOESY enhancement on H-7β (δ 1.35), H-12β (δ 1.90) and H-1. The coupling constant of 9.5 Hz between H-6 and H-5 (δ 1.65) indicated the *trans* di-axial arrangement between H-5 and H-6.

The NOESY correlations between the methyl group signal at δ 1.41 (H_3-11)/H-5, H_3-11/Ha-12 (δ2.12), H_3-11/H-3α and H_3-11/H-3β revealed the equatorial orientation for the methyl on the brominated six-membered ring. Moreover, additional NOESY interactions between the methyl at δ 1.41 (H_3-11) and H-14β (δ 1.14) revealed the relative orientations of the two ring systems.

Thus, NOESY effects between H-14β/H-16 (δ 3.90) and H-14β/H_3-20 (δ 1.03) suggested axial positions for of H-16 and the methyl (H_3-19) on the second brominated six-membered ring.
The irradiation of the methyl at δ 1.10 (H_3-19) induced positive signal at δ 2.52 (H-14α) and at δ 2.16 (H-17 β), thus suggested the axial orientation for the methyl (H_3-19) and the H-17α proton. The NOESY interaction between H-16 and H-18β (δ 1.29) indicated the axial orientation of H-18 β..

The spectral data and NOESY data supported the identification as angasiol acetate. However, the assignments of the two bromomethine protons were interchangeable in the previous report (Atta Ur Rahman et al., 1991). Moreover, based on the HMBC and HSQC experiments, the assignments for the four methyl groups of (+) angasiol acetate in the first report should be reassigned.

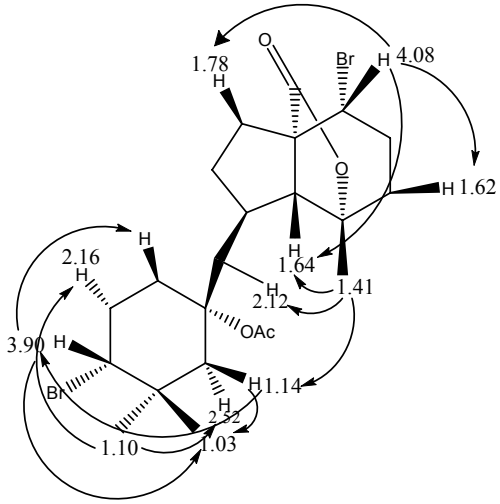

Figure 8. Selected NOESY correlations of (-)-angasiol acetate (**144**)

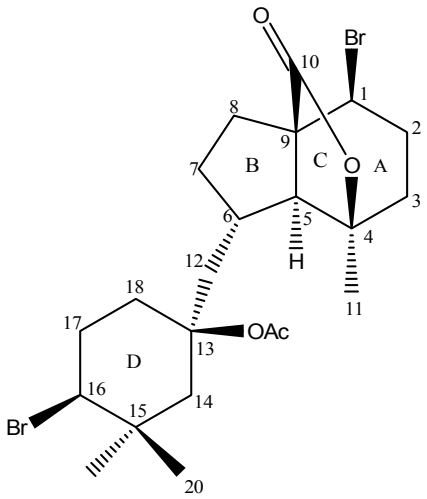

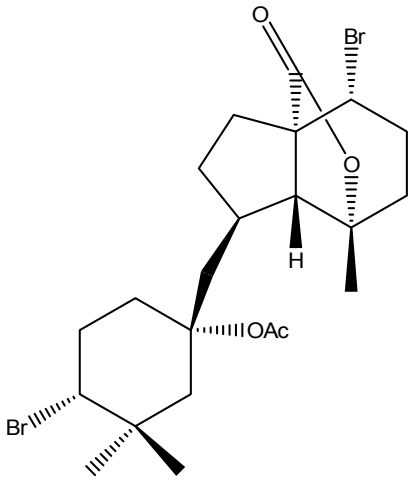

(85) (+)-angasiol acetate (**144**) = *ent*-(**85**), (-)-angasiol acetate

(-)-Angasiol (**143**)					
No	$\delta^{13}C$	$\delta^{1}H$	Multiplicities (Hz)	Selected NOESY	HMBC
1	51.6	4.10	dd 11.9, 6.0	H-2α, H-2β, H-3β, H-8α, H-5	C2, C5, C9,C10
2α	32.9	2.42	dtd 14.6, 6.1, 1.1	H-1, H-3β	C1, C3, C4, C9
2β	32.9	2.10	dddd 14.6, 12.4, 11.8, 6.8	H-1,	C1, C3
3α	38.2	1.63	ddd 14.1, 12.4, 6.1	H_3-11, H-2β, H-1	C2
3β		1.93	ddd 14.1, 6.8, 1.1		C2, C4,C5, C9, C-11
4	83.7				
5	63.5	1.65	br d 9.7	H-1	C1, C3, C6, C9, C10
6	35.9	2.19	br ddddd 10.4, 9.7, 8.7, 8.6, 1.1	H-5, H_3-11, H-12b	C4, C5, C12, C13
7α	32.1	1.41	m		
7β		2.12	dddd 13.1, 9.3, 8.7, 5.3		C6, C9
8α	31.7	1.79	dddd 14.1, 11.5, 5.5, 0.4		C9, C10
8β		2.37	br ddd 14.1, 9.3, 5.8		C1, C9, C10
9	61.7				
10	176.7				
11	21.3	1.45	s	H-3β, H-12b	C3, C4, C5
12a	51.4	1.35	dd 14.2, 10.4	H-7β, H-5, H-18β, H-18α	C6, C7, C13, C14, C18
12b		1.73	dd 14, 1.7	H-6, H_3-11	
13	72.6				
14α	50.0	1.28	dd 14.4, 0.5		C15, C19
14β		1.77	dd 14.5, 3.5		C13, C18
15	36.7				
16	65.4	3.90	dd 12.7, 3.8	H_3-19, H-17β, H-14α, H-18β	C19,C20
17α	30.4	2.34	tdt 13.5, 13.5, 12.7, 3.8	H-17β, H_3-20, H-14β, H-18α	C-16
17β		2.04	dddd 13.5, 4.0, 4.0, 3.3		
18α	39.9	1.62	ddd 14.1, 3.5, 3.5		
18β		1.42	m		
19	32.7	1.01	s	H16, H-14α, H-14β, H_3-20	C14, C16, C20
20	22.8	1.23	s	H-17α, H-14β, H_3-19	C14, C15, C16, C19

Table 4. NMR data for (-)-angasiol (**143**) at 600 (^{1}H) MHz and 75 MHz (^{13}C) in $CDCl_3$

(-)-Angasiol acetate (**144**)					
No	δ ^{13}C		δ ^{1}H	Selected NOESY	HMBC
1	51.5	4.08	dd 11.8, 5.9	H-3β, H-5, H-8β	C10, C9
2α	32.9	2.41	m		C1, C4
2β		2.10	m		C1
3α	38.2	1.92	m	H_3-11	C1, C2, C4
3β		1.62	ddd 14.0, 12.5, 6.1	H-8β, H_3-11	C1, C2, C11
4	83.6				
5	63.6	1.64	br d 9.5		C1, C11
6	36.7	2.05	m		
7α	31.0	2.04	m	H-7β, H-8α, H-8β	C6
7β		1.35	m	H-8β	
8α	31.5	2.35	m		C1, C9, C10
8β		1.78	m	H-1, H-8β, H-7α, H-7β, H-12β	C1, C10
9	61.5				
10	176.8				
11	21.3	1.41	s	Hα-12, H-3α, H-3β, H-5, Hα-13	C3, C4, C5
12a	44.3	2.12	dd 14.4, 1.4		C5, C11, C13
12b		1.90	dd 14.4, 7.0	H-8β	C4, C5
13	82.9				
14α	46.7	2.52	d 14.7	H-14β, H-16, H_3-20	C19, C20
14β		1.14	dd 14.7, 3.6	H-12a, H-14α, H_3-19, H_3-20	C13, C15
15	36.2				
16	64.6	3.90	dd 12.6, 4.0		C19, C20
17α	30.3	2.16	m		
17β		2.05	m		C13
18α	37.3	2.38	m		
18β		1.29	ddd 14.0, 14.0, 3.9		
19	21.9	1.10	s	H-14α, H-17α, H_3-20	C16
20	32.5	1.03	s	H-14α, H-14β, H-16, H_3-19	C16
OAc	22.9	2.01	s		C=O
C=O	171.0				

Table 5. NMR data for angasiol acetate (**143**) at 600 (^{1}H) MHz and 75 MHz (^{13}C) in $CDCl_3$

2.1.3 Halogenated Triterpene Polycylic Ethers

2.1.3.1 Armatol G (145)

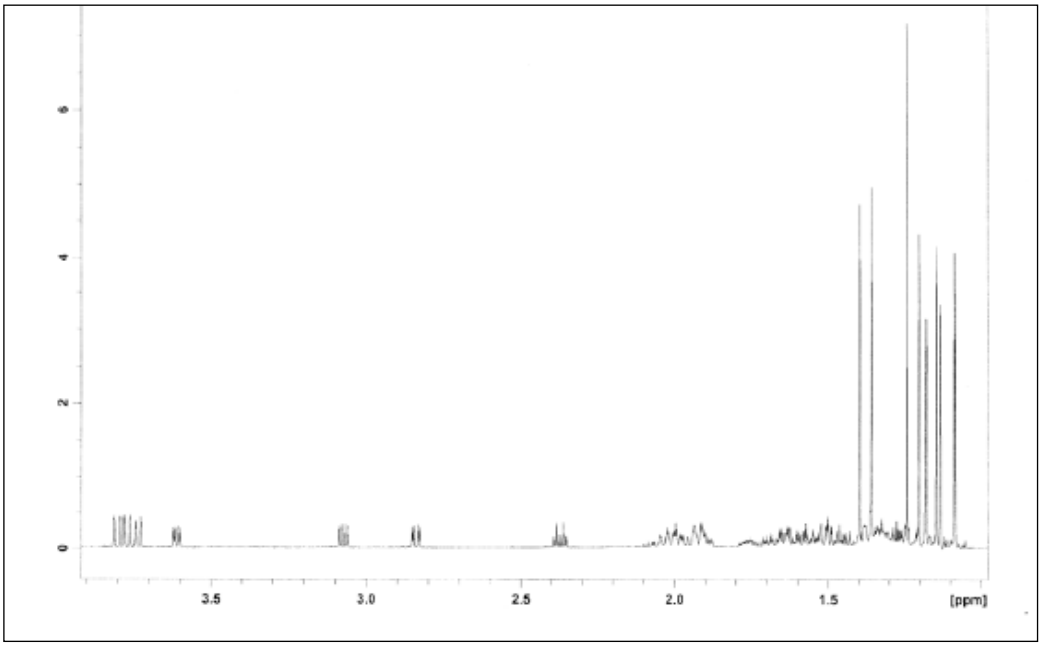

Figure 9. ^{1}H NMR spectrum of armatol G (**145**) at 600 MHz in C_6D_6

Seven new halogenated triterpene polycyclic ethers: armatol G, H, I and J together with aplysiol C, D and E were isolated from a freeze dried sample of *Chondria armata* collected at Hazard Bay, Orpheus Island. The freeze dried material was extracted with methanol and partioned between water and dichloromethane. The dichloromethane soluble fraction of the methanol extract was fractionated by vacuum liquid chromatography over silica gel and the further subjected to purification with HPLC (Phenomenex, Luna C-18 column) to afford the seven new polycyclic ethers.

Armatol G was isolated as a white solid, mp 184-186, $[\alpha]_D^{22}$ +58.7^{o}C (*c.* 0.08, $CHCl_3$) and the molecular formula $C_{30}H_{52}Br_2O_6$ was established on the basis of its molecular ion and from ^{13}C NMR spectral data. The presence of two bromine atoms was suggested by the characteristic 1:2:1 pattern of the molecular ion in the ESI positive ion mass spectrum and by two resonances at 60.7 and 60.2 ppm in the carbon spectrum. The ^{1}H NMR spectrum in C_6D_6 revealed signals for the presence of eight methyl groups at δ 1.20, 1.15, 1.40, 1.13, 1.24, 1.09, 1.18 and 1.36, four oxygenated methines at δ 3.07 (dd, 11.1, 5.3 Hz), 3.73 (dd, 10.3, 1.5Hz), 3.61 (dd, 9.5, 3.2 Hz) and 2.84 (dd, 11.3, 3.0 Hz), two bromomethines at δ 3.80 (dd, 11.1, 1.0 Hz) and 3.77 (brd, 10.7 Hz) and ten methylenes. The ^{13}C NMR spectrum accounted for thirty carbon atoms and the protonated carbons were all assigned using an HSQC experiment (Table 6). Spectral data was

indicative of a triterpene polycyclic ether, so an acetylation was undertaken to establish the nature of any alcohol functionality. This resulted in a mono-acetylated product where the proton signal that was formerly at δ 3.73 shifted downfield. Thus, a secondary alcohol was indicated.

Analysis of selective gradient TOCSY and COSY data together with HSQC data of the six methine protons enabled assignments to identify five sub units within the molecule. Selective gradient TOCSY experiments on two bromomethine protons (δ 3.80 and 3.77) allowed assignments of the protons on two brominated rings A and D. The bromomethine proton at δ 3.80 (H-3) showed correlations with the H-4 protons (δ 2.0 and 1.92), H-5 protons (δ 1.58 and 1.36) and H_3-26 (δ 1.13), while the bromomethine proton at δ 3.77 (H-22) correlated with the H-21 protons (δ 2.03 and 1.89), H-20 protons (δ 1.63 and 1.38) and H_3-29 (δ 1.18). Three additional sub units were established based on data from the other four methine protons. A gradient selective TOCSY experiment on the methine proton at δ 3.07 (H-7) induced positive signals for the H-8 protons (δ 1.69 and 1.45) and H-9 protons (δ 2.37 and 1.26). Irradiation of signal at δ 3.73 (H-11) induced positive signals for the H-12 protons (δ 1.98 and 1.54), H-13 protons (δ 1.76 and 1.63) and the methine proton at δ 3.61 (H-14). The same signals were produced by irradiation at δ 3.61 (H-14). The last sub unit of the molecule was identified based on the TOCSY data from the H-18 proton (δ 2.84). Thus, the methine proton signal at δ 2.84 showed correlations with the H-17 protons (δ 1.92 and 1.32) and the H-16 protons (δ 1.50). The sequence of methylene groups within the TOCSY spin systems was elucidated from a COSY spectrum. Therefore, selective gradient TOCSY and COSY experiments enabled five spin systems within the molecule to be identified: C3—C6—C26, C7—C9, C11—C14, C16—C18 and C29—C19—C22.

Furthermore, HMBC and NOESY data enabled these sub units to be linked. An HMBC correlation between H-7 (δ 3.07) and C-2 (77.9 ppm) showed the presence of the ether ring A and this was confirmed by NOESY cross peak from H_3-1 (δ 1.20) and H-3 (δ 3.80) to H-7 (δ 3.07). Two other cyclic ether rings (C and D) were also indicated by the HMBC correlation of the H-14 signal (δ 3.61) with C-19 (80.0 ppm) and the correlation between the H-18 signal (δ 2.84) and C-23 (78.0 ppm) respectively. The presence of ring C was also confirmed from the NOESY correlation between H-14 and H_3-29 (δ 1.18) and ring D was confirmed from the NOESY correlation between H-18 and H_3-30 (δ 1.15) and between H-18 (δ 2.84) and H-22 (δ 3.77). On the other hand, another additional cyclic ethereal group (ring B) was shown to be present based on the NOESY cross peak correlation between H-11 (δ 3.73) and H_3-26 (δ 1.13) despite the absence of HMBC correlations. Because C-11 is a secondary alcohol, the ether link should be at C-10.

Relative stereochemistry of armatol G was proposed based on selected NOESY correlation and ^{1}H-^{1}H coupling constants. Irradiation of bromomethine proton H-3 (δ 3.80) induced the positive NOESY correlations to H_3-1(δ 1.20), H-7 (δ 3.07), H-4α (δ 1.92) and H-5α (δ 1.36) while irradiation of H_3-1 (δ 1.20) also induced NOESY correlations with H-3 (δ 3.80), H-7 (δ 3.07) and H_3-25 (δ1.40). Furthermore, irradiation of H-7 (δ 3.07) induced the NOESY correlations of H_3-1 (δ 1.20), H-3 (δ 3.80), H-8α (δ 1.69), H-5α (δ 1.36) and H-9α proton (δ 1.26). The NOESY correlations among H-3 (δ 3.80), H_3-1 (δ 1.20) and H-7 (δ 3.07) suggested that the relative stereochemistry at C-3 and C-7 were R^* and S^* respectively. The absence of a NOESY interaction between H-7 and H_3-26 established the relative stereochemistry of the A/B ring junction as ***trans***, thus implying that the relative configuration at C-6 was R^*.

Irradiation of the H-9β proton (δ 2.37) gave NOESY correlations with H-9α (δ 1.26), H-11 (δ 3.73) and both the H-8 protons. The methine proton at δ 3.73 (H-11) had correlations with H_3-26 (δ 1.13), H-9β (δ 2.37), one H-12 proton (δ 1.98) and one H-13 proton (δ 1.76). These correlations suggested that the relative configuration at C-10 was S^*. More interestingly, the NOESY correlation between H-11 and H_3-26 established that relative stereochemistry in ring B linkage as *anti* (with respect to the H_3-26 / H_3-27 stereochemistry) and this was supported by the absence of NOESY correlations between H-11 and H_3-27 (δ 1.24) and between H_3-26 (δ 1.13) and H_3-27 (δ 1.24).

The methine proton at δ 3.61 (H-14) had NOESY correlations to the H-12 protons (δ 1.98 and 1.54), H-13 protons (δ 1.76 and 1.63), H-17β (δ 1.92) and to H_3-29 (δ 1.18). The strong NOESY interaction between H-14 and H_3-29 revealed that the relative stereochemistry of ring C linkage as *syn*. H-18 (δ 2.84) had strong cross peak correlations to the H-20α (δ 1.38), the bromomethine proton H-22 (δ 3.77) and H_3-30 (δ 1.15). It also had NOESY correlations to H-17 protons (δ 1.92 and 1.32) and the H-16α proton (δ 1.50). The absence of a NOESY interaction between H-18 and H_3-29 (δ 1.18) indicated that the relative stereochemistry of the C/D ring junction as *trans*. Irradiation of the bromomethine proton at δ 3.77 (H-22) induced NOESY correlations to H-18 (δ 2.84), H_3-30 (δ 1.15), the H-20α proton (δ 1.38) and H-21 protons (δ 2.03 and 1.89). These NOESY interactions among H-18, H-22 and H_3-30 implied that the relative stereochemistry of C-18, C-19 and C-22 were $18R^*$, $19S^*$ and $20S^*$.

With the objective of confirming the structure of armatol G, a suitable single crystal, grown carefully from a toluene / cyclohexane mixture (1:1), was used for an X-ray diffraction study. The result (Figure 9) established the absolute configuration of all the chiral centres of armatol

G. The molecular packing exhibits intermolecular H-bonding between OH (6) and OH (5) in adjacent molecules, and there is intra-molecular H-bonding between OH (5) and O (3). The coupling constants for H-11 (dd, J = 10.3, 1.5 Hz) and H-14 (dd, J = 9.5, 3.2 Hz) indicates a lack of rotation around single bonds in the uncylised unit of the structure. This is supported by intra-molecular H-bonding between OH (5) and O (3) of the molecule observed in the crystal. This H-bonding, which appeared to still be present in non-polar NMR solvents, enabled the relative stereochemistry of the two bicyclic rings to be related through NOESY correlations. NOESY correlations observed from H-11 (δ 3.73) to one H-12 proton (δ 1.98) and one H-13 proton (δ 1.76) together with the absence of a NOESY correlation between H-11/H_3-27 (δ 1.24) indicated that the relative configuration at C-11 was *R*.

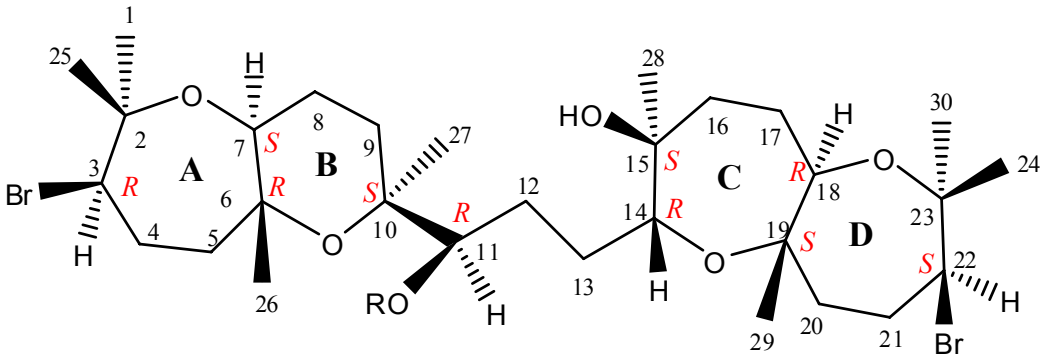

(**145**) R = H (armatol G)
(140) R = OAc (armatol H)

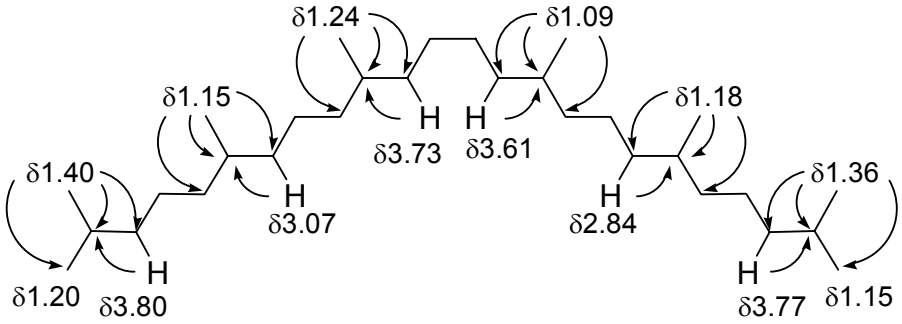

Figure 10. Arrows depict selected key HMBC correlations from tertiary methyl and methine groups that were used to link the five spin systems to form a squalene-derived carbon skeleton for Armatol G.

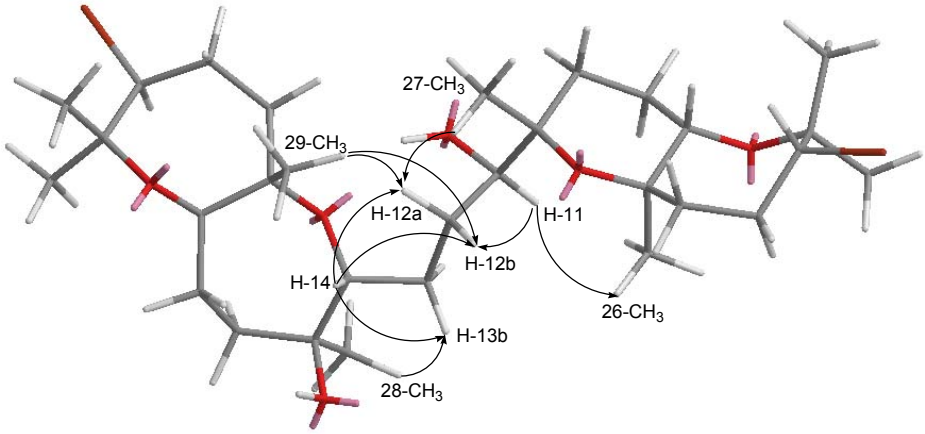

Figure 11. Arrows depict the key NOESY correlations on an MM2 energy minimised Chem3D model of for Armatol G (**145**) that enabled relative stereochemistry of the two ring systems to be related.

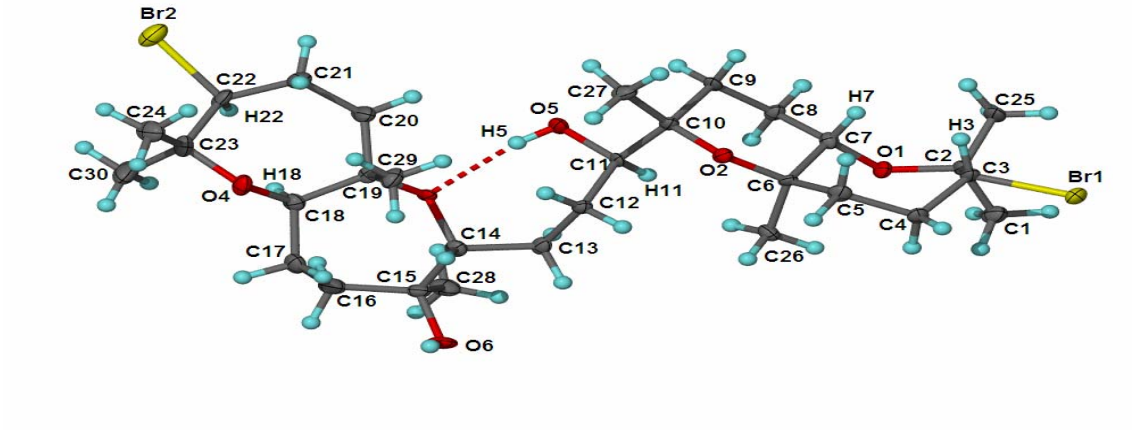

Figure 12. The X-ray structure of armatol G (**145**) showing H-bonding of the tertiary OH group on the uncyclised portion of the terpene backbone to one of the ether oxygens.

2.1.3.2 Armatol H (140)

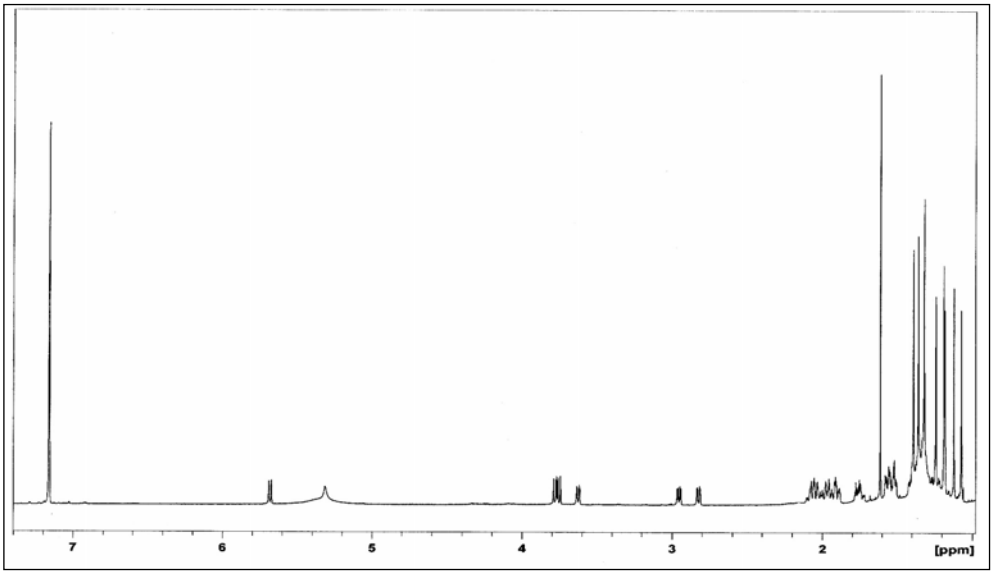

Figure 13. ^{1}H NMR spectrum of armatol H **(140)** at 600MHz in C_6D_6

The formula of armatol H, $[\alpha]_D^{22}$ +13.88°C (*c.* 0.32, in $CHCl_3$) was determined to be $C_{32}H_{53}Br_2O_7$ from high-resolution mass spectrometric measurement of the protonated molecular ion produced by electrospray ionization. As its ^{1}H and ^{13}C NMR spectra exhibited no double bonds, armatol H should be an acetylated tetracyclic triterpene polyether.

The ^{1}H NMR spectrum showed six methine protons in the low field region at δ 2.82, 2.95, 3.62, 3.75, 3.78, and 5.68. The downfield doublet at δ 5.68 which corresponds to the carbon signal at 74.2 ppm in the ^{13}C NMR spectrum indicated ester attachment, and a three proton singlet at δ 1.61 in the ^{1}H NMR spectrum together with a carbonyl signal at 170.4 ppm in the ^{13}C NMR spectrum indicated the existence of secondary acetate group. Moreover, the presence of two bromine atoms was suggested by the characteristic 1:2:1 pattern of the molecular ion in the ESI mass spectrum and by the presence of two methine carbons resonating at 60.1 and 59.8 ppm in the ^{13}C NMR spectrum with proton signals at δ 3.78 and 3.75 respectively as shown by the HSQC data.

The spectroscopic data for armatol H **(140)** was very similar to that for armatol G (**145**) except for the presence of signals attributed to the secondary acetate group and its point of attachment. The relative stereochemistry of armatol H was then determined by means of 1D selective NOESY spectra and by comparison with spectral data and the X-ray structure of armatol G. The structure of armatol H was confirmed by acetylation of armatol G, which provides identical spectral data to those of armatol H.

Armatol G (145)				Armatol H (140)		
C	$\delta^{13}C$	$\delta^{1}H$, mult., J (Hz)	HMBC ^{1}H to ^{13}C	$\delta^{13}C$	δ ^{1}H, mult., J (Hz)	HMBC ^{1}H to ^{13}C
1	25.0	1.20, s	C2, C3, C25	24.9	1.19, s	C1, C2
2	77.9			77.7		
3	60.7	3.80, dd , 11.1, 1.0	C1, C2, C25	60.1	3.78, d, 10.6	C2, C4, C5, C25
4	32.3	1.92, m	C3, C5	31.7	1.90, m	
		2.00, m			1.98, m	C2, C3
5	45.8	1.36, m		44.9	1.32, m	
		1.58, m			1.57, m	C6, C7
6	76.8			76.8		
7	72.5	3.07, dd, 11.1, 5.3	C2, C6, C8, C9, C26	72.4	2.95, dd, 11.6, 4.7	C2, C5
8	24.4	1.69, m	C7	24.2	1.39, m	
		1.45, m	C7, C9		2.04, m	
9	31.9	1.26, m	C7, C11	33.3	1.25, m	
		2.37, d/t, 13.9, 4.9	C7, C8, C10, C11		1.76, m	
10	76.7			74.6		
11	74.8	3.73, dd, 10.3, 1.5	C10, C13, C27	74.2	5.68, dd, 11.1, 1.2	C10, C13, C27, OAc
12	28.7	1.54, m		27.4	1.95, m	
		1.98, m	C10, C13, C14		2.08, m	
13	29.6	1.63, m	C14	28.5	1.54, m	
		1.76, m	C11, C12		1.74, m	
14	76.6	3.61, dd, 9.5, 3.2	C15, C19, C28	76.4	3.62, dd, 10.0, 1.5	C13, C15, C19, C28
15	75.4			74.7		
16	41.5	1.50, m	C15, C18	40.9	1.48	
		1.50, m			1.52	C14, C15, C18
17	27.6	1.32, m		27.3	1.32, m	
		1.92, m	C15		1.96, m	
18	79.1	2.84, dd, 11.3, 3.0	C17, C19, C20, C23, C29	78.8	2.82, dd, 11.3, 2.9	C16, C17, C19, C20, C23, C29
19	80.0			79.1		
20	44.6	1.38, m		44.4	1.41, m	
		1.63, m	C18, C19		1.56, m	C21
21	32.2	1.89, m		31.9	1.90, m	
		2.03, m	C20, C22, C23		2.03, m	C20, C22, C23
22	60.2	3.77, brd, 10.7	C20, C21, C23, C24, C30	59.8	3.75, d, 11.2	C20, C21, C23, C24
23	78.0			77.5		
24	24.8	1.36, s	C22, C23, C30	25.7	1.36, s	C22, C23, C30
25	26.2	1.40, s	C1, C2, C3	25.7	1.39, s	C1, C2
26	21.7	1.13, d, 0.9	C5, C7	20.9	1.24, s	C5, C6. C7
27	25.1	1.24, s	C9, C10, C11	24.9	1.32, s	C9, C10, C11
28	25.6	1.09, s	C14, C15, C16	25.1	1.07, s	C14, C15, C16
29	17.1	1.18, brs	C19, C20	16.9	1.18, s	C18, C19, C20
30	26.1	1.15, s	C22, C23, C24	24.4	1.12, s	C22, C23, C24
OAc				20.5	1.61, s	OAc (CO group)
C=O				170.4		

Table 6. NMR data for armatol G (**145**) and H **(140)** at 600 (^{1}H) MHz and 150 MHz (^{13}C) in C_6D_6

2.1.3.3 Armatol I (141)

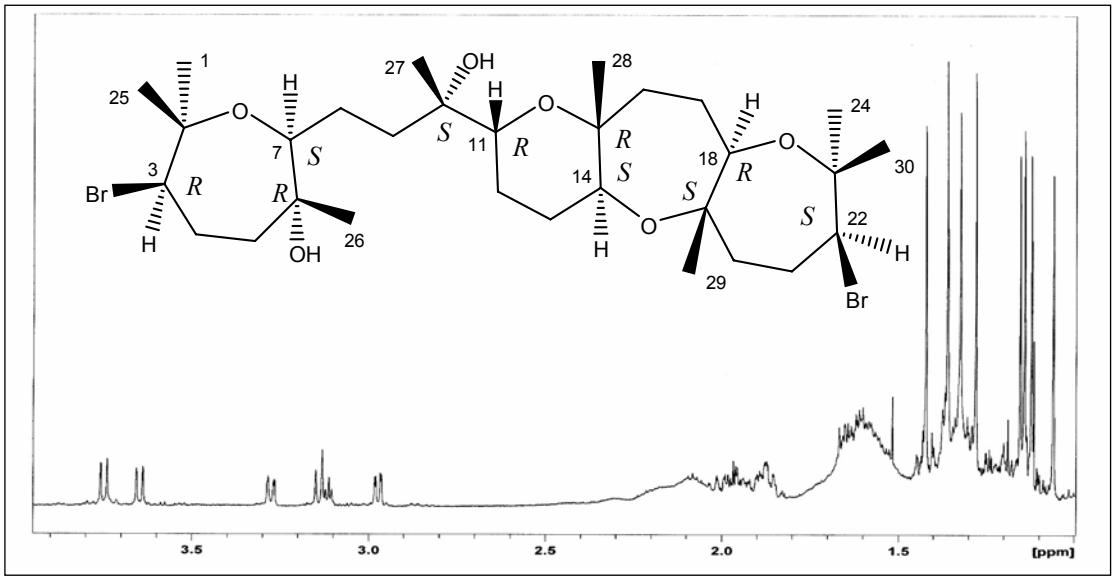

Figure 14. ^{1}H NMR spectrum of armatol I **(141)** at 600 MHz in C_6D_6

Armatol I was isolated as an amorphous white solid, mp 159-162, $[\alpha]_D^{22}$ +13.9^{o}C (*c.* 0.53 $CHCl_3$). The molecular formula was determined as $C_{30}H_{52}Br_2O_6$, indicative of a tetracyclic triterpene polycyclic ether, by high resolution ESI positive ion mass spectrometry. The presence of two bromine atoms was suggested by the characteristic pattern 1:2:1 of the molecular ion from the mass spectrum and by two signals at δ 60.6 and 59.9 ppm in the carbon spectrum which corresponded to the two bromomethine signals at δ 3.75 (H-3) and 3.65 (H-22). The ^{13}C NMR spectrum confirmed the molecular formula and showed the presence of eight methyl groups, ten methylene groups, four oxygenated methines, two brominated methine groups, as well as six quaternary carbon centres, which were α to oxygens**.** All the protonated carbons were assigned using an HSQC experiment.The ^{1}H NMR spectrum exhibited in the lowfield region six methine signals at δ 3.75, 3.65, 3.28, 3.14, 3.12 and 2.97 identified as H-3, H-22, H-11, H-18, H-14 and H-7 respectively.

Analysis of selective gradient TOCSY and COSY spectra together with HSQC-derived assignments of the six methine protons enabled assignments to identify the sub units of the molecule. A series of selective gradient TOCSY spectra showed that these six methine signals were coupled to the ten methylene groups. Signals at δ 3.75, 3.65, 3.14 and 2.97 were each linked to two different contiguous methylene groups while the methine signals at δ 3.28 and 3.12 were each linked to another pair of adjacent methylene signals. The methine signal at δ 3.75 (H-3) was linked to the methylene signals at δ 1.89, 2.01 (H_2-4), δ 1.14, 1.43 (H_2-5) and H_3-26 (δ 1.06). The methine proton signal at δ 2.97 (H-7) correlated with the methylene signals

at δ 1.60, 1.93 (H_2-8) and δ 1.98, 1.32 (H_2-9). The signals at δ 3.28 (H-11) and 3.12 (H-14) were each correlated with methylene signals at δ 1.56, 1.65 (H_2-12) and δ 1.54, 1.64 (H_2-13). The proton signal at δ 3.14 (H-18) had correlations with the methylene signals at δ 1.87, 1.39 (H_2-17), δ 1.64, 1.42 (H_2-16) and a methyl signal at δ 1.12 (H_3-28). Finally the signal at δ 3.65 correlated with the methylene at δ 1.86, 1.95 (H_2-21) and the remaining methylene at δ 1.29, 1.21 (H_2-20). The sequence of the spin systems was confirmed from a COSY spectum. Therefore, selective gradient TOCSY and COSY experiments enabled five sub units of the molecule: C3—C5—C26, C7—C9, C11—C14, C16—C18 and C20—C22 to be established.

Furthermore, HMBC data allowed the spin systems to be connected together with the quaternary carbon atoms bearing methyl groups. Thus in the HMBC spectrum, both H_3-1 (δ 1.33) and H_3-25 (δ 1.42) showed correlations to C-2 (77.3 ppm) and C-3 (60.6 ppm), H_3-26 (δ 1.06) showed correlations to C-5 (45.9 ppm), C-6 (73.7 ppm) and C-7 (77.5 ppm), H_3-27 (δ 1.28) showed correlations to C-9 (35.3 ppm), C-10 (73.1 ppm) and C-11 (75.1 ppm), H_3-28 (δ 1.12) showed correlations to C-14 (71.2 ppm), C-15 (77.5 ppm) and C-16 (42.0 ppm), H_3-29 (δ 1.14) showed correlations to C-18 (76.1 ppm), C-19 (78.8 ppm) and C-20 (40.0 ppm), while both H_3-24 (δ 1.16) and H_3-30 (δ 1.36) showed correlations to C-22 (59.9 ppm) and C-23 (77.6 ppm) The presence of three cyclic ethereal groups (rings A, C and D) was indicated by HMBC correlations (C-2/H-7, C-19/H-14 and C-23/H-18). Thus, a long range correlation between H-7 (δ 2.97) and C-2 (77.3 ppm) and a correlation from H_3.1 (δ 1.33) to C-2 (77.3 ppm) indicated the presence of ring A. Ring C was confirmed from the correlation from H-14 (δ 3.12) to C-19 (78.8 ppm) while ring D was established from the correlation from H-18 (δ 3.14) to C-23 (77.6 ppm). On the other hand, the fourth cyclic ethereal group (ring B) was indicated by NOESY correlations between H-11 (δ 3.28) and H_3-28 (δ 1.12) despite the absence of HMBC correlations. The other two quaternary carbons which were α to oxygen implied the location of OH groups. Thus, HMBC long range correlations from the methyl signal at δ 1.06 (H_3-26) and the methylene proton signals at δ 1.43 (H-5β) and 1.89 (H-4α) to the carbon signal at 73.7 ppm (C-6) together with the correlations from the methyl signal at δ 1.28 (H_3-27) and the methylene proton signal at δ 1.98 (H-9b) to the carbon signal at 73.1 ppm (C-10) indicated C-6 and C-10 as the location of the two hydroxyl groups.

The relative stereochemistry of armatol I was proposed based on selective gradient NOESY experiments. Irradiation of the bromomethine proton signal at δ 3.75 (H-3) induced NOESY correlations to the H-5α proton (δ 1.14), the H-4 protons (δ 1.89 and 2.01), H-7 (δ 2.97) and the H_3-1 protons (δ 1.33). The H_3-1 signal (δ 1.33) was in turn correlated with signals at δ 3.75 (H-3), δ 2.97 (H-7) and δ 1.42 (H_3-25). In contrast, irradiation of H_3-26 (δ 1.06) induced

correlations to H-4β (δ 2.01), H-5β (δ 1.43) and H-8a (δ 1.60) while no correlations were observed to H-3 (δ 3.75) or H-7 (δ 2.97). The methine proton signal at δ 2.97 (H-7) also had strong correlations with the H-3 proton signal (δ 3.75) and the H_3-1 proton signal (δ 1.33) in addition to correlations with the H-5α proton at δ 1.14, H-8b (δ 1.93) and H-9b (δ 1.98). The NOESY correlations among H-3 (δ 3.75), H-7 (δ 2.97) and H_3-1 (δ 1.33) and the absence of NOESY correlations between H_3-26 (δ 1.06) and the signals at H-3 (δ 3.75), H-7 (δ 2.97) and H_3-1 (δ 1.33) allowed the relative stereochemistry of OH group at C-6 to be deduced and indicated the relative configuration at C-2, C-6 and C-7 as $2R^*$, $6R^*$ and $7S^*$ respectively.

The methine proton at δ 3.12 (H-14) had NOESY correlations with H-12α (δ 1.65), H-16α (δ 1.42) and H-20α (δ 1.21). Hence, the NOESY correlations between H-11 and H_3-28 and the absence of NOESY correlations between H-14 and H_3-28 enabled the relative configuration at C-11, C-14 and C-15 to be established as 11*R**, 14*S** and 15*R** respectively and indicated the relative stereochemistry of the B/C ring junction as *trans* in nature. In addition, the absence of a NOESY correlation between H-14 and H_3-29 (δ 1.14) implied that the relative configuration of the ether linkage in ring C was *anti*.

Irradiation of the methine proton signal at δ 3.14 (H-18) induced NOESY correlations to the H-21α proton (δ 1.86), the H-16α proton (δ 1.42), H-22 (δ 3.65) and H_3-24 (δ 1.16). H_3-24 (δ 1.16) in turn showed correlations with H-22 (δ 3.65), the methine proton signal at δ 3.14 (H-18) and the H_3-30 signal (δ 1.36). The absence of a NOESY correlation between H-18 and H_3-29 (δ 1.14) suggested that the relative configuration of the C/D ring junction was *trans*. The bromomethine proton at δ 3.65 (H-22) also showed correlations with the methine proton signal at δ 3.14 (H-18), the methyl signals at δ 1.16 (H_3-24) and δ 1.36 (H_3-30) and the methylene proton signals at δ 1.86 (H-21α) and 1.21 (H-20α).

Irradiation of the methine proton signal at δ 3.28 (H-11) induced NOESY correlations to the H-9b proton (δ 1.98), H-13β proton (δ 1.54), H_3-27 (δ 1.28) and H_3-28 (δ 1.12). H_3-28 (δ 1.12) also had correlations with the signals for H-17β (δ 1.87) and the H-16 protons (δ 1.42 and 1.64). Moreover, irradiation of H_3-27 (δ 1.28) induced NOESY correlations to H-11 (δ 3.28) and H-9b (δ 1.98). The correlations observed from H-7 to the H-9b proton (δ 1.98), from H_3-27 (δ 1.28) to H-9b proton (δ 1.98) and from the H-11 proton (δ 3.28) to H-9b proton (δ 1.98) indicated the conformation of the uncyclised portion of the structure and allowed the relative stereochemistry of the OH group to be deduced and thus, the relative configuration of C-10 to be established as 10*S**. Moreover, they allowed the relative stereochemistry of ring A to be related to the relative stereochemistries of rings B, C and D.

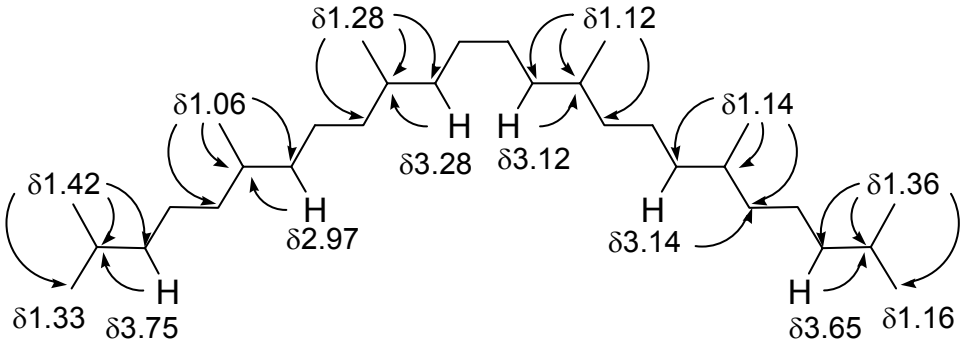

Figure 15. Arrows depict selected key HMBC correlations from tertiary methyl and methine groups that were used to link the five spin systems to form a squalene-derived carbon skeleton for Armatol I.

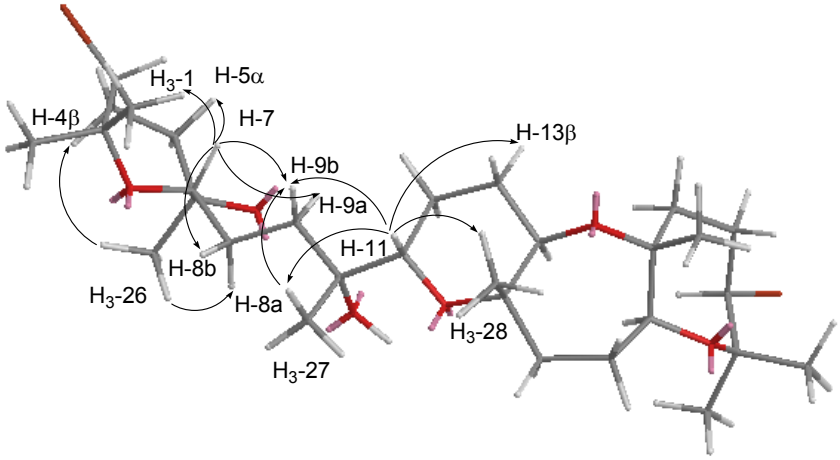

Figure 16**.** Arrows depict the key NOESY correlations on an MM2 energy minimised Chem3D model of Armatol I (**141**) that enabled relative stereochemistry of the two ring systems to be related.

2.1.3.4 Armatol J (146)

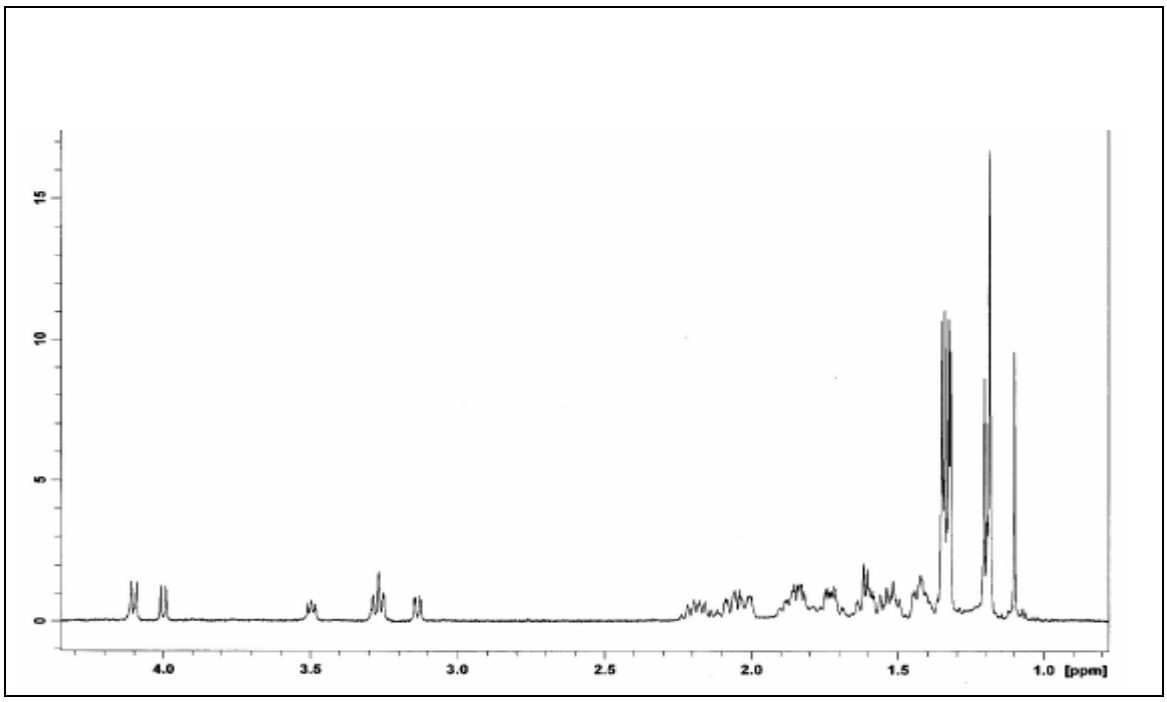

Figure 17. ^{1}H NMR spectrum for armatol J **(146)** at 600 (^{1}H) MHz in $CDCl_3$

Armatol J was isolated as an amorphous white solid, $[\alpha]_D^{22}$ +14.3°C (*c.* 0.29 $CHCl_3$). The molecular formula of armatol J was determined to be $C_{30}H_{52}Br_2O_6$ by high resolution ESI-MS and therefore, four degrees of unsaturation were indicated. As its ^{1}H and ^{13}C NMR spectra revealed no unsaturated bonds, armatol J should be tetracylic. The presence of two bromine atoms was suggested by the characteristic 1:2:1 pattern of the molecular ion in the HRESI mass spectrum and by two resonances at 60.4 and 59.7 ppm in the carbon spectrum. These two carbon signals correspond to the two bromomethine signals at δ 4.00 and δ 4.10 respectively in the ^{1}H NMR spectrum.

The ^{1}H NMR spectrum exhibited an additional four methine proton signals at δ 3.14, 3.26, 3.28 and 3.50, indicative of a triterpene polycyclic ether. Analysis of selective gradient TOCSY experiments showed that these six methine signals were contained within five spin systems. The methine signals at δ 4.00, 4.10, 3.26 and 3.14 were each linked to two different methylene groups while signals at δ 3.28 and δ 3.50 were associated with the same two methylene groups. Thus, the signal resonating at δ 4.00 (H-3) was correlated with methylene signals at δ 2.19, 2.07 (H_2-4), 1.85, 1.57 (H_2-5) and a methyl signal at δ 1.19 (H_3-26). The methine signal at δ 3.26 (H-7) showed correlations to the methylenes at δ 1.89, 1.25 (H_2-8) and 1.52, 1.43 (H_2-9). The

signal at δ 3.28 (H-11) was linked to the methylene signals at δ 1.63, 1.40 (H_2-12) and 1.61 (H_2-13) and also linked to the methine proton at δ 3.50 (H-14). The signal resonating at δ 3.14 (H-18) was linked to the methylene signals at δ 2.03, 1.43 (H_2-17) and at δ 1.85, 1.71 (H_2-16) and to a methyl signal at δ 1.19 (H_3-28). The bromomethine signal at δ 4.10 (H-22) showed correlations to methylene signals at δ 2.07, 2.19 (H_2-21) and δ 1.52, 1.73 (H_2-20) and the methyl signal at δ 1.20 (H_3-29). The sequence of these TOSCY spin systems was elucidated from a COSY spectrum. Hence, five partial structures C3—C5—C26, C7—C9, C11—C14, C28—C16—C18 and C29—C20—C22 were constructed.

The HMBC data allowed the five partial structures to be connected with quaternary carbons bearing methyl groups. Thus, HMBC correlations from δ 1.19 (H_3-26) to C-5 (45.4 ppm), C-6 (74.1 ppm) and C-7 (77.6 ppm) were used to link C-5 to C-7, while correlations from δ 1.10 (H_3-27) to C-9 (33.7 ppm), C-10 (73.2 ppm) and C-11 (75.5 ppm) linked C-9 to C-11. HMBC correlations from δ 1.19 (H_3-28) to C-14 (70.4 ppm), C-15 (76.8 ppm) and C-16 (40.3 ppm) were then used to link C-14 to C-16, while correlations from δ 1.20 (H_3-29) to C-18 (77.3 ppm), C-19 (78.1 ppm) and C-20 (44.4 ppm) linked C-18 to C-20.

HMBC and NOESY correlations enabled the ether linkages to be established. Thus, an HMBC correlation from δ 3.26 (H-7) to C-2 (76.9 ppm) together with correlations from the two methyl signals at δ 1.34 (H_3-1) and 1.35 (H_3-25) to C-2 and C-3 established the presence of ether ring A. This ring was also supported by a NOESY correlation between δ 3.26 (H-7) and δ 1.34 (H_3-1). HMBC correlations from H-18 (δ 3.14) and H-22 (δ 4.10) to C-23 (77.2 ppm) confirmed the presence of ether ring D. The two methyl signals at δ 1.32 (H_3-24) and δ 1.33 (H_3-30) also exhibited HMBC correlations to the C-23 signal. This ring was also confirmed by a NOESY correlation between H-22 (δ 4.10) and H-18 (δ 3.14). On the other hand, the presence of the ether linkages in rings B and C were confirmed by NOESY correlations between H-11 (δ 3.28) and methyl signal at δ 1.19 (H_3-28) and between H-14 (δ 3.50) and H_3-29 (δ 1.20) respectively despite the absence of HMBC correlations.

The relative stereochemistry of armatol J was proposed based on selective gradient NOESY experiments and ^{1}H-^{1}H coupling constants. H-3 had a NOESY correlation to the H-4α proton (δ 2.07) and NOESY cross peak correlations to the H_3-1 signal (δ 1.34), the H-5α proton signal (δ 1.57) and to methine proton signal at δ 3.26 (H-7). This methine proton (δ 3.26) also had in turn a cross peak correlation to the bromomethine proton H-3 (δ 4.00). This allowed the stereochemistry of the OH group at C-6 to be deduced because of the absence of a NOESY interaction between H-7 and H_3-26 (δ 1.19). This permitted determination of the relative

stereochemistry at C-3, C-6 and C-7 as 3*R**, 6*R** and 7*S**. Thus, the relative stereochemistry of ring A was identical to armatol C (Ciavatta et al., 2001) and armatol I.

H-11(δ 3.28) had a NOESY correlation to H_3-27 (δ 1.10) and other correlations to H_3-28 (δ 1.19), H-13α (δ 1.61) and H-12α (δ 1.63) and therefore the stereochemistry of the ring B ether link had H-11 (δ 3.28) and H_3-28 in a ***syn*** configuration. The methine proton H-14 showed correlations to the H_3-29 signal (δ 1.20), H-13β (δ 1.61) and H-17β (δ 2.03). The correlations between signals for H-14 and H_3-29 indicated that H-14 and H_3-29 were in a ***syn*** configuration compared to ***anti*** arrangement in armatol I. Finally, the bromomethine proton H-22 (δ 4.10) had NOESY correlations to the H_3-30 signal (δ 1.33), the H-21α signal (δ 2.07), the H-20α proton signal (δ 1.52) and to the methine H-18 signal (δ 3.14). These NOESY correlations together with the absence of correlations from H-14 to H_3-28 and from H-18 to H_3-29 established the B-C and C-D ring junctions as ***trans***, and hence led to a ***syn-trans-syn-trans*** arrangement for the tricyclic ring system B-D, whereas armatol I was ***syn-trans-anti-trans***.

The 11*S**, 14*R**, 15*S**, 18*R**, 19*S**, 22*S** stereochemistry for the tricyclic ring system had previously been reported in armatols B and C (Ciavatta et al., 2001), and comparison of the ^{13}C NMR data for carbon atoms 10-24 and 27-30 with literature values showed excellent agreement for all carbon shifts except two quaternary ether carbons (C15 and C23) which were shifted about 0.5 ppm, perhaps by H-bonding. Although in the 2001 paper on armatols, no evidence whatever was presented to relate the relative stereochemistry of ring A to those of the B-D ring system in armatol C, the absolute stereochemistry for armatol C was proposed as 3*R,* 6*R,* 7*S, 10*,* 11*R,* 14*R,* 15*R,* 18*S,* 19*R,* 22*R* (* = undetermined). Armatol J would then appear to diastereomeric with armatol C in the relationship between the A ring and B-D ring relative stereochemistries. So armatol J is predicted to be 3*R*,* 6*R*,* 7*S*,* 10*S*,* 11*S*,* 14*R*,* 15*S*,* 18*R*,* 19*S*,* 22*S** which compares with the absolute stereochemistry determined by X-ray crystallography for armatol G: 3*R*,* 6*R*,* 7*S*,* 10*S** 11*R*,* 14*R*,* 15*S*,* 18*R*,* 19*S*,* 22*S**.

The NOESY correlations between H-7 and H-8α (δ 1.89) and between H_3-27 (δ 1.10) and H-8β (δ 1.25) together with the NOESY correlation between H-11 (δ 3.28) and H_3-27 indicated the conformation of the uncyclised part of the molecule and enabled the relative stereochemistry of the OH group at C10 to be deduced. Thus, the relative configuration of C-10 to be established as 10*S**. Moreover, this allowed the relative stereochemistry of ring A to be related to the relative stereochemistries of rings B-D.

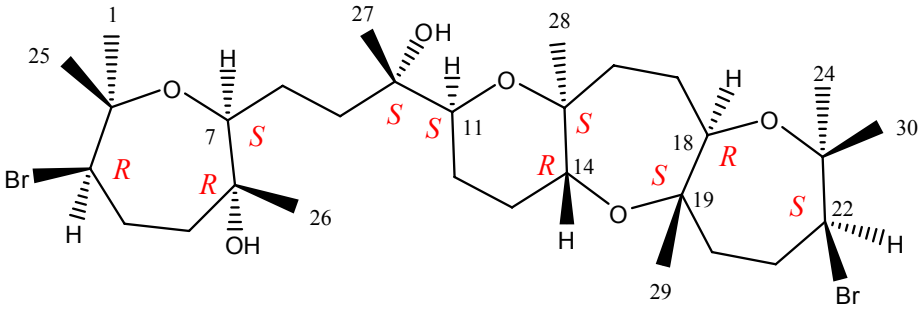

(146) armatol J

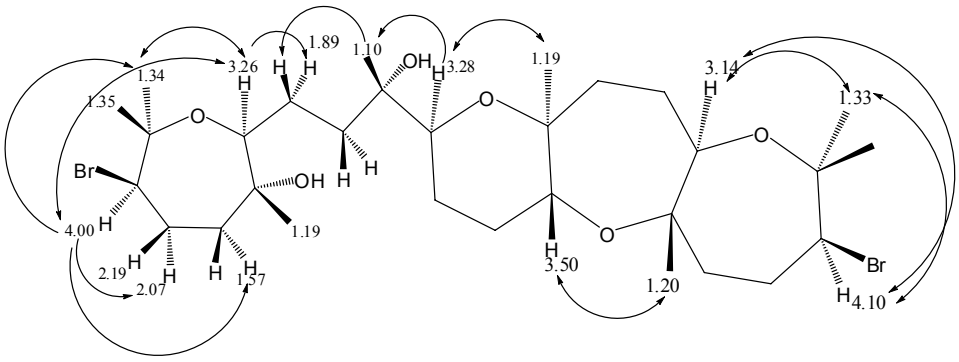

Figure 18 . Selected NOESY correlations of armatol J (**146**)

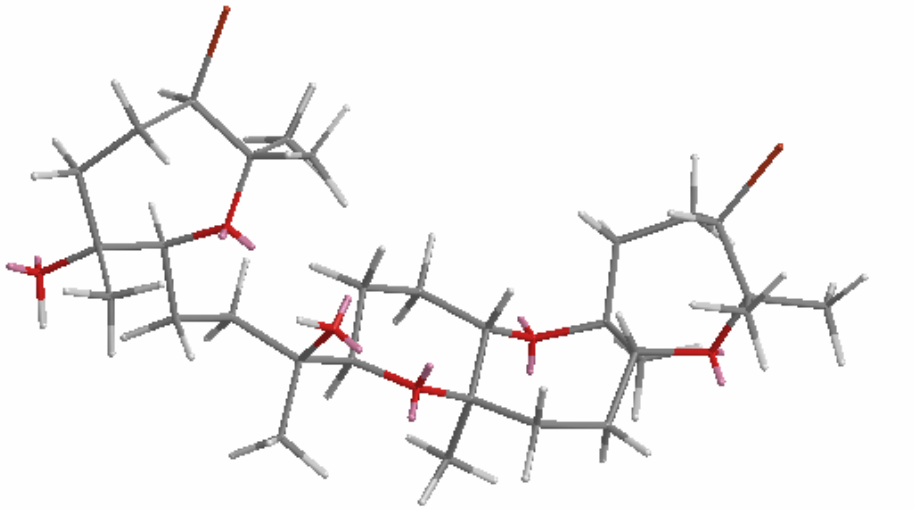

Figure 19**.** MM2 minimised Chem3D model of armatol J **(146)** based on stereochemistry predicted by observed 1D NOESY enhancements and coupling constants

	Armatol I (141)			Armatol J (146)		
C	$\delta^{13}C$	$\delta^{1}H$, mult., J (Hz)	HMBC ^{1}H to ^{13}C	$\delta^{13}C$	δ ^{1}H, mult., J (Hz)	HMBC ^{1}H to ^{13}C
1	25.4	1.33, s	C2, C3	25.3	1.34, s	C2, C3, C25
2	77.3			76.9		
3	60.6	3.75, dd , 10.9, 1.1	C2, C4, C5, C25	60.4	4.00, brd, 10.6	C2, C4, C5,C6, C25
4	31.7	1.89, m	C2, C3, C5, C6	31.4	2.07, m	C2, C6
		2.01, m			2.19, m	
5	45.9	1.14, m	C3, C7	45.4	1.57, m	
		1.43, m	C6		1.85, m	C6
6	73.7			74.1		
7	77.5	2.97, dd, 9.6, 2.2	C2, C5, C6, C8, C9, C26	77.6	3.26, dd, 9.4, 1.8	C2, C5, C6, C9,
8	24.0	1.60, m	C7	23.6	1.89, m	
		1.93, m	C9,C10		1.25, m	
9	35.3	1.32, m	C10, C11	33.7	1.52, m	C7
		1.98, m	C8		1.43, m	
10	73.1			73.2		
11	75.1	3.28, dd, 10.9, 2.2	C9, C10, C12, C27	75.5	3.28, brd, 11.3	C10, C12
12	25.3	1.65, m	C12	25.2	1.63, m	
		1.56, m	C14, C15		1.40, m	
13	28.2	1.64, m		27.1	1.61, m	C14, C15
		1.54, m			1.61, m	
14	71.2	3.12, dd, 11.0, 4.5	C15, C16, C28	70.4	3.50, dd, 9.3, 6.7	C13, C16, C18, C28
15	77.5			76.8		
16	42.0	1.42, m		40.3	1.85, m	C18
		1.64, m	C14, C17		1.71, m	
17	28.6	1.39, m		28.6	1.43,m	
		1.87, m	C15		2.03, m	C18
18	76.1	3.14, dd, 11.5, 1.1	C16, C17, C20, C29	77.3	3.14, dd, 11.3, 2.4	C16, C19, C20, C23
19	78.8			78.1		
20	40.0	1.21, m		44.4	1.52, m	C18
		1.29, m			1.73, m	
21	31.8	1.86, m	C22	31.4	2.07, m	
		1.95, m			2.19, m	
22	59.9	3.65, dd, 11.2, 1.2	C20, C21, C23, C30	59.7	4.10, brd, 11.0	C20, C21, C23, C24, C30
23	77.6			77.2		
24	24.5	1.16, s	C22, C23, C30	25.2	1.32, s	C22, C23, C30
25	26.2	1.42, s	C1, C2, C3	25.6	1.35, s	C1, C2, C3
26	21.2	1.06, s	C5, C6, C7	21.3	1.19, s	C5, C6
27	23.8	1.28, s	C9, C10, C11	23.5	1.10, s	C9, C10, C11
28	16.2	1.12, s	C14, C15, C16	19.7	1.19, s	C14, C15, C16
29	20.9	1.14, s	C18, C19, 20	16.6	1.20, s	C19, C20
30	25.7	1.36, s	C22, C23, C24	24.3	1.33, s	C22, C23, C24

Table 7. NMR data for armatol I **(141)** (in C_6D_6) and J **(146)** (in $CDCl_3$) at 600 MHz ^{13}C NMR data at 150 MHz was referred to C_6D_6 (128.0 ppm) for armatol I and $CDCl_3$ (77.0 ppm) for armatol J

2.1.3.5 Aplysiol C (147)

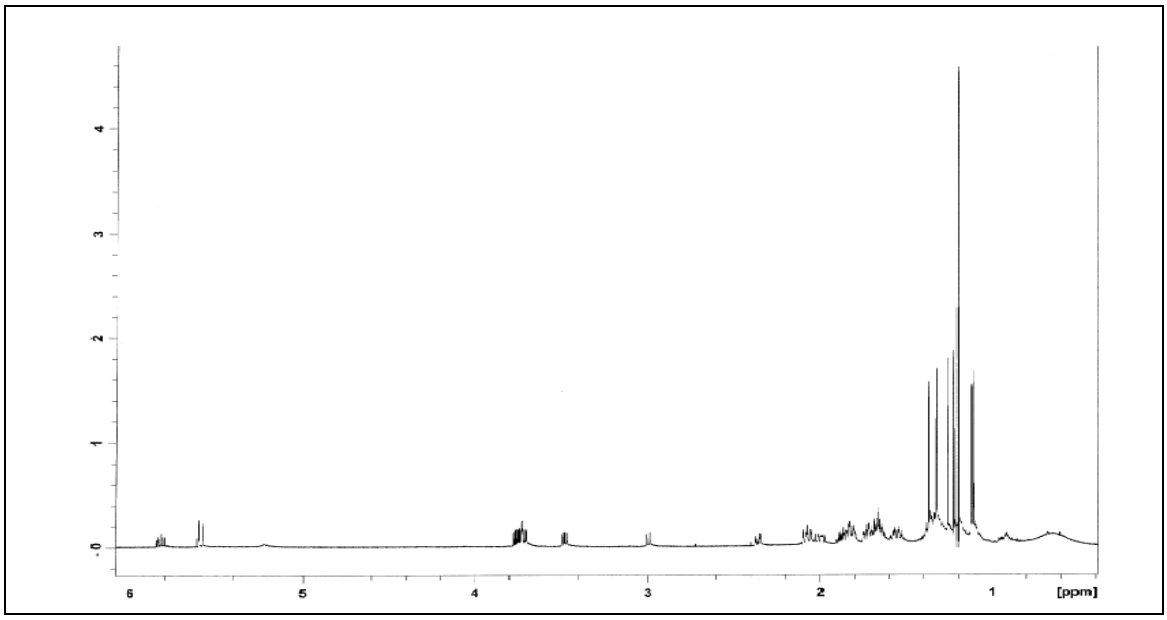

Figure 20. ^{1}H NMR spectrum of Aplysiol C **(147)** at 600 MHz in C_6D_6

A new brominated triterpene polyether, aplysiol C, $[\alpha]_D^{22}$ +11.9°C (*c.* 0.1 in $CHCl_3$) was isolated as a colourless oil. The molecular formula of aplysiol C was determined as $C_{30}H_{51}BrO_6$ from ESI-MS. The ^{13}C NMR spectrum confirmed the molecular formula and showed the presence of eight methyl groups, nine methylene groups, four oxygenated methine groups, one brominated methine group, two olefinic carbon atoms as well as six quaternary carbon centres. All the protonated carbons were assigned using an HSQC experiment. The ESI-MS (positive mode) spectrum showed ion cluster at *m/z* 609 and 611 ($M+Na^+$) with equal intensities, thus indicating the presence of one bromine atom in the molecule which corresponded with the brominated methine proton signal at δ 3.73 (dd 12.4, 4.1 Hz, H-3) in the ^{1}H-NMR spectrum. In addition, the ^{1}H-NMR spectrum in C_6D_6 (Table 9) revealed signals due to two olefinic protons at δ 5.84 (ddd 15.5, 8.2, 6.7 Hz, H-21) and δ 5.59 (d 15.5 Hz, H-22), four oxygenated methine proton signals at δ 3.00 (dd 11.6, 2.5 Hz, H-7), 3.48 (dd 11.1, 7.5 Hz, H-11), 3.72 (dd 11.9, 3.5 Hz, H-14) and 3.77 (dd 9.7, 5.5 Hz, H-18), ten methylene proton groups and eight tertiary methyl groups which were indicated by the presence of seven singlets at δ 1.11, 1.12, 1.20 (integrated for six protons), 1.22, 1.26, 1.32 and 1.37.

Analysis of selective gradient TOCSY and COSY spectra, together with HSQC correlations for the five methine protons and a vinyl proton allowed the spin systems of the molecule to be identified. Two methine protons with signals at δ 3.48 (H-11) and 3.72 (H-14) were each

coupled to a pair of methylene signals at δ 1.54, 1.83 (H_2-12) and δ 1.68, 1.71 (H_2-13). The sequence of this spin system was confirmed by the COSY experiment. In the COSY spectrum, the signal that resonated at δ 3.48 was correlated with methylene protons at δ 1.54 and 1.83. These methylene protons were coupled with each other and the δ 1.83 proton was in turn linked with another methylene group at δ 1.68, 1.71 (H_2-13). Furthermore, the signal at δ 3.72 (H-14) showed correlations with the same methylene protons (H_2-13).

The other methine proton signals at δ 3.00 (H-7), 3.73 (H-3) and 3.77 (H-18) were each linked to two different contiguous methylene groups from gradient selective TOCSY data. The methine proton signal at δ 3.73 (H-3) was correlated with the methylene groups at δ 2.05, 1.88 (H_2-4) and δ 1.33, 1.67 (H_2-5). The methine proton at δ 3.00 (H-7) was correlated with the methylene proton signal at δ 1.37, 1.74 (H_2-8) and 1.57, 1.82 (H_2-9) and also correlated to a methyl group at δ 1.22 (H_3-27). Irradiation of the signal at δ 3.77 (H-18) induced signals at δ 1.66, 1.85 (H_2-17) and 1.65, 1.99 (H_2-16). The last spin system was identified by irradiation of the vinyl proton at δ 5.84 (H-21) which correlated with only one methylene group at δ 2.37, 2.07 (H_2-20) and another vinyl proton at δ 5.59 (H-22). The sequences of methylene proton groups within the spin systems were confirmed from a COSY experiment. Therefore, selective gradient TOCSY, COSY and HSQC experiments enabled five sub units of the molecule: C3—C5, C7—C9—C27, C11—C14, C16—C18 and C20—C22 to be established.

Furthermore, HMBC data allowed the five spin systems to be connected with quaternary carbon atoms bearing methyl groups. Strong HMBC correlations from the methyls at δ 1.32 (H_3-1) and 1.37 (H_3-25) to the carbons resonating at 75.0 ppm (C-2) and the bromomethine carbon at 58.7 ppm (C-3) revealed that these two methyl groups were attached to C-2 which in turn linked to C-3. The HMBC correlation from the methine proton at δ 3.73 to C-2 confirmed the position of the geminal dimethyl group. HMBC correlations from H_3-26 (δ 1.12) to C-5 (37.0 ppm), C-6 (74.4 ppm) and C-7 (86.7 ppm) linked C-5 to C-7, while HMBC correlations from H_3-27 (δ 1.22) to C-9 (38.7 ppm), C-10 (71.5 ppm) and C-11 (76.7 ppm) linked C-9 to C-11. In addition, HMBC correlations from H_3-28 (δ 1.11) to C-14 (75.5 ppm), C-15 (84.2 ppm) and C-16 (36.5 ppm) linked C-14 to C-16, while HMBC correlations from H_3-29 (δ 1.26) to C-18 (85.9 ppm), C-19 (72.4 ppm) and C-20 (41.2 ppm) linked C-18 to C-20. The mutual HMBC correlations between the equivalent *gem*-dimethyl signals at δ 1.20 (C-24/30) and their correlations to the oxygenated quaternary carbon resonating at 70.0 ppm (C-23) and to the alkene carbon at 141.7 ppm (C-22) were used to complete the carbon skeleton.

The presence of ring A was established by mutual NOESY correlations between methyl signals at δ 1.37 (H_3-25) and δ 1.12 (H_3-26) despite the absence of HMBC correlations across the ether bridge. The presence of ring B was indicated by HMBC correlations from the methine protons at δ 3.00 (H-7) and δ 3.48 (H-11) to carbons resonating at 76.7 ppm (C-11) and 86.7 ppm (C-7) respectively and also confirmed by a strong mutual NOESY correlation between the methine protons at δ 3.00 (H-7) and δ 3.48 (H-11). NOESY and HMBC correlations were not particularly helpful when it came to determination of the cyclisation positions for the remaining two ether linkages. In particular, no HMBC correlations were observed from either δ 3.72 (H-14) or 3.77 (H-18) that were indicative of ether linkages, so logically the first of the remaining ether linkages could be either be between C-10 and C-14 or C-10 and C-15. If the C-10 to C-14 linkage was present, then the remaining ring would link C-15 to either C-18 or C-19. On the other hand, if the C-10 to C-15 linkage was present, C-14 would link to either C-18 or C-19. The presence of two oxygenated quaternary carbon atoms with ^{13}C NMR shifts of 84.5 and 86.0 ppm was suggestive of a 5-membered ether linkage (Blunt et al., 1978; Sakemi et al., 1986; Suzuki et al., 1993; Manriquez et al., 2001 and Manzo et al., 2007), which would only occur for the C10-C14/C15-C18 linkages. A search of the literature revealed that the linkage between C-15 and C-18 was also present within the known related structure, aplysiol B (**130**) (Manzo et al., 2007). A comparison of the ^{13}C NMR data for the ring system B-D showed excellent agreement (see Table 8).

	Aplysiol B	Aplysiol C
Carbon	^{13}C	^{13}C
1	31.0	31.0
2	74.9	74.9
3	59.1	59.1
4	28.2	28.3
5	37.1	37.1
6	74.4	74.2
7	86.5	86.5
8	23.0	23.0
9	38.6	38.7
10	71.4	71.5
11	76.6	76.5
12	21.3	21.5
13	21.4	21.3
14	75.4	75.4
15	84.3	84.3
16	35.8	35.8
17	25.9	25.9
18	86.4	85.8

Table 8. ^{13}C NMR data for the Carbon skeleton rings A-D for aplysiol B (Manzo et al., 2007) and aplysiol C at 150MHz in $CDCl_3$ with chemical shifts (ppm) referenced to $CDCl_3$ (77.0 ppm).

The relative configuration of the chiral centres was determined by the proximity of the substituent based on NOESY correlations and the magnitude of coupling constant which established the same stereochemistry for the ABC ring system as thyrsiferol (Blunt et al., 1978). Moreover, the A-D ring system showed identical stereochemistry to aplysiol B (Manzo et al., 2007). The observed NOESY correlation between H-3 (δ 3.73) and H_3-1 (δ 1.32), together with the NOESY correlation between H_3-25 (δ 1.37) and H_3-26 (δ 1.12) suggested the relative configuration at C-3 and C-6 as *R** and *S** respectively. The NOESY correlations from H_3-1 to both H-3 and H-7 together with a weak NOESY correlation between H-7 and H_3-26 suggested the relative configuration at C-7 as *R** in nature. Moreover, strong NOESY correlation between H-7 and H-11 and the absence of a NOESY correlation between H-11 and H_3-27 (δ 1.22) enabled the relative stereochemistry of the ring B ether linkage and ring B/C junction to be deduced as ***syn*** and ***trans*** respectively.

The NOESY correlation between H_3-27 (δ 1.22) and H_3-28 (δ 1.11) indicated that the stereochemistry of the ring C ether linkage had H_3-27 and H-14 in an ***anti*** configuration. NOESY data was also indicative of a boat conformation for ring C, as had previously been observed in thyrsyferol (**105**) (Blunt et al., 1978). NOESY correlations observed between H-11 (δ 3.48) and H-13α (δ 1.71) together with correlations between H-13α (δ 1.71) and H_3-28 (δ 1.11) allowed the relative configuration at C-15 to be deduced as *R**. The similarity of NMR data for aplysiols B and C are indicative of them having the same stereochemistries at C-15, C-18 and C-19. The discussion of the stereochemistry of aplysiol B by Manzo et al., 2007 shows a model to explain the nuclear Overhauser effects observed in a ROESY experiment, where the model has ***anti*** geometry for the carbon chain about the ring D ether linkage. However, the structure drawn in that paper for aplysiol B has ***syn*** geometry for the carbon chain about the ring D ether linkage, and C-18, which is labeled as (*R*) is actually depicted as having the (*S*) configuration. The structure shown below for Aplysiol C is in line with their model for aplysiol B, with an *R* configuration at C-18.

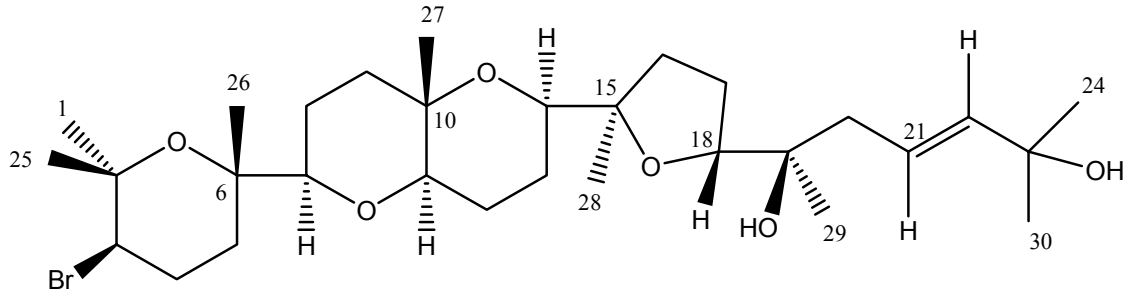

aplysiol C **(147)**

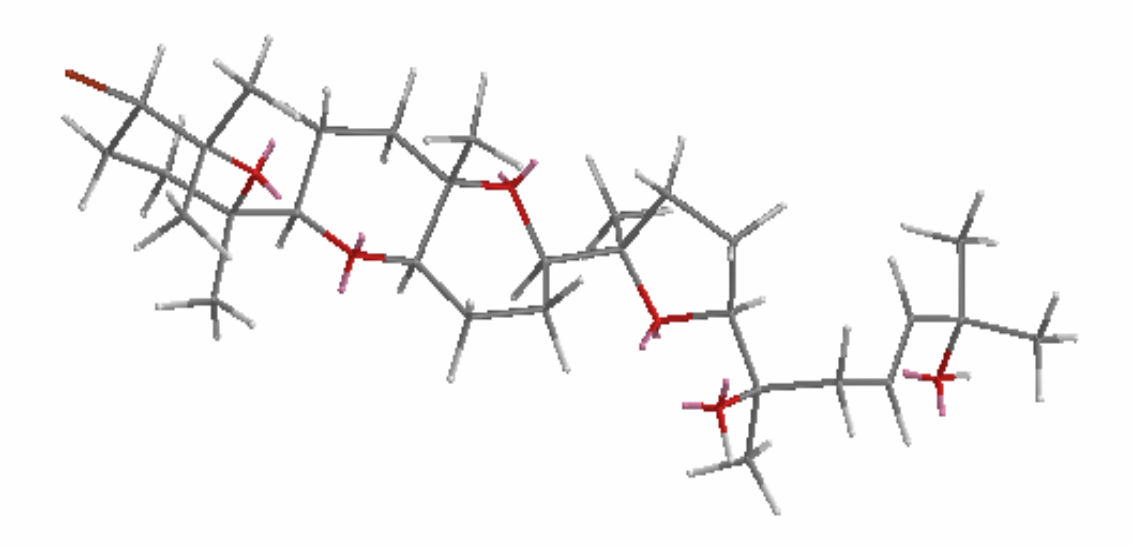

Figure 21. MM2 minimised Chem3D model of aplysiol C based on stereochemistry predicted by observed 1D NOESY correlations and coupling constants

2.1.3.6 Aplysiol D (148)

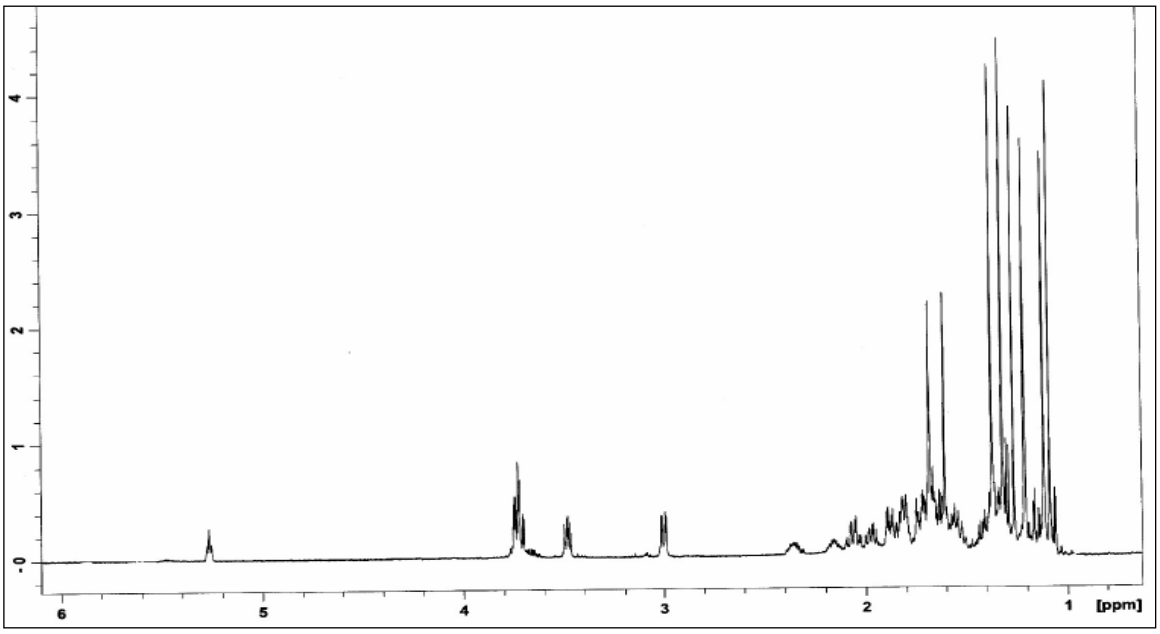

Figure 22. ^{1}H NMR spectrum of aplysiol D at 600 MHz in C_6D_6

A second, closely related new brominated triterpene polyether, aplysiol D was also isolated. Analysis of the ^{1}H NMR spectrum in C_6D_6 (Table 9) revealed a signal due to a bromomethine proton at δ 3.73 (H-3), an olefinic protons at δ 5.26 (H-22) and four oxygenated methine protons at δ 3.00 (H-7), 3.48 (H-11), 3.70 (H-14) and 3.72 (H-18). Furthermore, the ^{1}H-NMR spectrum exhibited six tertiary methyl groups which were indicated by the presence of six singlets at δ 1.08, 1.12, 1.21, 1.32, 1.37 and two allylic methyl groups at δ 1.61 and 1.68. In addition, a number of methylene proton signals were present between δ 1.32 and 2.35. The proton signals were assigned to their respective carbon atoms by an HSQC experiment.

Selective gradient TOCSY and COSY experiment allowed the spin systems of the molecule to be determined. Thus, in the TOCSY experiment, Irradiation of the bromomethine proton at δ 3.73 (H-3) enhanced the methylene signals at δ 2.07 and 1.88 (H_2-4) and 1.67 and 1.32 (H_2-5). The methine proton at δ 3.0 (H-7) showed correlations with the methylene proton signals at δ 1.37 and 1.74 (H_2-8) and 1.81 and 1.56 (H_2-9) as well as the methyl signal at δ 1.21 (H_3-27). The methine protons at δ 3.48 (H-11) and 3.70 (H-14) were in a spin system that also contained a pair of methylene group: δ 1.52 and 1.81 (H_2-12) and δ 1.68 (H_2-13). The signal at δ 3.72 (H-18) showed correlations with the methylene proton signals at δ 1.82 and 1.62 (H_2-17) as well as δ 1.97 and 1.62 (H_2-16). The double bond proton at δ 5.26 was linked to the methylene groups with signals at δ 2.35 and 2.15 (H_2-22) and at δ 1.65 and 1.40 (H_2-21) as well as the methyl

groups at δ 1.26 (H_3-29), δ 1.68 (H_3-24) and 1.61 (H_3-30). The sequences of these spin systems were determined from a COSY experiment. Therefore, selective gradient TOCSY, COSY and HSQC experiments enabled five sub units of the molecule: C3—C5, C7—C9—C27, C11—C14, C15—C18 and C19—C24(—C30) to be established.

The spectroscopic data for aplysiol D was very closely related to that of aplysiol C except for the presence of only one signal attributed to the olefinic proton at C-22. Thus, the same ABCD ring system as that of aplysiol C (**147**) was indicated. A terminal gem-dimethyl substituted double bond replaced the terminal alcohol functionality of aplysiol C. The relative stereochemistry of aplysiol D was then determined by means of 1D selective NOESY spectra which indicated the same configuration with aplsyiol C in all chiral centres.

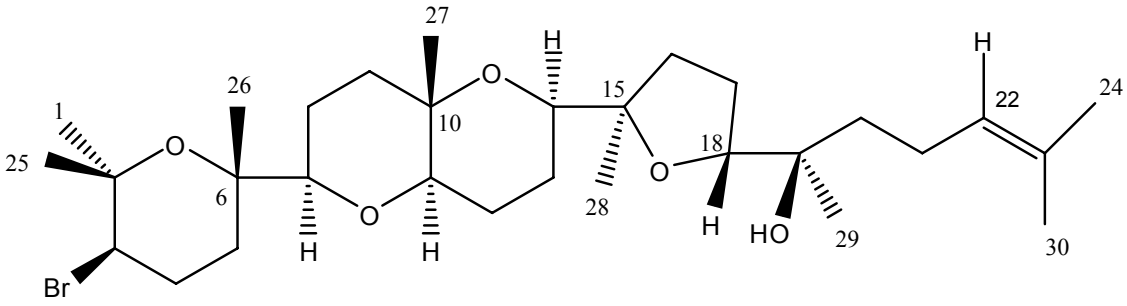

Aplysiol D (148)

Aplysiol C **(147)**					Aplysiol D **(148)**			
C	δ ^{13}C	δ ^{1}H	Multiplicities	HMBC	δ ^{13}C	δ ^{1}H	Multiplicities	HMBC
1	31.0	1.32	s	C2, C3,C25	31.4	1.32	s	C2, C3,C25
2	75.0				75.2			
3	58.7	3.73	dd 12.4, 4.1	C1, C2, C25,C4, C5	59.2	3.73	dd 12.4, 3.8	C2, C25
4	28.1	1.88	m		28.7	1.88	m	
		2.05	dd 12.9, 3.7	C2		2.07	m	C2
5	37	1.67	m		37.6	1.67	m	C2
		1.33	m			1.32	m	C2
6	74.4				74.6			
7	86.7	3.00	dd 11.6, 2.5	C6, C9, C11, C26	87.3	3.00	dd 11.6, 2.6	C5, C6, C11
8	22.9	1.74	m		23. 9	1.74	m	
		1.37	m			1.37	m	
9	38.7	1.57	m	C10, C27	39.3	1.56	m	C10
		1.82	m			1.81	m	C7, C10
10	71.5				71.5			
11	76.7	3.48	dd 11.1, 7.5	C7, C9, C10, C27	77.1	3.48	dd 11.1, 7.5	C7, C9, C10, C27
12	21.6	1.83	m	C10, C11	21.9	1.81	m	C11
		1.54	m	C11, C14		1.52	m	
13	21.6	1.71	m	C11, C12, C14	22	1.68	m	
		1.68	m	C12		1.68	m	
14	75.5	3.72	dd 11.9, 3.5	C13, C15, C16	75.8	3.70	dd 11.8, 3.7	
15	84.2				84.5			
16	36.5	1.99	m	C14, C15, C17,C28	36.8	1.97	m	C14, C15
		1.65	m	C18, C28		1.62	m	C17
17	25.9	1.66	m	C18	26.3	1.62	m	
		1.85	m	C18		1.82	m	C18
18	85.9	3.77	dd 9.7, 5.5	C16, C20, C29	86.9	3.72	m	C14, C29
19	72.4				72.2			
20	41.2	2.37	m	C18, C19, C21, C22, C29	38.4	1.65	m	C18
		2.07	m	C18, C19, C21, C22, C29		1.40	m	
21	121.8	5.84	ddd 15.5, 8.2, 6.7	C20,C23	22.8	2.35		C20
						2.15		C20
22	141.7	5.59	d 15.5	C20,C23	125.6	5.26	t sept, 7.1, 1.4	C30
23	70.0				131.2			
24	29.8	1.20	s	C22, C23, C30	25.9	1.68	s	C22, C23, C30
25	23.6	1.37	s	C1,C2, C3	23.9	1.37	s	C1,C2, C3
26	19.7	1.12	s	C5, C6, C7	20.3	1.12	s	C5, C6, C7
27	21.6	1.22	s	C9, C10, C11	21.8	1.21	s	C9, C10, C11
28	21.3	1.11	s	C14, C15, C16	21.7	1.08	s	C14, C15, C16
29	24.4	1.26	s	C18, C19, C20	24.7	1.26	s	C18, C19, C20
30	29.8	1.20	s	C22, C23, C24	17.7	1.61	s	C22, C23, C24

Table 9. NMR data for aplysiol C **(147)** and D **(148)** at 600 MHz (^{1}H) and 150 MHz (^{13}C) in C_6D_6

2.1.3.7 Aplysiol E (149)

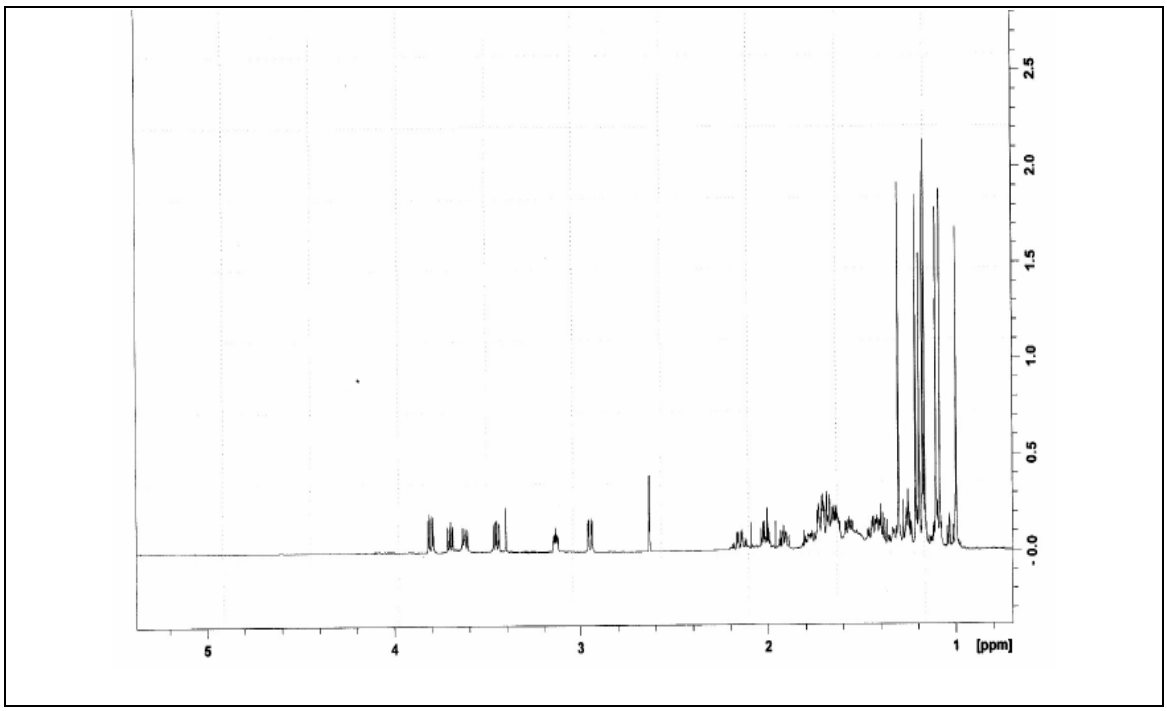

Figure 23. ^{1}H NMR spectrum of aplysiol E **(149)** at 600 MHz in $CDCl_3$

The molecular formula of aplysiol E was determined as $C_{30}H_{52}BrClO_7$ from high-resolution mass spectrometric measurement of the $[M-H]^-$ ion produced by negative ion electrospray ionization. As the NMR data showed no double bond protons, the presence of four rings were required for the molecule. All the protonated carbons were assigned using an HSQC experiment. Analysis of the ^{1}H NMR spectrum exhibited seven methine signals in the low field region at δ 3.90 (dd 12.4, 4.1 Hz, H-3), 3.80 (dd 9.5, 5.8 Hz, H-18), 3.70 (dd 8.4, 6.8, H-14), 3.56 (dd 11.2, 7.3, H-11), 3.22 (ddd 7.1, 4.4, 2.4 Hz, H-21), 3.04 (dd 11.5, 2.5 Hz, H-7) and 2.72 (d 2.5 Hz, H-22). Furthermore, the ^{1}H NMR spectrum revealed eight tertiary methyl groups indicated by the presence of eight singlet signals at δ 1.08, 1.17, 1.19, 1.25, 1.26, 1.28, 1.29 and 1.39.

Selective gradient TOCSY and COSY experiments together with HSQC correlations for the methine protons allowed assignment of the spin systems within the molecule. Irradiation of the bromomethine proton at δ 3.90 induced TOCSY signals for two methylene groups at δ 2.25, 2.10 (H_2-4) and δ 1.81, 1.53 (H_2-5) and a methyl signal at δ 1.19 (H_3-26). The methine signal at δ 3.04 was also linked to two methylene groups at δ 1.72, 1.41 (H_2-8) and δ 1.73, 1.51 (H_2-9) and a methyl signal at δ 1.17 (H_3-27). The methine proton signals at δ 3.56 (H-11) and at δ 3.70 (H-14) were coupled to a pair of methylene groups: δ 1.87, 1.49 (H_2-12) and δ 1.78, 1.76

(H_2-13). The methine proton signal at δ 3.80 (H-18) showed correlations with two methylene groups at δ 1.77, 1.80 (H_2-17), δ 1.65, 1.99 (H_2-16) and a methyl signal at δ 1.08 (H_3-28). The other two methine proton signals, at δ 3.22 (H-21) and 2.72 (H-22), were both in the same spin system as another methylene proton signals at δ 1.81, 1.47 (H_2-20). The sequence of these spin systems was determined from a COSY experiment. Therefore, selective gradient TOCSY, COSY and HSQC experiments allowed five spin systems: C3-C5-C26, C7-C9-C27, C11-C14, C28-C16-C18 and C20-C22 to be established.

The HMBC experiment allowed the spin systems to be connected with quaternary carbons and their methyl substituent. Strong HMBC correlations from the methyl signal at δ 1.26 (H_3-1) and 1.39 (H_3-25) to the carbons resonating at 74.9 ppm (C-2) and 59.0 ppm (C-3) revealed that these two methyls were attached to C-2 (74.9 ppm). The mutual HMBC correlations between the bromomethine proton at δ 3.90 with the two methyl carbon signal at 30.9 ppm (C-1) and 23.5ppm (C-25) and also the HMBC correlation from the bromomethine proton at δ 3.73 to C-2 (74.9 ppm) confirmed the position of the methyl groups. HMBC correlations from H_3-26 (δ 1.19) to C-5 (37.2 ppm), C-6 (74.2 ppm) and C-7 (86.5 ppm) linked C-5 to C-7, while HMBC correlations from H_3-27 (δ 1.17) to C-9 (38.7 ppm), C-10 (71.2 ppm) and C-11 (76.7 ppm) linked C-9 to C-11. In addition, HMBC correlations from H_3-28 (δ 1.08) to C-14 (75.1 ppm), C-15 (84.1 ppm) and C-16 (35.6 ppm) linked C-14 to C-16, while HMBC correlations from H_3-29 (δ 1.28) to C-18 (85.7 ppm), C-19 (72.0 ppm) and C-20 (39.5 ppm) linked C-18 to C-20. The mutual HMBC correlations between the non-equivalent *gem*-dimethyl signals at δ 1.25 and 1.29 (C-24/30) and their correlations to the oxygenated quaternary carbon resonating at 67.6 ppm (C-23) were used to complete the carbon skeleton.

The mutual strong NOESY correlations between the two methyls at δ 1.39 (H_3-25) and δ 1.19 (H_3-26) established the presence of ring A despite the absence of HMBC correlations. The strong HMBC correlation from H-7 (δ 3.04) to the carbon resonating at 76.7 ppm (C-11) and from H-11 (δ 3.56) to the carbon signal at 86.4 ppm (C-7) indicated the presence of ring B and the stereochemistry was determined from the strong mutual NOESY correlations between H-7 (δ 3.04) and H-11 (δ 3.56).

As was the case for aplysiol C, NOESY and HMBC correlations were not helpful for the determination of the cyclisation positions for rings C and D. Rings C and D were then determined to be the same as for aplysiol C based on the very similar NMR data particularly the presence of two oxygenated quaternary carbon atoms with ^{13}C NMR shifts of 84.1 and 85.7 ppm, which was suggestive of a 5-membered ether linkage (Blunt et al., 1978; Sakemi et al.,

1986; Suzuki et al., 1993; Manriquez et al., 2001 and Manzo et al., 2007). A comparison of the ^{13}C NMR data for the ring system B-D showed excellent agreement with aplysiols B (**130**) (Manzo et al., 2007) and C **(147)**.

The relative stereochemistry at chiral centres, with the exception of C-21 and C-22, was deduced as being identical with that observed for aplysiol C based on the correlations from NOESY experiment and the identical NMR data for the ring system. The NOESY effects among the methine proton signal at δ 3.80 (H-18), the methyl signal at 1.28 (H_3-29) and the chloromethine proton signal at δ 3.22 (H-21) together with the NOESY correlations observed among H-21, H-22 and H_3-29 allowed the relative configuration at C-21 and C-22 to be deduced as ***R***. The coupling constant for H-22 (2.5 Hz) was not indicative of free rotation and presumably indicated H-bonding. From the H-21 and H-22 coupling constants, an estimate of dihedral angles can be made. A model with 21*R*, 22*R* stereochemistry where the 19 and 22 OH groups were H-bonded was energy minimized in MM2 (Chem 3D) to afford dihedral angles in accordance with observed coupling constants.

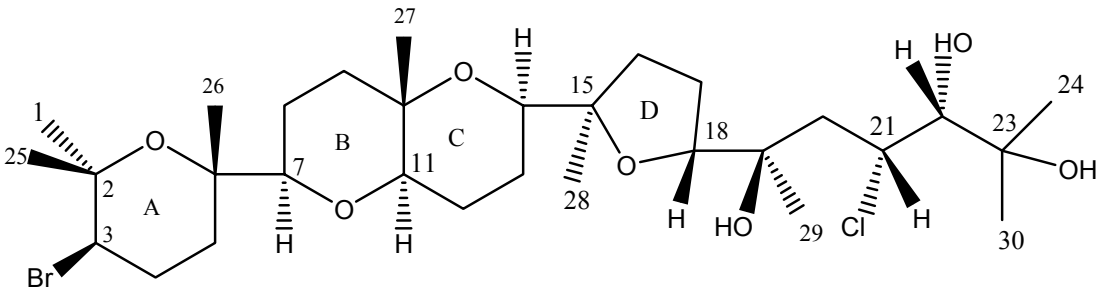

aplysiol E **(149)**

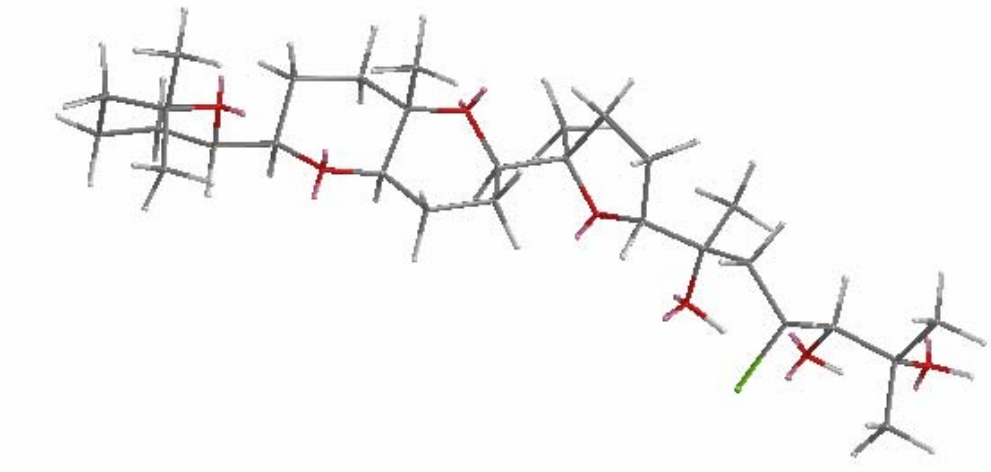

Figure 24**.** MM2 minimised Chem3D model of aplysiol E (**149)** based on stereochemistry predicted by observed 1D NOESY correlatios and coupling constants

Aplysiol C (**147**)			Aplysiol E (**149**)			
C	δ^{13} C	δ^{1}H	δ^{13} C	δ^{1}H	Multiplicities	HMBC
1	31.2	1.26	30.9	1.26	s	C2, C3,C25
2	75.1		74.9			
3	59.3	3.89	59.0	3.90	dd 12.4, 4.1	C1, C2, C25
4	28.5	2.10	28.2	2.10	m	
		2.25		2.25	m	C2
5	37.3	1.81	37.2	1.81	m	C3
		1.53		1.53	m	
6	74.4		74.2			
7	86.7	3.04	86.5	3.04	dd 11.5, 2.5	C5, C6, C8, C11, C26
8	23.2	1.72	23.0	1.72	m	C7, C9
		1.41		1.41	m	
9	38.9	1.53	38.7	1.51	m	C7, C10
		1.81		1.73	m	C7, C10
10	71.7		71.2			
11	76.7	3.55	76.7	3.56	dd 11.2, 7.3	C7, C9, C10, C12
12	21.7	1.87	21.2	1.87	m	C10, C11, C13
		1.51		1.49	m	C13
13	21.5	1.77	21.5	1.78	m	C12
		1.77		1.76	m	C11, C12, C14
14	75.6	3.70	75.1	3.70	dd 8.4, 6.8	C13, C15, C16
15	84.5		84.1			
16	36.0	1.98	35.6	1.99	m	
		1.66		1.65	m	
17	26.1	1.81	26.1	1.77	m	C15
		1.81		1.80	m	C19
18	86.0	3.72	85.7	3.80	dd 9.5, 5.8	
19	72.6		72.0			
20	40.7	2.25	39.5	1.81	m	C19, C21
		2.06		1.47	m	C19, C21, C22
21	122.3	5.68	52.4	3.22	ddd 7.1, 4.4, 2.4	C20
22	141.7	5.68	64.1	2.72	d 2.5	C20, C21, C23
23	70.9		67.6			
24	30.0	1.32	25.0	1.25	s	C22, C23, C30
25	23.9	1.39	23.5	1.39	s	C1,C2, C3
26	20.3	1.19	19.9	1.19	s	C5, C6, C7
27	21.8	1.17	21.6	1.17	s	C9, C10, C11
28	21.5	1.09	21.6	1.08	s	C14, C15, C16
29	24.7	1.14	24.6	1.28	s	C18, C19, C20
30	30.0	1.32	27.8	1.29	s	C22, C23, C24

Table 10. NMR data for aplsyiol C (**147**) and E (**149**) at 600 MHz (^{1}H) and 150 MHz (^{13}C) in $CDCl_3$

2.1.3.8 Intricatetraol (126)

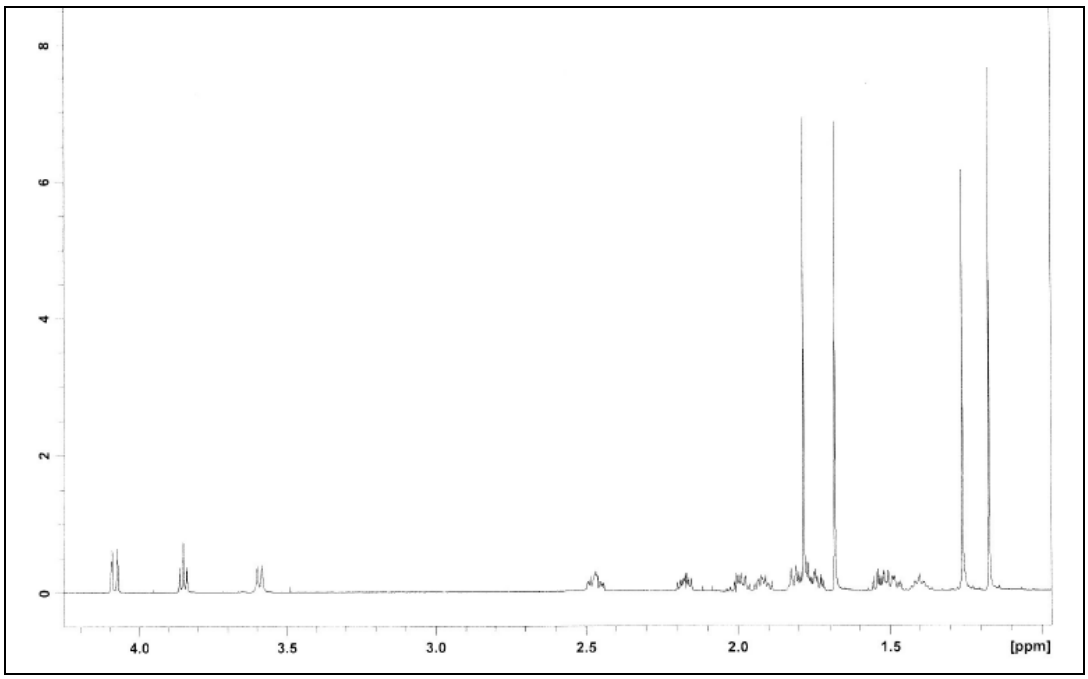

Figure 25. ^{1}H NMR spectrum for intricatetraol (**126**) at 600 MHz in $CDCl_3$

Intricatetraol, $[\alpha]_D^{22}$ +52.5°C [(*c.* 0.17 in $CHCl_3$), $[\alpha]_D^{20}$ Lit +53.0° (Suzuki et al., 1993)], was obtained as a colourless oil. The molecular formula of intricatetraol was determined to be $C_{30}H_{54}Br_2Cl_2O_6$ based on high resolutions ESIMS measurement. However, the ^{13}C NMR data only exhibited 15 carbon signals so was indicative of a symmetrical structure. The ^{1}H NMR spectrum of intricatetraol contained signals for four methyl groups at δ 1.17, 1.26, 1.68 and 1.75, five methylenes, one halomethine proton at δ 4.09 (dd 10.9, 1.4 Hz), and two oxygenated protons at δ 3.58 (br d 10.1 Hz) and 3.85 (t 7.3 Hz). Both the ^{1}H NMR and ^{13}C NMR data were more indicative of a sesquiterpene and thus indicated the presence of C_2 symmetry in intricatetraol.

Gradient selective TOCSY, HSQC and COSY experiments on the three methine protons allowed the three spin systems of the molecule to be identified. Thus, in the TOCSY experiment, irradiation of the methine proton at δ 4.09 induced signals from two methylene groups at δ 2.46 and 1.78 and at δ 1.75 and 1.48. The methine proton at δ 3.85 showed correlations with methylene proton signals at δ 1.98 and 1.91 and δ 2.17 and 1.53. The signal at δ 3.58 was coupled to a methylene group with signals at δ 1.82 and 1.78. These sequences were also confirmed by a COSY experiment.

HMBC data allowed the spin systems to be connected with the quaternary carbons bearing methyl groups. Hence, HMBC correlations from the methyl signals at δ 1.75 (H_3-25/30) and δ

1.68 (H_3-1/24) to the carbon resonances at 72.0 ppm (C-2/23) and 66.9 ppm (C-3/22) indicated these methyls are formed a gem-dimethyl group on a carbon bearing an electronegative heteroatom with an adjacent methine group that also carried an electronegative heteroatom. The *gem*- dimethyl group was also linked to the spin system of the methine proton at δ 4.09 on C-3/22 by strong correlation from the H-3/22 signal at δ 4.09 to the carbon at 72.0 ppm (C-2). The HMBC correlations from the methyl at δ 1.26 (H_3-26) to the quaternary carbon signals at 73.8 ppm (C-6/19), the methylene carbon at 37.1 ppm (C-5) and the methine carbon at 84.2 ppm (C-7) established the connections for the spin systems based on the methine protons signals at δ 4.09 (H-3/22) and δ 3.85 (H-7/18). The connection of the two spin systems was also confirmed by the correlation from H-7 to the methyl carbon signal at 24.2 ppm (C-26/29) and the quaternary carbon signal for C-6/19.

HMBC correlations from the methine proton at δ 3.58 (H-11/14) to the quaternary carbon resonating at 86.1 ppm (C-10/15) and the methylene carbon at 31.7 ppm (C-9/16) allowed the connection the above two spin systems. This was also supported by the correlation from the methyl signal at δ 1.17 (H_3-27/28) to the quaternary carbon resonating at 86.1 ppm (C-10/15), the carbon resonating at 31.7 ppm (C-9/16) and to the methine carbon signal at 77.6 ppm (C-11/14).

According to the molecular formula, intricatetraol contained six oxygen atoms and required two degree of unsaturation. However, four oxygenated carbons (C-6/19 at 73.8 ppm, C-7/18 at 84.2 ppm, C-10/15 at 86.1 ppm and C-11 at 77.6 ppm) were observed in the ^{13}C NMR data for half of the molecule, which suggested an ether bridged linkage between C-7 and C-11. The presence of this ring was established from the mutual NOESY correlations between the methyl signal at δ 1.17 (H_3-27/28) and the methine proton at δ 3.85 (H-7/18) despite the absence of an HMBC correlation.

The NMR data of this metabolite were very similar to those reported for intricatetraol isolated from *Laurencia intricata* (Suzuki et al., 1993). However, some differences were observed in the H and ^{13}C NMR data. In the H NMR spectrum, the differences were observed for signals from the methylene protons H_2-5/20 at δ 1.75 and 1.48, the H_2-12/13 protons at δ 1.82 and 1.78 and H_2-8/17 at δ 1.91and 1.98. These protons were previously reported with a single proton resonance frequency in each case i.e they were reported to resonate at δ 1.50 (H_2-5/20), δ 1.75 (H_2-12/13) and at δ 1.90 (H_2-8/17). In ^{13}C NMR data, the difference was observed for C-3 (66.9 ppm) which was previously reported at 67.5 ppm. This is likely to be concentration effect. The similarity of the NMR data and the value of the specific optical rotation suggested the metabolite is in fact intricatetraol. The relative stereochemistries of two oxalane rings in

intricateraol isolated from *Laurencia intricata* were proposed by the authors of the first report (Suzuki et al., 1993) and the absolute stereochemistry of intricatetraol was determined by chemical synthesis (Yoshiki et al., 2007a).

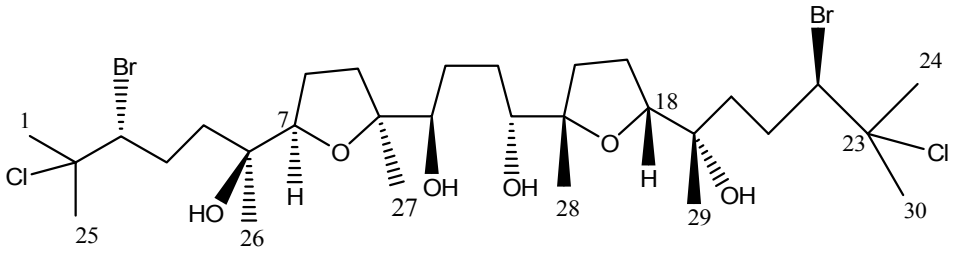

intricatetraol (**126**)

Position	Intricatetraol (**126**)			Observed HMBC
	$\delta^{13}C$	$\delta\ ^{1}H$	Multiplicities	
1(24)	27.5	1.68	s	C-2 (23), C-3 (22), C-25 (30)
2 (23)	72.0			
3 (22)	66.9	4.09	dd, 10.9, 1.4 Hz	C-1 (24), C-2 (23), C-5 (20)
4 (21)	28.9	1.78	m	C-2 (23), C-3 (22)
		2.46	m	C-6 (19)
5 (20)	37.1	1.48	m	
		1.75	m	
6 (19)	73.8			
7 (18)	84.2	3.85	t , 7.3 Hz	C-26 (29), C-8(17), C-6 (19)
8 (17)	26.6	1.98	m	C-7 (18), C-6 (19)
		1.91	m	
9 (16)	31.7	1.53	m	
		2.17	m	
10 (15)	86.1			
11 (14)	77.6	3.58	br d, 10.1 Hz	C-12 (13), C-9 (16), C-10 (15) C-27 (28)
12 (13)	29.4	1.78	m	
		1.82	m	
25 (30)	32.9	1.75	s	
26 (29)	24.2	1.26	s	C-5 (20), C-7 (18), C-6 (19)
27 (28)	23.9	1.17	s	C-9 (16), C-11 (14), C-10 (15)

Table 11. NMR data for intricatetraol (**126**) at 600 MHz (^{1}H) and 150 MHz (^{13}C) in $CDCl_3$

2.1.4 Diketopiperazine (dihydrodysamide C) (150)

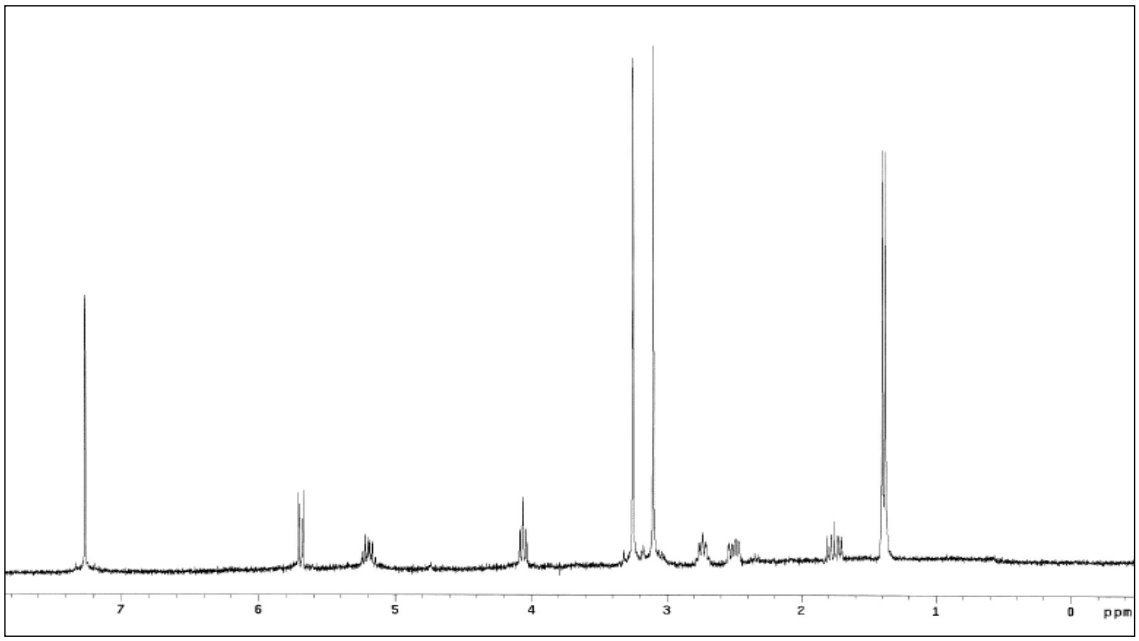

Figure 26. ^{1}H NMR spectrum for dihydrodysamide C (**150**) at 300 MHz in $CDCl_3$

Dihydrodysamide C was isolated as an optically active colourless oil with $[\alpha]_D^{22}$ = -91.7^{0}C (*c.* 0.11 in CHCl3). The ^{1}H NMR spectrum of dihydrodysamide C (**150**) showed two *N*-methyl singlets at δ 3.24 and δ 3.09, a methyl doublet at δ 1.36 (*J* = 6.6 Hz, integrated for 6 H), three methine protons at δ 2.73, 4.05 and 5.20, a methylene group at δ 1.75 and 2.49 and a vinyl proton at δ 5.69. The ^{13}C NMR spectrum showed the presence 14 carbon signals and the protonated carbons were all assigned using an HSQC experiment. The presence of two trichloromethyl groups was evident from the characteristic ^{13}C NMR signals at 105.1 and 104.1 ppm. The carbon signals at 159.7 and 165.4 ppm together with the carbon resonates at 33.9 and 31.4 ppm, which corresponded to the methyl proton signals at δ 3.09 and δ 3.24 respectively in the HSQC experiment, suggested the presence of two CONMe groups. In addition, the presence of a trisubstituted double bond was revealed by signals resonating at 123.8 and 131.7 ppm in the carbon spectrum and supported by a vinyl proton signal at δ 5.69 in ^{1}H NMR spectrum. The remainder of the ^{13}C NMR was accounted for two methyl signals at 17.5 and 18.4 ppm, one methylene signal at 37.6 and three methine carbons at 51.4, 51.6 and 61.9 ppm.

The TOCSY and COSY data together with results from HSQC experiment allowed two spin systems to be identified in the molecule. In the TOCSY spectrum, H-3 (δ 5.69) showed correlations with the methine proton signal at δ 5.20 (H-4) and a methyl doublet signal at δ 1.36

(H_3-5). The methine proton at δ 4.05 (H-2') was correlated with the methylene protons at δ 1.75 and 2.49 (H_2-3'), the *N*-methyl proton signals at δ 3.24, the methine proton signal at δ 2.73 and also the methyl signal at δ 1.36 (H_3-5'). The sequence of the spin systems was also elucidated by a COSY experiment.

The HMBC experiment enabled the two spin systems to be connected with the N-methyl groups and the quaternary carbons. Thus, HMBC correlations observed from the N-methyl at δ 3.24 (NMe-7) to the carbon resonances at 131.7 (C-2) and 165.5 ppm confirmed the location of olefinic bond at C-2 and the carbon resonating at 165.5 ppm at C-1. Another N-methyl at δ 3.09 (NMe-7') showed correlations with the carbons resonating at 61.7 and 159.7 ppm, and thus suggested that the carbon resonating at 61.7 and 159.7 ppm were located at C-2' and C-1' respectively. The methyl signal at δ 1.36 showed a correlation with the carbon signal at 105.1 ppm and thus indicated the location of C-6. This was also supported by an HMBC correlation from H-3 to the carbon signal at 105.1 ppm. The methylene proton signal at 2.49 (H_{2b}-3') was correlated to the carbon signal at 104.1 ppm, thus indicating the location of C-6'. Moreover, the methyl signal at δ 1.36 (actually 2 different methyl doublets) was also correlated with the methine carbon signals at 51.4 and 51.6 ppm in addition to the methylene carbon signal at 37.6 ppm (C-3'). Hence, the assignments for C-4, C-4'and C-3' were indicated.

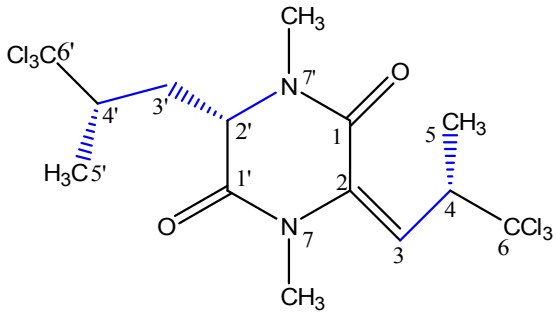

(**150**) dihydrodysamide C

	Dihydrodysamide C(**150**)			
Position	$\delta^{13}C$	δ ^{1}H	Multiplicities	Selected HMBC correlations
1	159.7			
2	131.7			
3	123.8	5.69	d, 9.4 Hz	C-6
4	51.4	5.2	m	
5	18.4	1.36	d, 6.6 Hz	C-3, C-4, C-6
6	105.1			
1'	165.4			
2'	61.9	4.05	t, 6.8 Hz	C-1, C-1’
3'	37.6	1.75	m	C-6’
		2.49	ddd, 1.7 7.3, 14.2 Hz	C-6’
4'	51.6	2.73	m	
5'	17.5	1.36	d, 6.6 Hz	C-3’, C-4’,C-6’
6'	104.1			
NMe (7)	31.4	3.24	s	C-1’, C-2
NMe (7’)	33.9	3.09	s	C-1, C-2’

Table 12. NMR data for dihydrodysamide C (**150**) at 300MHz (^{1}H) and 150 MHz (^{13}C) in $CDCl_3$

The NMR data of this molecule were identical with the previous reports of diketopiperazine (Kazlauskas et al., 1978 and Dumdei et al., 1997), thus suggesting the same stereochemistry. The stereochemistry at the four stereogenic centres was proposed to be 2*S*, 2'*S*, 4*S*, and 4'*S* by Dumdei et al (1997). The absolute configuration with all-*S* stereochemistry has been consistent with other hexachlorinated diketopiperazines isolated from *Dysidea herbacea* (Su et al., 1993, Dumdei et al., 1997 and Fu et al., 1998).

Dysidea herbacea was also prevalent in the area where the *Chondria* sample was collected, so it is likely that the *Chondria* sample may have been contaminated by *Dysidea herbacea* (e.g. growing on rocks along with *D. herbacea*) or that the *Chondria* sample had absorbed some diketopiperazine (exuded by *D. herbacea*) from the water column. It is also possible that microorganisms that produce diketopiperazines in *D. herbacea* may be compatible with *Chondria armata*.

2.2 Cytotoxicity Assays for isolated metabolites

Cytotoxicity assays involving the P388D1 mouse lymphoma cell line (See Table 13) revealed that the known diketopiperazine, dihydrodysamide C, and a new triterpene polyether, armatol J were the most cytostatic of all the purified metabolites tested, both with IC_{50} values of 5μg/ml. The other two new triterpene polycyclic ethers, armatol G and aplysiol C, showed moderate activity with IC_{50} value of 18 and 25 μg/ml respectively. Armatol H and I had been reported to have moderate cytotoxic activity with IC_{50} values of 5.8 and 6.3 μg/ml respectively (Agrawal and Bowden, 2007). In contrast, the C_{15} acetogenins (laurenyne and obtusenyne) and the known triterpene polyether, intricatetraol showed weak cytotoxic activity while angasiol and angasiol acetate were found to be inactive. (-) (*Z*)-pinnatifidenyne and aplysiols D and E were not tested due to decomposition of the compounds.

Compound	IC_{50} (μg/ml)
Armatol G (**145**)	18
Armatol J (**146**)	5
Aplysiol C (**147**)	25
Obtusenyne (**27**)	26
Laurenyne (**26**)	36
(-)-Angasiol (1**43**)	>50
(-)-Angasiol acetate (**144**)	50
Intricatetraol (**126**)	31
Dihydrodisamide C (**150**)	5

Table 13. Cytotoxic activity of pure compounds isolated in this study

Further cytotoxicity assays should be undetaken to investigate whether the more potent compounds, diketopiperazine (dihydrodisamide C) and armatol J, target specific types of cancer. It would be beneficial to retest these compounds against at least five different cancer lines: breast cancer (MCF7), acute promyeolocytic leukemia (HL-60), glioma (SF-268), a large cell lung cancer (NCI-H460), and mouse neuroblastoma/glioma hybrid (NG-108) as these cell lines are the standard cell line panel for preliminary screening as proposed by the National Cancer Institute.

CHAPTER 3

Experimental Part

3.1 General

3.1.1 High-Performance Liquid Chromatography

Preparative high-performance liquid chromatography (HPLC) was performed using a GBC LC 1150 HPLC pump, a Rheodyne 7725i manual injector with a 2.5 ml sample loop, and various C-18 columns (described under individual separation procedures). Samples were observed at multiple UV/Vis wavelengths simultaneously with a GBC LC 5100 Photodiode Array Dector (PDA) and WinChrom Chromatography Data System (Version 1.3.1) software. Flow rates ranged from 1-3 ml/min. Distilled water and LR grade acetonitrile were filtered through a Millipore 0.45 μm HA (water) or FH (acetonitrile) membrane filter, and degassed by sparging with helium for 15 minutes.

3.1.2 Spectroscopy

NMR spectra were measured at 300 MHz on a Varian Mercury spectrometer and at 600 MHz on a Bruker Avance spectrometer with cryoprobe. Optical rotations were observed on a Jasco P-1020 digital polarimeter.

Melting points (m.p.) were determined with a Stuart Scientific SMP1 melting point apparatus. Infrared (IR) spectra were taken in AR grade $CHCl_3$ using a Nicolet Nexus Fourier Transform IR spectrometer. Electro spray ionisation mass spectrometry (ESI-MS) was performed in HPLC grade MeOH with a Bruker BioApex 47e Fourier Transform Ion Cyclotron Resonance Mass Spectrometer by Ms. Cherrie Motti at the Australian Institute of Marine Science, Townsville.

3.1.3 X-ray Crystallographic Details for Armatol G

Crystal data for Armatol G: $C_{30}H_{52}Br_2O_6$, M = 668.54, 0.30 × 0.10 × 0.05 mm^3, monoclinic, space group $P2_1$ (No. 4), a = 11.746(2), b = 7.1226(14), c = 18.855(4) Å, β = 99.42(3)°, V = 1556.1(5) Å^3, Z = 2, D_c = 1.427 g/cm^3, F_{000} = 700, Bruker X8 Apex II CCD, MoKα radiation, λ = 0.71073 Å, T = 123(1)K, $2\theta_{max}$ = 60.1°, 13576 reflections collected, 7026 unique (R_{int} = 0.0465). Final *GooF* = 0.980, *R1* = 0.0522, *wR2* = 0.0959, *R* indices based on 4780 reflections

with I >2sigma(I) (refinement on F^2), 353 parameters, 1 restraint. Lp and absorption corrections applied, μ = 2.644 mm^{-1}. Absolute structure parameter = 0.015(10) (Flack, H. D. *Acta Cryst*. **1983**, *A39*, 876-881).

3.2 Isolation and fractionation of the dichloromethane extract of *Chondria armata*.

3.2.1 Plant material and extraction

Chondria armata was collected from Hazard Bay, Orpheus Island by Professor Rocky DeNys and frozen until extraction. The freeze dried alga (70.1 gram) was extracted three times with dichloromethane (CH_2Cl_2) 250 mL. The solvent was removed on a rotary evaporator to afford a crude extract (0.629 g) which was rapidly chromatographed on silica gel under vacuum eluted with 25 ml each of 25% CH_2Cl_2/hexane, 50% CH_2Cl_2/hexane, 100% CH_2Cl_2, 10% ethyl acetate (EtOAc) in CH_2Cl_2, 20% EtOAc/CH_2Cl_2, 50% EtOAc/CH_2Cl_2, 100% EtOAc, 10% methanol (MeOH) in EtOAc and 100% MeOH (fractions 1-9)

Fraction 1 eluted with 25% CH_2Cl_2 in hexane was purified by reverse phase HPLC on a C_{18} column (10 x 250 mm) eluted with 87% acetonitrile at a flow rate of 2 ml/min. The fraction with retention time 17.2 min was transferred to a separating funnel, diluted with water and extracted with dichloromethane. The water layer was removed and the dichloromethane layer was evaporated under reduced pressure to afford pinnatifidenyne (4.5 mg, 0.0064 %)

Fraction 2 eluted with 25% CH_2Cl_2 in hexane was a mixture of 3*Z*-laurenyne and obtusenyne. This mixture was separated by reverse phase HPLC on a C_{18} column (10 x 250 mm) eluted with 75 % acetonitrile at a flow rate of 2 ml/min. The fractions with retention times of 24.3 min and 26.8 min were separately transferred to a separating funnel, diluted with water and extracted with dichloromethane. The water layer was removed and the dichloromethane layer was further evaporated under reduced pressure to afford 3*Z* laurenyne (13 mg, 0.019 %) and 3*Z,6R,*7*R*-obtusenyne (20 mg, 0.028 %).

The fraction eluted with 10% ethyl acetate in dichloromethane was further purified through HPLC on a reverse phase column using 79% CH_3CN as the mobile phase to yield angasiol (45.7 mg) and angasiol acetate (3.03 mg).

Intricatetraol (2.74 mg) was obtained after the purification through HPLC on a reverse phase HPLC column from the fraction eluted with 100% ethyl acetate.

Physical properties of pure metabolites isolated

Z-Pinnatifidenyne (142). Colourless oil; $[\alpha]_D^{22}$ = -17.3^0 ($CDCl_3$, *c*. 0.03); $[\alpha]_D^{25}$Lit = + 39^0 ($CHCl_3$, *c*. 13.8) ^{1}H and ^{13}C NMR data, Table 1.

Z-Laurenyne (26). Colourless oil; $[\alpha]_D^{22}$ = + 20^0 ($CHCl_3$, *c*. 0.01); $[\alpha]_D$ Lit = + 30.4^0 ($CHCl_3$, *c*. 0.63); ^{1}H and ^{13}C NMR data, Table 2.

(+)-3*Z*,6*R*,7*R*-Obtusenyne (**27**). Colourless oil; $[\alpha]_D^{22}$ = + 20.7^0($CHCl_3$, c. 0.32); $[\alpha]_D$ Lit = + 10^0 ($CHCl_3$, *c*. 0.2) ^{1}H and ^{13}C NMR data, Table 3.

(-)-Angasiol (143)

White crystals; mp 190-192; $[\alpha]_D^{22}$ -5.9^0 (*c.* 0.24 in $CHCl_3$); Found: [M-HBr +Na^+], 419.1180; $C_{20}H_{29}BrO_3Na$ requires 419.1192; ν_{max} ($CHCl_3$) 3501 cm^{-1}, 1762 cm^{-1}.

^{1}H NMR spectrum ($CDCl_3$): Refer to Table 4

^{13}C NMR spectrum ($CDCl_3$): Refer to Table 4

(-)-Angasiol acetate(144)

White crystals; $[\alpha]_D^{22}$ -2.5^0(*c.* 0.19 in $CHCl_3$); Found [M+Na]$^+$, 541.0571; $C_{22}H_{32}Br_2O_4Na$ requires 541.0560

^{1}H NMR spectrum ($CDCl_3$): Refer to Table 5

^{13}C NMR spectrum ($CDCl_3$): Refer to Table 5

Intricatetraol (126)

Colourless oil; $[\alpha]_D^{22}$ +52.5^0 (*c.* 0.17 in $CHCl_3$), $[\alpha]_D^{20}$ Lit +53.0^0 (Suzuki et al., 1993); Found: [M+Na]$^+$, 763.1536; $C_{30}H_{54}{}^{79}Br_2{}^{35}Cl_2O_6Na$ requires [M+Na]$^+$, 763.1536.

^{1}H NMR spectrum ($CDCl_3$): Refer to Table 11

^{13}C NMR spectrum ($CDCl_3$): Refer to Table 11

3.3 Isolation and fractionation of the methanol extract from a recollection of *Chondria armata*.

3.3.1 Plant material and extraction

Plant material was collected from Hazard Bay, Orpheus Island and frozen until extraction. The freeze-dried alga (140 gram, dried weight) was extracted four times with 450 mL MeOH and the extractions were combined. The solvent was removed at 40°C under vacuum on a rotary evaporator (Büchi) to give crude methanol extract (2.845 g). The methanol extract was partitioned with water and CH_2Cl_2. After removal of the solvent, the CH_2Cl_2 soluble fraction (1.145 g) of the methanol extract was obtained.

3.3.2 Fractionation and Isolation

The CH_2Cl_2 fraction (organic extract) was resuspended in a minimal amount of hexane:CH_2Cl_2 (1:1) and applied to a glass column (i.d. 3 cm, length 12 cm) that had been packed with silica gel (60 H, thin layer chromatography grade; Merck) and solvated with hexane. The column was eluted under vacuum with 25 ml each of 10% CH_2Cl_2 in hexane, 25% CH_2Cl_2/hexane, 50% CH_2Cl_2/hexane, 100% CH_2Cl_2, 10% ethyl acetate (EtOAc) in CH_2Cl_2, 20% EtOAc/CH_2Cl_2, 50% EtOAc/CH_2Cl_2, 100% EtOAc, 10% methanol (MeOH) in EtOAc and 100% MeOH (fractions 1-10). The solvent was removed from each fraction at 30-40°C under vacuum on a rotary evaporator. Fractions eight (100% EtOAc, 240 mg) was further separated using column chromatography with 20 mL of hexane: EtOAc: acetone (2:1:0.5). Fraction 8.2 (98 mg) was purified by reverse phase HPLC [Phenomenex, Luna C18 column, 10µm, 10 x 250 mm] eluted with 90% CH_3CN at a flow rate of 2 mL/min using a diode array detector monitored at 201 nm to afford armatol I (10 mg, 0.07%) with retention time 30 minutes**,** armatol G (3.1 mg, 0.002%) with retention time of 23.4 minutes, armatol J (5.4 mg, 0.004 %) with retention time 41 minutes, aplysiol E (3 mg, 0.002 %) with retention time 43 minutes and aplsyiol C (9.1 mg, 0.06 %) with retention time 61 minutes.

Fraction seven (67 mg) eluted with 50% of ethyl acetate in dichloromethane was further purified with reverse phase HPLC [Phenomenex, Luna C18 column, 10µm, 10 x 250 mm] eluted with 95% CH_3CN at a flow rate of 2 mL/min using a diode array detector monitored at 198 nm to yield armatol H (24.2 mg, 0.02 %) with retention time 25 minutes and a trace amount of armatol J.

Fraction six (30 mg) eluted with 20% ethyl acetate in dichloromethane was further purified with reverse HPLC [Phenomenex, Luna C18 column, 10µm, 10 x 250 mm] eluted with 95% CH_3CN at a flow rate of 2 mL/min using a diode array detector monitored at 199 nm to afford aplsysiol D (14 mg, 0.01 %) with retention time 49.9 minutes.

Fraction five (50 mg) eluted with 10% ethyl acetate in dichloromethane was also further purified with reverse phase HPLC [Phenomenex, Luna C18 column, 10µm, 10 x 250 mm] eluted with 85% CH_3CN at a flow rate of 1 mL/min using a diode array detector monitored at 201 nm to afford the diketopiperazine, dihydrodysamide C (3.08 mg, 0.0022 %) with retention time 38 minutes.

Acetylation of armatol G

Armatol G (1 mg) was treated with acetic anhydride (1 mL) in pyridine (1 mL) for 24 hours at room temperature. The solvent (acetic anhydride and pyridine) was removed under high vacuum. The ^{1}H NMR spectrum was identical with that of armatol H.

Physical properties of pure metabolites isolate

Armatol G (145)

White solid; mp 184-186; $[\alpha]_D^{22}$ +58.7 (*c.* 0.08, $CHCl_3$); (Found: $[M+Na]^+$, 689.2002. $C_{30}H_{52}O_6{}^{79}Br_2Na$ requires $[M+Na]^+$, 689.2023)

^{1}H NMR spectrum (C_6D_6): Refer to Table 6

^{13}C NMR spectrum (C_6D_6): Refer to Table 6

Armatol H (140)

Clear oil; $[\alpha]_D^{22}$ +13.88 (*c.* 0.32, $CHCl_3$); (Found: $[M+Na]^+$, 731.2128. $C_{32}H_{54}O_7{}^{79}Br_2Na$ requires $[M+Na]^+$, 731.2133);

^{1}H NMR spectrum (C_6D_6): Refer to Table 6

^{13}C NMR spectrum (C_6D_6): Refer to Table 6

^{1}H NMR spectrum ($CDCl_3$): 5.28, dd, *J* 10.4, 1.6 Hz, H-11; 4.14, dd, *J* 11.0, 1.1 Hz, H-22; 4.12, dd, *J* 10.9, 1.2 Hz, H-3; 3.51, dd, *J* 10.0, 2.5 Hz, H-14; 3.26, dd, *J* 11.2, 4.9 Hz, H-7; 3.13, dd, *J* 11.3, 3.0 Hz, H-18; 2.24, m, H_2-4; 2.08, m, H_2-21; 1.91, m, H-17a, 1.41, m, H-17b; 1.78, m, H-8a, 1.45, m, H-8b; 1.77, m, H-12a, 1.63, m, H-12b; 1.70, m, H-9a, 1.34, m, H-9b; 1.75, m, H-16a, 1.65, m, H-16b; 1.74, m, H-5a, 1.49, m, H-5b; 1.53, m, H_2-20; 1.44, m, H-13a, 1.20, m, H-13b; 1.34, s, H_3-25; 1.34, s, H_3-24; 1.33, s, H_3-1; 1.21, s, H_3-30; 1.20, s, H_3-26; 1.19, s, H_3-29; 1.09, s, H_3-27; 1.08, s, H_3-28.

^{13}C NMR spectrum ($CDCl_3$): 170.4, OAc; 20.5, OAc; 79.1, C-19; 78.9, C-6; 78.4, C-18; 77.6, C-2; 77.5, C-23; 75.7, C-14; 74.2, C-10; 74.0, C-11; 72.0, C-7; 60.0, C-4; 59.8, C-22; 44.7, C-5; 44.3, C-20; 40.6, C-16; 32.6, C-9; 31.7, C-4; 31.6, C-21; 27.6, C-13; 26.8, C-17; 26.4, C-12; 25.5, C-25; 25.5, C-24; 25.0, C-28; 24.7, C-27; 24.6, C-1; 24.4, C-30; 23.4, C-8; 20.8, C-20; 16.8, C-29.

Armatol I (141)

White solid; mp 159-162; $[\alpha]_D^{22}$ +13.9 (*c.* 0.53 $CHCl_3$); (Found: $[M+Na]^+$, 689.2024. $C_{30}H_{52}O_6{}^{79}Br_2Na$ requires $[M+Na]^+$, 689.2023);

^{1}H NMR spectrum (C_6D_6): Refer to Table 7

^{13}C NMR spectrum (C_6D_6): Refer to Table 7

^{1}H NMR spectrum ($CDCl_3$): 4.17, d, *J* 10.2 Hz, H-22; 3.98, d, *J* 10.2 Hz, H-3; 3.51, d, *J* 10.2 Hz, H-18; 3.26-3.24, m, H-11 and H-7; 2.10, m, H_2-4; 2.1, m, H_2-21; 1.93, m, H-8a, 1.60, m, H-8b; 1.86, m, H-12a, 1.53, m, H-12b; 1.75, m, H-20a, 1.54, m, H-20b; 1.68, m, H-16a, 1.43, m, H-16b; 1.67, m, H-13a, 1.59, m, H-13b; 1.63, m, H-17a, 1.36, m, H-17b; 1.19, m, H-9a, 1.18, m, H-9b; 1.35, s, H_3-1; 1.35, s, H_3-24; 1.34, s, H_3-25; 1.34, s, H_3-30; 1.19, s, H_3-26; 1.12 s, H_3-28; 1.11, s, H_3-27; 1.11, s, H_3-29.

^{13}C NMR spectrum ($CDCl_3$): 78.7, C-19; 77.7, C-23; 77.3, C-2; 77.0, C-7; 75.9, C-18; 74.8, C-11; 74.2, C-6; 73.1, C-10; 71.2, C-14; 60.3, C-3; 59.4, C-22; 45.6, C-5; 41.8, C-16; 39.9, C-20; 34.0, C-9; 31.6, C-21; 31.3, C-4; 28.1, C-17; 27.2, 26.0, C-1; 25.3, C-12; 25.4, C-30; 25.3, C-25; 24.5, C-24; 23.6, C-8; 23.6, C-27; 21.3, C-26; 20.6, C-29; 16.1 , C-28.

Armatol J (146)

White solid; $[\alpha]_D^{22}$ +14.3^0 (*c.* 0.29, $CHCl_3$); (Found: $[M+Na]^+$, 689.2069. $C_{30}H_{52}O_6{}^{79}Br_2Na$ requires $[M+Na]^+$, 689.2023);

^{1}H NMR spectrum (C_6D_6): Refer to Table 7

^{13}C NMR spectrum (C_6D_6): Refer to Table 7

Aplsyiol C (147)

Clear oil; $[\alpha]_D^{22}$ +11.9^0 (*c.* 0.1 in $CHCl_3$); (Found: $[M+Na]^+$, 609.2741. $C_{30}H_{51}O_6Br$ Na requires $[M+Na]^+$, 609.2758)

^{1}H NMR spectrum (C_6D_6): Refer to Table 9

^{13}C NMR spectrum (C_6D_6): Refer to Table 9

^{1}H NMR spectrum ($CDCl_3$): Refer to Table 10

^{13}C NMR spectrum ($CDCl_3$): Refer to Table 10

Aplysiol D (148)

Clear oil;

^{1}H NMR spectrum (C_6D_6): Refer to Table 9

^{13}C NMR spectrum (C_6D_6): Refer to Table 9

Aplysiol E (149)

Clear oil; (Found: [M-H^+], 637.2514. $C_{30}H_{52}O_7BrCl$ requires [M-H^+], 637.2512)

^{1}H NMR spectrum ($CDCl_3$): Refer to Table 10

^{13}C NMR spectrum ($CDCl_3$): Refer to Table 10

Dihydrodysamide C (**150**)

Clear oil; $[\alpha]_D^{22} = -91.7^0$ (*c.* 0.11 in CHCl3)

^{1}H NMR spectrum ($CDCl_3$): Refer to Table 12

^{13}C NMR spectrum ($CDCl_3$): Refer to Table 12

3.4 Cytotoxicity Assays

Cytotoxicity assays were undertaken by Dr. Anna-Marie Babey (School of Veterinary and Biomedical Science, JCU). Cytotoxicity was assessed *in vitro* against the P388D1 mouse lymphoma cell line using the sulphorhodamine (SRB) method (Houghton et al., 2007). The ability of seven pure compounds to inhibit the growth of the P388D1 mouse lymphoma cell line was assessed.

References

Agrawal, M., Bowden F. B., 2007**.** Isolation and Structure Elucidation of Cytotoxic Compounds from Marine Organisms. Unpublished Dissertation**.**

Atta-ur-Rahman., Alvi, K. A., Abbas, S. A., Sultana, T., Shameel, M., Choudhary, M. I., Clardy, J. C., 1991**.** A Diterpenoid Lactone from *Aplysia juliana*. J. Nat. Prod.54, (3), 886-888.

Aydomus Z., Imre, S., Ersoy, L. and Wray, V. 2004. Halogenated secondary metabolites from *Laurencia obtusa*. Nat. Prod. Res. 18(1), 43-49.

Bergmann, W., Feeney, R. J., 1950. The Isolation of a New Thymine Pentoside from Sponges. J. Am.Chem Soc 72, (6), 2809-2810.

Bergmann, W., Feeney, R. J., 1951. Contributions To The Study of Marine Products. XXXII. The Nucleosides of Sponges. J Org Chem 16, (6), 981-987.

Bergmann, W., Burke, D. C., 1955. Contributions To The Study of Marine Products. XXXIX. The Nucleosides of Sponges. III.1 Spongothymidine and Spongouridine 2. J Org Chem 20, (11), 1501-1507.

Blunt, J. W., Hartshorn, M. P., McLennan, T. J., Munro, M. H. G., Robinson, W. T., Yorke, S. C., 1978**.** Thyrsiferol: a squalene-derived metabolite of. Tetrahedron Lett. 19, (1), 69-72.

Boyd, M.R., 1989. Status of the NCI preclinical anti-tumor drug discovery screen, Principles, Practice Oncol. 3, 12.

Brennan, M. R., Kim, I. K., Erickson, K. L., **1993.** Kahukuenes, new Diterpenoids from the Marine Alga *Laurencia majuscula*. J. Nat. Prod 56, (1), 76-84.

Briand, A., Kornprobst, J.-M., Al-Easa, H. S., Rizk, A. F. M., Toupet, L., 1997**.** (-)-Paniculatol, a new ent-labdane bromoditerpene from *Laurencia paniculata*. Tetrahedron Lett.38, (19), 3399-3400.

Caccamese, S., Azzolina, R., Duesler, E. N., Paul, I. C., Rinehart, K. L., 1980. Laurencienyne, a new acetylenic cyclic ether from the marine red alga. Tetrahedron Lett. 21, (24), 2299-2302.

Ciavatta, M. L., Wahidulla, S.; D'Souza, L., Scognamiglio, G., Cimino, G., 2001**.** New bromotriterpene polyethers from the Indian alga *Chondria armata*. Tetrahedron 57, (3), 617-623.

Coll, J. C., Wright, A. D., 1989. Tropical Marine Algae. IV. Novel Metabolites from the Red Alga *Laurencia implicata* (Rhodophyta, Rhodophyceae, Ceramiales, Rhodomelaceae). Aust. J. Chem. 42, (10), 1685-1693.

de Silva, D. E., Schwartz, R. E., Scheuer, P. J., Shoolery, J. N., 1983. Srilankenyne, a new metabolite from the sea hare Aplysia oculifera. *J Org Chem* 48, (3), 395-396.

Dumdei, E. J., Simpson, J. S., Garson, M. J., Byriel, K. A., Kennard, C. H. L., 1997**.** New Chlorinated Metabolites from the Tropical Marine Sponge *Dysidea herbacea*. Aust. J. Chem. 50, (2), 139-144.

Falshaw, C. P., King, T. J., Imre, S., Islimyeli, S., Thomson, R. H., 1980**.** Laurenyne, a new acetylene from *Laurencia obtusa*: crystal structure and absolute configuration. Tetrahedron Lett. 21, (51), 4951-4954.

Fenical, W., Sims, J. J., Radlick, P., 1973**.** Chondriol, a halogenated acetylene from the marine alga *Chondria oppositiclada.* Tetrahedron Lett.14, (4), 313-316.

Fenical, W., B. Gifkins, K., Clardy, J., 1974. X-ray determination of chondriol; a re-assignment of structure. Tetrahedron Lett. 15, (16), 1507-1510.

Fenical, W., Sims, J. J., 1974**.** Cycloeudesmol, an antibiotic cyclopropane containing sesquiterpene from the marine alga, *Chondria oppositiclada* Dawson. Tetrahedron Lett. 15, (13), 1137-1140.

Fernandez, J. J., Souto, M. L., Norte, M., 2000**.** Marine polyether triterpenes. Nat.Prod. Rep. 17, (3), 235-246.

Findlay, J. A., Li, G. 2002. Novel terpenoids from the sea hare *Aplysia punctata*. Can. J. Chem. 80(12), 1697-1707.

Fu, X., Ferreira, M. L. G., Schmitz, F. J., Kelly-Borges, M., 1998**.** New Diketopiperazines from the Sponge Dysidea chlorea. J. Nat. Prod. 61, (10), 1226-1231.

Fukuzawa, A., Miyamoto, M., Kumagai, Y., Abiko, A.., Takaya, Y., Masamune, Tadashi., 1985. Structure of new bromoditerpenes, pinnatols, from the marine red alga *Laurencia pinnata* Yamada. Chem. Lett. 8, 1259-1262.

Fukuzawa, A., Aye, M., Takaya, Y., Fukui, H., Masamune, T., Murai, A., 1989. Laureoxolane, a new bromo ether from *Laurencia nipponica*. Tetrahedron Lett 30, (28), 3665-3668.

Giordano, F., Mayol, L., Notaro, G., Piccialli, V., Sica, Donato., 1990. Structure and absolute configuration of two new polybrominated C15 acetogenins from the sponge *Mycale rotalis*. J. Chem. Soc., Chem. Commun. 1559 - 1561.

González, A. G., Martín, J. D., Martín, V. S., Norte, M., Pérez, R., Ruano, J. Z., Drexler, S. A., Clardy, J., 1982**.** Non-terpenoid C-15 metabolites from the red seaweed *Laurencia pinnatifida*. Tetrahedron 38, (7), 1009-1014.

Gonzalez, A. G., Arteaga, J. M., Fernandez, J. J., Martin, J. D., Norte, M., Ruano, J. Z., 1984. Terpenoids of the red alga *Laurencia pinnatifida*. Tetrahedron 40, (14), 2751-2755.

Gopichand, Y., Schmitz, F. J., Shelley, J., Atta-ur-Rahman., Van der Helm, D., 1981**.** Marine natural products: halogenated acetylenic ethers from the sea hare *Aplysia dactylomela*. J. Org. Chem. 46, (25), 5192-5197.

Hall, J G., Reiss, J A., 1986. Elatenyne - a pyrano[3,2-b]pyranyl vinyl acetylene from the red alga *Laurencia elata.* Aust. J. Chem. 39(9), 1401-9.

Higgs, M. D., John Faulkner, D., 1982**.** Diterpene from *Laurencia obtusa*. Phytochemistry 21, (3), 789-791.

Houghton, P., Fang, R., Techatanawat, I., Steventon, G., Hylands, P. J., Lee, C. C.,2007. The sulphorhodamine (SRB) assay and other approaches to testing plant extracts and

derived compounds for activities related to reputed anticancer activity. Methods 42, (4), 377-387.

Howard, B. M., Fenical, W., 1978**.** Structures of the irieols, new dibromoditerpenoids of a unique skeletal class from the marine red alga *Laurencia irieii*. J. Org. Chem. 43, (23), 4401-4408.

Howard, B. M., Schulte, G. R., Fenical, W., Solheim, B., Clardy, J., 1980**.** Three new vinyl acetylenes from the marine red alga *Laurencia*. Tetrahedron 36, (12), 1747-1751.

Iliopoulou, D., Vagias, C., Harvala, C., Roussis, V., 2002**.** C15 Acetogenins from the red alga *Laurencia obtusa*. Phytochemistry 59, (1), 111-116.

Iliopoulou, D., Mihopoulos, N., Roussis, V., Vagias, C., 2003a**.** New Brominated Labdane Diterpenes from the Red Alga *Laurencia obtusa*. J. Nat. Prod. 66, (9), 1225-1228.

Iliopoulou, D., Mihopoulos, N., Vagias, C., Papazafiri, P., Roussis, V., 2003b**.** Novel Cytotoxic Brominated Diterpenes from the Red Alga *Laurencia obtusa*. J. Org. Chem. 68, (20), 7667-7674.

Irie, T., Suzuki, M., Masamune, T., 1968**.** Laurencin, a constituent of *Laurencia glandulifera* Kützing. Tetrahedron 24, (11), 4193-4205.

Ji, N.-Y., Li, X.-M., Li, K., Wang, B.-G., 2007a. Laurendecumallenes A-B and Laurendecumenynes A-B, Halogenated Nonterpenoid C15-Acetogenins from the Marine Red Alga *Laurencia decumbens*. J Nat Prod. 70, (9), 1499-1502.

Ji, N.-Y., Li, X.-M., Li, K., Ding, L.-P., Gloer, J. B., Wang, B.-G., 2007b**.** Diterpenes, Sesquiterpenes, and a C15-Acetogenin from the Marine Red Alga *Laurencia mariannensis*. J. Nat. Prod. 70, (12), 1901-1905.

Ji, N.-Y., Li, X.-M., Chui C-M., Wang, B.-G., 2007c**.** Terpenes and Polybromoindoles from the Marine Red Alga *Laurencia decumbens* (Rhodomelaceae). Helvetica Chim. Acta 90, (9), 1731-1736.

Ji, N.-Y., Li, X.-M., Chui C-M., Wang, B.-G., 2007d**.** Two new brominated diterpenes from *Laurencia decumbens*. Chi.Chem.Lett. 18, (8), 957-959.

Kazlauskas, R., Murphy, P. T., Wells, R. J., 1978**.** A diketopiperazine derived from trichloroleucine from the sponge. Tetrahedron Lett. 19, (49), 4945-4948.

Kigoshi, H., Shizuri, Y., Niwa, H., Yamada, K., 1981**.** Laurencenyne, a plausible precursor of various nonterpenoid C15-compounds, and neolaurencenyne from the red alga. Tetrahedron Lett. 22, (47), 4729-4732.

Kikuchi, H., Suzuki, T., Kurosawa, E., Suzuki, Minoru., 1991. Constituents of marine plants. 78. The structure of notoryne, a halogenated C15 nonterpenoid with a novel carbon skeleton from the red alga *Laurencia nipponica* Yamada. Bull. Chem. Soc. 64(6), 1763-75.

Kim, K., Brennan, M. R., Erickson, K. L., 1989**.** Lauroxolanes from the marine alga. Tetrahedron Lett.30, (14), 1757-1760.

King, T. J., Imre, S., Öztunc, A., Thomson, R. H., 1979**.** Obtusenyne, a new acetylenic nine-membrered cyclic ether from *Laurencia obtusa*. Tetrahedron Lett. 20, (16), 1453-1454.

Kinnel, R. B., Dieter, R. K., Meinwald, J., Van Engen, D., Clardy, J., Eisner, T., Stallard, M. O., Fenical, W., 1979. Brasilenyne and cis-dihydrorhodophytin: Antifeedant medium-ring haloethers from a sea hare (*Aplysia brasiliana*). Proceedings of the National Academy of Sciences of the United States of America 76(8), 3576-3579.

Kuniyoshi, M., Wahome, P. G., Miono, T., Hashimoto, T., Yokoyama, M., Shrestha, K. L., Higa, T., 2005**.** Terpenoids from *Laurencia luzonensis*. J. Nat. Prod. 68, (9), 1314-1317.

Lyakhova, E. G., Kalinovsky, A. I., Kolesnikova, S. A., Vaskovsky, V. E., Stonik, V. A., 2004**.** Halogenated diterpenoids from the red alga *Laurencia nipponica*. Phytochemistry 65, (18), 2527-2532.

Manríquez, C. P., Souto, M. L., Gavín, J. A., Norte, M., Fernández, J. J., 2001**.** Several new squalene-derived triterpenes from Laurencia. *Tetrahedron* 57, (15), 3117-3123.

Manzo, E., Ciavatta, M. L., Gavagnin, M., Puliti, R., Mollo, E., Guo, Y.-W., Mattia, C. A., Mazzarella, L., Cimino, G., 2005**.** Structure and absolute stereochemistry of novel C15-halogenated acetogenins from the anaspidean mollusc *Aplysia dactylomela*. Tetrahedron 61, (31), 7456-7460.

Manzo, E., Gavagnin, M., Bifulco, G., Cimino, P., Di Micco, S., Ciavatta, M. L., Guo, Y. W., Cimino, G., 2007**.** Aplysiols A and B, squalene-derived polyethers from the mantle of the sea hare *Aplysia dactylomela*. Tetrahedron 63, (40), 9970-9978.

Matsuo, Y., Suzuki, M., Masuda, M., 1995. Enshuol , a novel squalene-derived pentacyclic triterpene alcohol from a new species of the red algal genus *Laurencia*. Chem. Lett. 11, 1043-1044.

McDonald, F. J., Campbell, D. C., Vanderah, D. J., Schmitz, F. J., Washecheck, D. M., Burks, J. E., Van der Helm, D., 1975**.** Marine natural products. Dactylyne, an acetylenic dibromochloro ether from the sea hare *Aplysia dactylomela*. J. Org. Chem. 40, (5), 665-666.

McPhail, K. L., Davies-Coleman, M. T., 2005. (3Z)-Bromofucin from a South African sea hare. *Nat. Prod. Res.* 19, (5), 449 - 452.

Mohammed, K. A., Hossain, C. F., Zhang, L.; Bruick, R. K., Zhou, Y. D., Nagle, D. G., 2004**.** Laurenditerpenol, a New Diterpene from the Tropical Marine Alga *Laurencia intricata* that Potently Inhibits HIF-1 Mediated Hypoxic Signaling in Breast Tumor Cells. *J. Nat. Prod.* 67, (12), 2002-2007.

Newman, D. J., Cragg, G. M., 2004. Marine Natural Products and Related Compounds in Clinical and Advanced Preclinical Trials. J Nat Prod 67, (8), 1216-1238.

Newman, D. J., Cragg, G. M., 2007. Natural Products as Sources of New Drugs over the Last 25 Years. J Nat Prod 70, (3), 461-477.

Norte, M., Fernandez, J.J., Cataldo, F., Gonzalez, A.G., 1989a.
(E)-Dihydrorhodophytin, A C15 acetogenin from the red alga *Laurencia pinnatifida.* Phytochemistry 28, (2), 647-649.

Norte, M., Fernandez, J., Ruano, J. Z., 1989b.Three new bromo ethers from the red alga *Laurencia obtusa*. Tetrahedron 45, (18), 5987-5994.

Norte, M., Gonzalez, A. G., Cataldo, F., Rodríguez, M. L., Brito, I., 1991**.** New examples of acyclic and cyclic C-15 acetogenins from *Laurencia pinnatifida*. Reassignment of the absolute configuration for *E* and *Z* pinnatifidienyne. Tetrahedron 47, (45), 9411-9418.

Norte, M., Fernández, J., Souto, M. L., García-Grávalos, M. D., 1996**.** Two new antitumoral polyether squalene derivatives. Tetrahedron Lett. 37, (15), 2671-2674.

Norte, M., Fernández, J., Souto, M. L., García-Grávalos, M. D., 1997a**.** Thyrsenols A and B, Two Unusual polyether squalene derivatives. Tetrahedron 53, (9), 3173-3178.

Norte, M., Fernández, J., Souto, M. L., 1997b**.** New polyether squalene derivatives from *Laurencia*. Tetrahedron 53, (13), 4649-4654.

Notaro, G., Piccialli, V., Sica, D., Mayol, L., Giordano, F., 1992**.** A Further C15 Nonterpenoid Polybromoether from the Encrusting Sponge *Mycale rotalis*. J. Nat. Prod 55, (5), 626-632.

Ojika, M., Nemoto, T., Yamada, K., 1993. Doliculols A and B, the non-halogenated C15 acetogenins with cyclic ether from the sea hare Dolabella auricularia. Tetrahedron Lett. 34, (21), 3461-3462.

Oztunc A., Imre S., Lotter H., Wagner H., 1989. Ent-13-Epiconcinndiol From the Red Alga *Chondria tenuissima* and Its Absolute Configuration. Phytochemistry 28, (12), 3403-3404.

Pettit, G. R., Herald, C. L., Einck, J. J., Vanell, L. D., Brown, P., Gust, D., 1978**.** Isolation and structure of angasiol. J. Org. Chem 43, (24), 4685-4686.

Pettit, G. R., Herald, C. L., Doubek, D. L., Herald, D. L.; Arnold, E., Clardy, J.,1982. Isolation and structure of bryostatin 1. J Am Chem Soc 104, (24), 6846.

Roberge, M., Cinel, B., Anderson, H. J., Lim, L., Jiang, X., Xu, L., Bigg, C. M., Kelly, M. T., Andersen, R. J., 2000**.** Cell-based Screen for Antimitotic Agents and Identification of Analogues of Rhizoxin, Eleutherobin, and Paclitaxel in Natural Extracts. Cancer Res 60, (18), 5052-5058.

Rochfort, S. J., Capon, R. J., 1996**.** Parguerenes Revisited: New Brominated Diterpenes From the Southern Australian Marine Red Alga *Laurencia filiformis*. Aust. J. Chem. 49, (1), 19-26.

Rowinsky, E K., 1997. The development and clinical utility of the taxane class of antimicrotubule chemotherapy agents. Annu. Rev Medicine 48, 353-74.

Sakemi, S., Higa, T., Jefford, C. W., Bernardinelli, G., 1986**.** Venustatriol. A new, anti-viral, triterpene tetracyclic ether from *Laurencia venusta*. Tetrahedron Lett. 27, (36), 4287-4290.

San-Martin, A., Darias, J., Soto, H., Contreras, C., Herrera, J. S., Rovirosa, J., 1997**.** A New C15 Acetogenin from the Marine Alga *Laurencia claviformis*. Nat. Prod. Res. 10, (4), 303 - 311.

Schmitz, F. J., Gopichand, Y., Michaud, D. P., Prasad, R.S., Remaley, S., Hossain, M. B., Rahman, A., Sengupta, P. K., van der Helm, D., 1981. Recent developments in research on metabolites from Caribbean marine invertebrates. Pure Appl. Chem. 53(4), 853-865.

Schulte, G. R., Chung, M. C. H., Scheuer, P. J., 1983**.** Two bicyclic C15 enynes from the sea hare Aplysia oculifera. J. Org. Chem 46, (19), 3870-3873.

Simmon T. L., Adrianasolo, E., McPhail, Kerry., Flat, Patricia., Gerwick, W.H., 2005. Marine Natural Product as Anticancer Drug. Mol. Cancer Ther 4, 333-342.

Sims J.J., Lin Y.H.G,. Wing M.R., Fenical W., 1973. Marine Natural Products. Concinndiol, A Bromo-diterpene Alcohol from the Red Alga, *Laurencia conncinna*. J.C.S Chem. Comm. 470-471.

Sims, James J., Donnell, M. S., Leary, J. V., Lacy, G. H. 1975. Antimicrobial agents from marine algae. Antimicrobial Agents and Chemotherapy 7(3), 320-321.

Su, J.-Y., Zhong, Y.-L., Zeng, L.-M., Wei, S., Wang, Q.-W., Mak, T. C. W., Zhou, Z.-Y., 1993**.** Three New Diketopiperazines from a Marine Sponge *Dysidea fragilis*. J. Nat.Prod 56, (4), 637-642.

Suenaga, K., Shibata, T., Takada, N., Kigoshi, H., Yamada, K., 1998**.** Aurilol, a Cytotoxic Bromotriterpene Isolated from the Sea Hare *Dolabella auricularia*. J. Nat. Prod 61, (4), 515-518.

Suzuki, T., Suzuki, M., Furusaki, A., Matsumoto, T., Kato, A., Imanaka, Y., Kurosawa, E., 1985**.** Teurilene and thyrsiferyl 23-acetate, meso and remarkably cytotoxic compounds from the marine red alga *Laurencia obtusa* (hudson) lamouroux. Tetrahedron Lett. 26, (10), 1329-1332.

Suzuki, T., Takeda S., Suzuki, M., Kurosawa, E., Kato A., Imanaka Y., 1987. Cytotoxic Squalene Derived Polyethers from the Marine Red Alga *Laurencia obtusa* (Hudson) Lamouroux. Chem. Lett. 2, 361-364.

Suzuki, M., Kurosawa, E., Kurata, K., 1988. Constituents of marine plants. Part 71. Venustanol , a brominated labdane diterpene from the red alga *Laurencia venusta*. Phytochemistry 27 (4), 1209-1210.

Suzuki, M., Matsuo, Y., Takeda, S., Suzuki, T., 1993**.** Intricatetraol, a halogenated triterpene alcohol from the red alga *Laurencia intricata*. Phytochemistry 33, (3), 651-656.

Suzuki, M., Matsuo, Y., Takahashi, Y., Masuda, M., 1995. Callicladol, a novel cytotoxic bromotriterpene polyether from a Vietnamese species of the red algal genus *Laurencia*. Chem Lett. 11, 1045-1046.

Suzuki, M., Takahashi, Y., Matsuo, Y., Masuda, M., 1996b**.** Pannosallene, a brominated C15 nonterpenoid from *Laurencia pannosa*. Phytochemistry 41, (4), 1101-1103.

Suzuki, M., Mizuno, Y., Matsuo, Y., Masuda, M., 1996a**.** Neoisoprelaurefucin, a halogenated C15 non-terpenoid compound from *Laurencia nipponica*. Phytochemistry 43, (1), 121-124.

Suzuki, M., Takahashi, Y., Matsuo, Y., Guiry, M. D., Masuda, M., 1997. Scanlonenyne, a novel halogenated C15 acetogenin from the red alga *Laurencia obtusa* in Irish waters. Tetrahedron 53, (12), 4271-4278.

Suzuki, M., Nakano, S., Takahashi, Y., Abe, T., Masuda, M., 1999. Bisezakyne-A and -B, halogenated C15 acetogenins from a Japanese *Laurencia* species. Phytochemistry 51, (5), 657-662.

Suzuki, M., Daitoh, M., Vairappan, C. S., Abe, T., Masuda, M., 2001**.** Novel Halogenated Metabolites from the Malaysian *Laurencia pannosa*. J. Nat. Prod**.,** 64, (5), 597-602.

Suzuki, M., Nakano, S., Takahashi, Y., Abe, T., Masuda, M., Takahashi, H., Kobayashi, K., 2002**.** Brominated Labdane-Type Diterpenoids from an Okinawan *Laurencia* sp. J. Nat. Prod. 65, (6), 801-804.

Takahashi, Y., Suzuki, M., Abe, T., Masuda, M., 1999. Japonenynes, halogenated C15 acetogenins from *Laurencia japonensis*. Phytochemistry 50, (5), 799-803.

Takahashi, Y., Daitoh, M., Suzuki, M., Abe, T., Masuda, M., 2002**.** Halogenated Metabolites from the New Okinawan Red Alga *Laurencia yonaguniensis*. J. Nat. Prod. 65, (3), 395-398.

Vairappan, C. S., Suzuki, M., Abe, T., Masuda, M., 2001a**.** Halogenated metabolites with antibacterial activity from the Okinawan *Laurencia* species. Phytochemistry 58, (3), 517-523.

Vairappan, C. S., Daitoh, M., Suzuki, M., Abe, T., Masuda, M., 2001b .Antibacterial halogenated metabolites from the Malaysian *Laurencia* species. Phytochemistry 58, (2), 291-297.

Vanderah, D. J., Schmitz, F. J., 1976**.** Marine natural products: isodactylyne, a halogenated acetylenic ether from the sea hare *Aplysia dactylomela*. J. Org. Chem. 41, (21), 3480-3481.

Yamamura, S., Hirata, Y., 1971. Naturally-occurring bromo-compound, aplysin - 20 from *Aplysia kurodai*. Bull. Chem. Soc. 44(9), 2560-2562.

Yoshiki, M., Tatsuya, O., Mamoru, T., Takeshi, T., 2007a. Total Synthesis and Determination of the Absolute Configuration of (+)-Intricatetraol. Angewandte Chemie International Edition 46, (7), 1132-1135.

Yoshiki, M., Hiromi, Y., Yoshihiro, N., 2007b**.** Assignment of the Absolute Configuration of the Marine Pentacyclic Polyether (+)-Enshuol by Total Synthesis13. Angewandte Chemie International Edition 46, (34), 6481-6484.

APPENDICES

APPENDIX 1.1

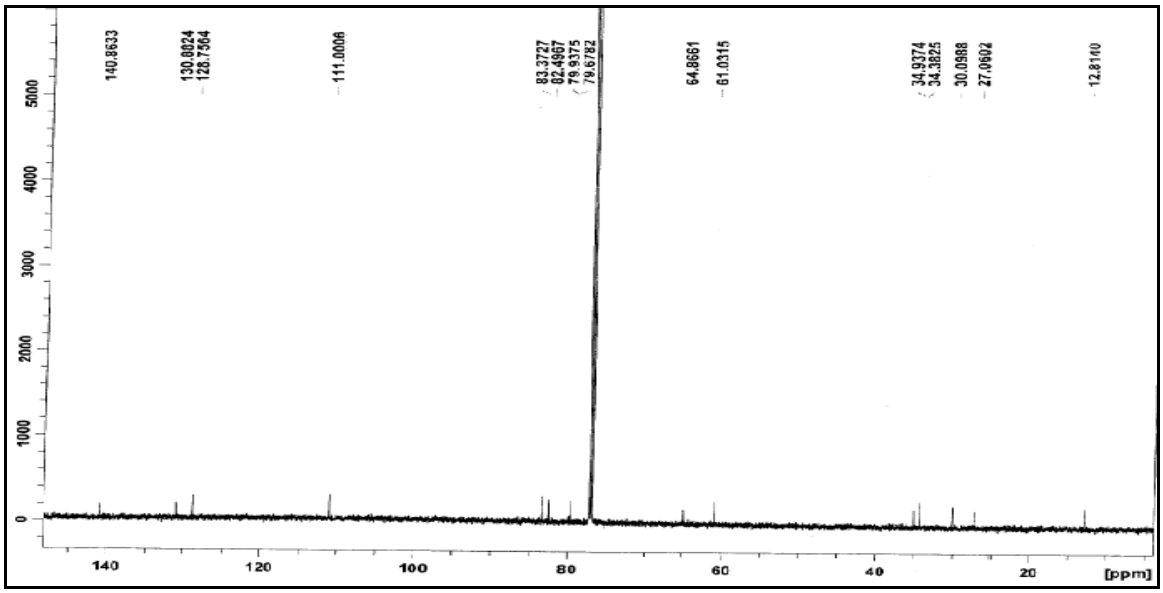

^{13}C NMR spectrum (75 MHz) of (-) (*Z*) pinnatifidenyne in $CDCl_3$

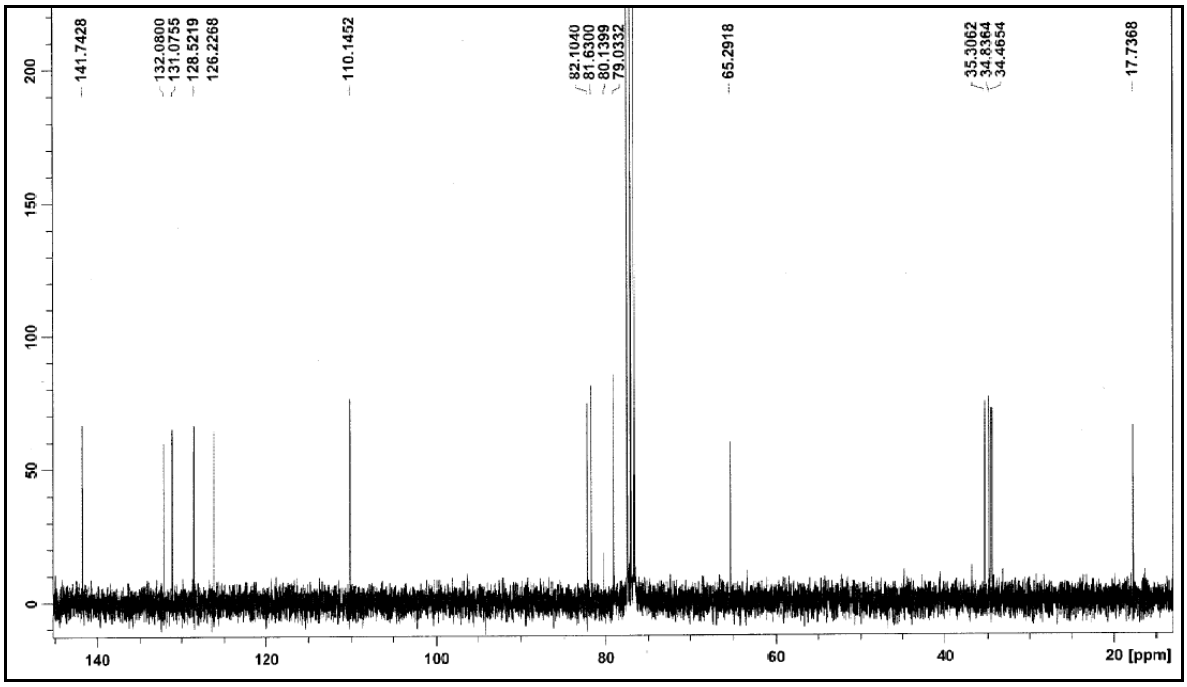

^{13}C NMR spectrum (75 MHz) of 3*Z*-laurenyne in $CDCl_3$

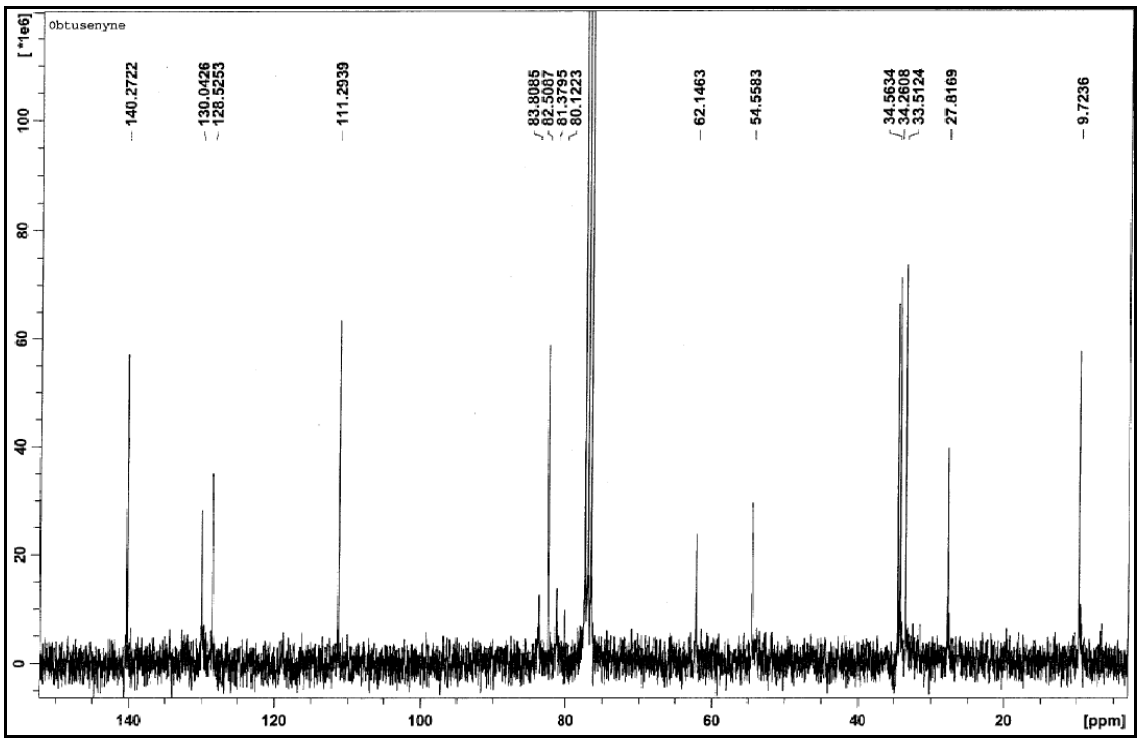

^{13}C NMR spectrum (75 MHz) of (+)-3*Z*,6*R*,7*R*-obtusenyne in $CDCl_3$

APPENDIX 1.2

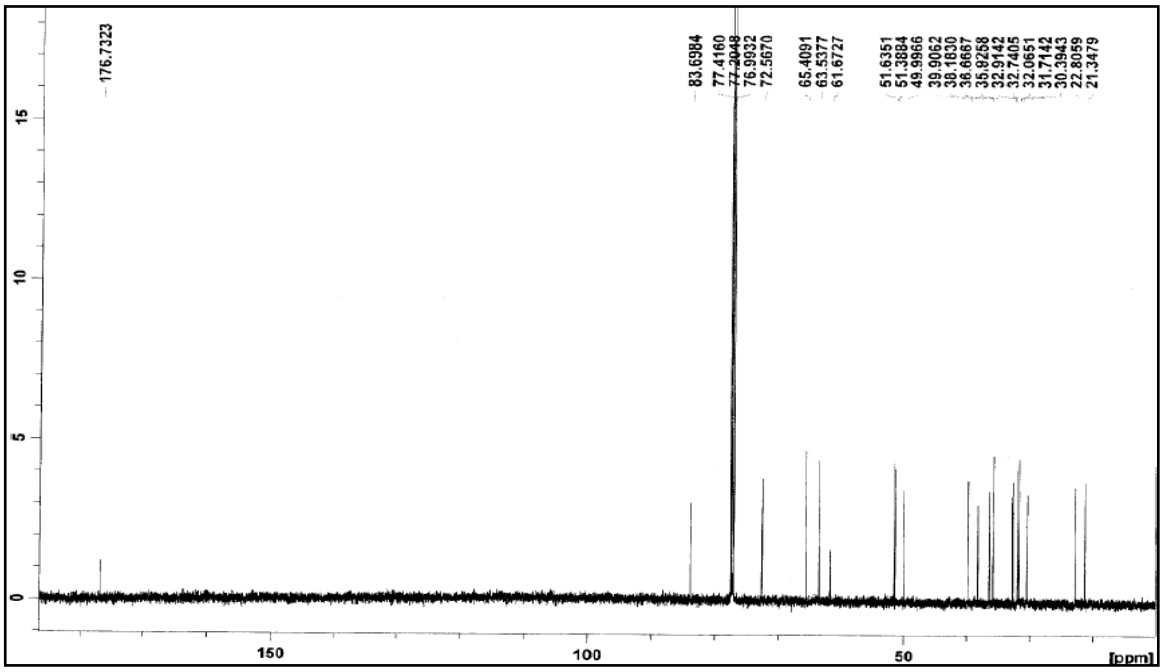

^{13}C NMR spectrum (75 MHz) of angasiol in $CDCl_3$

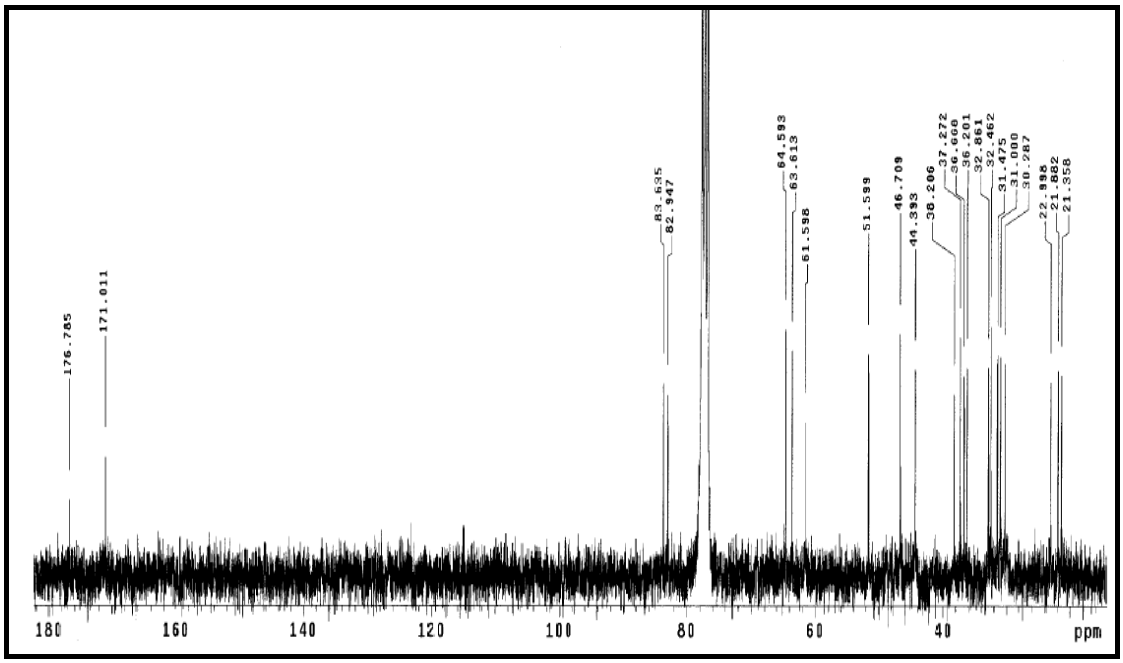

^{13}C NMR spectrum (75 MHz) of angasiol acetate $CDCl_3$

APPENDIX 1.3

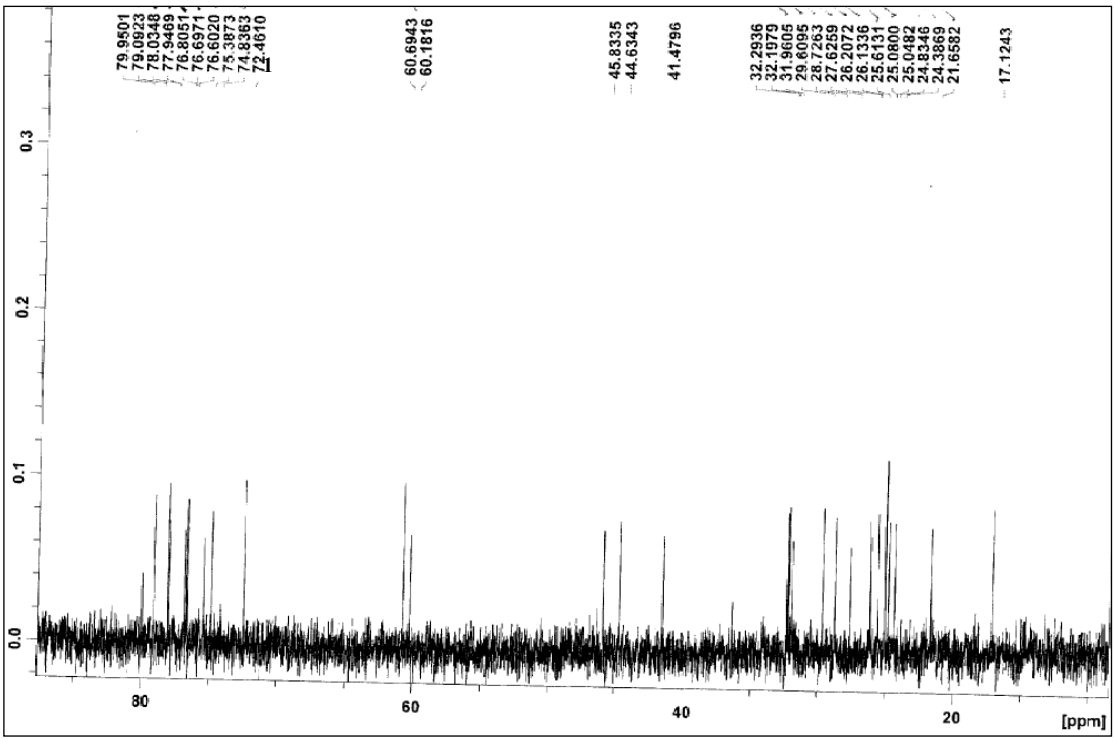

^{13}C NMR spectrum (150 MHz) for armatol G in C_6D_6

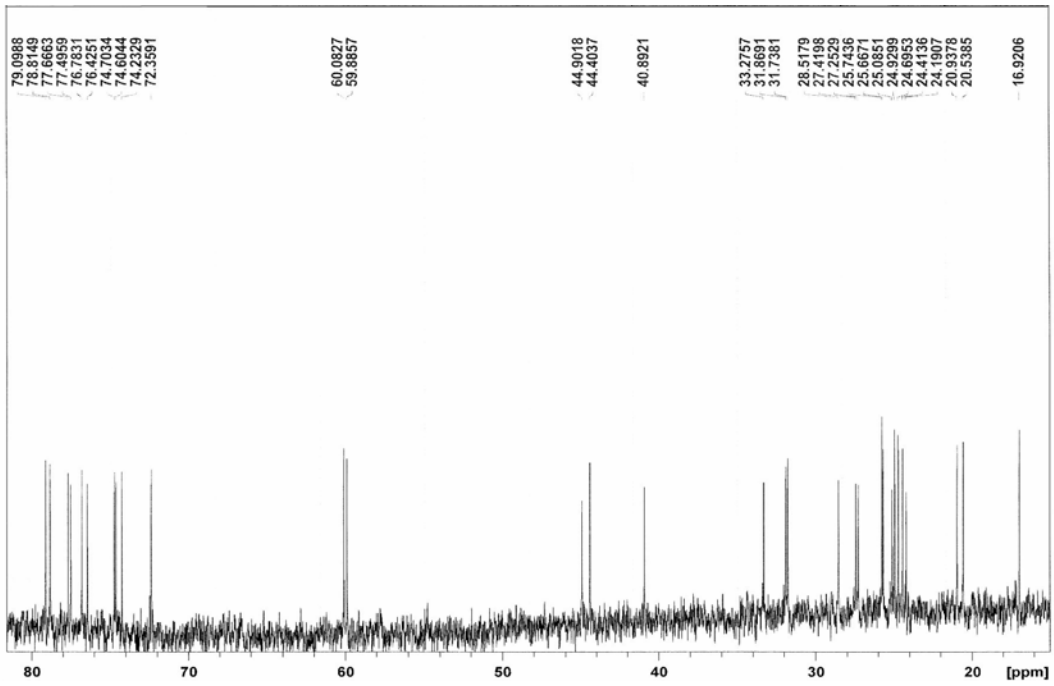

^{13}C NMR spectrum (150 MHz) of armatol H in C_6D_6

APPENDIX 1.4

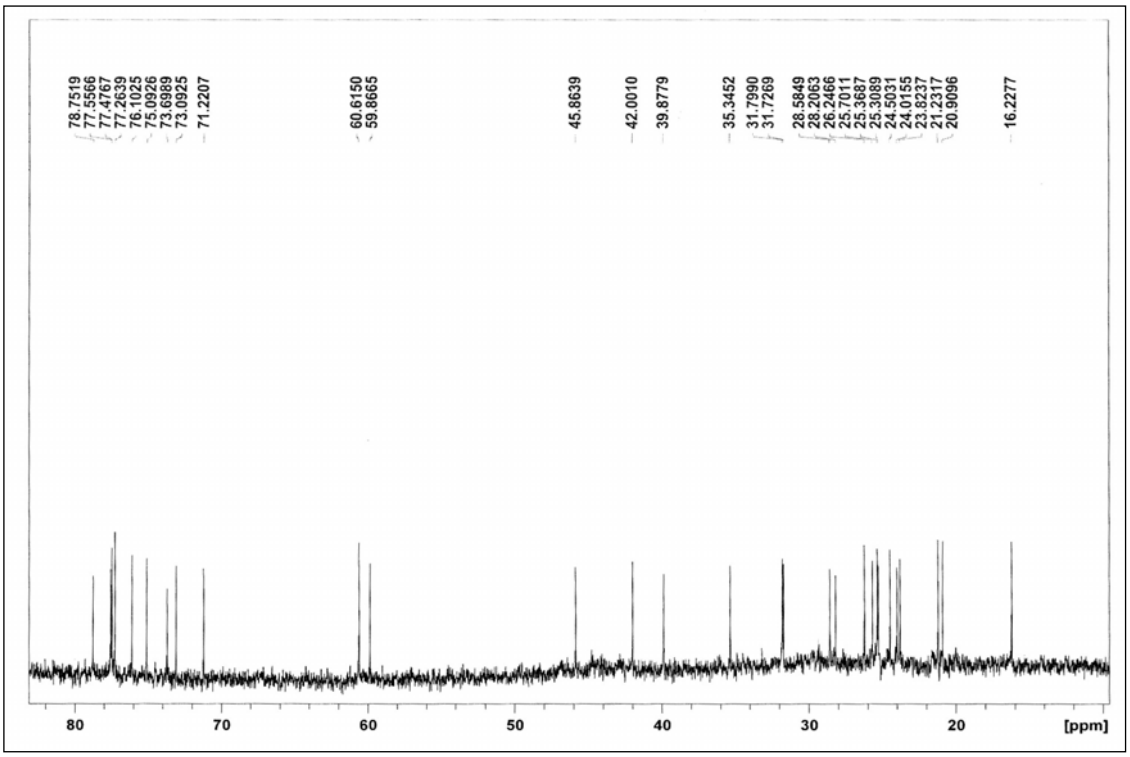

^{13}C NMR spectrum (150 MHz) of armatol I in C_6D_6

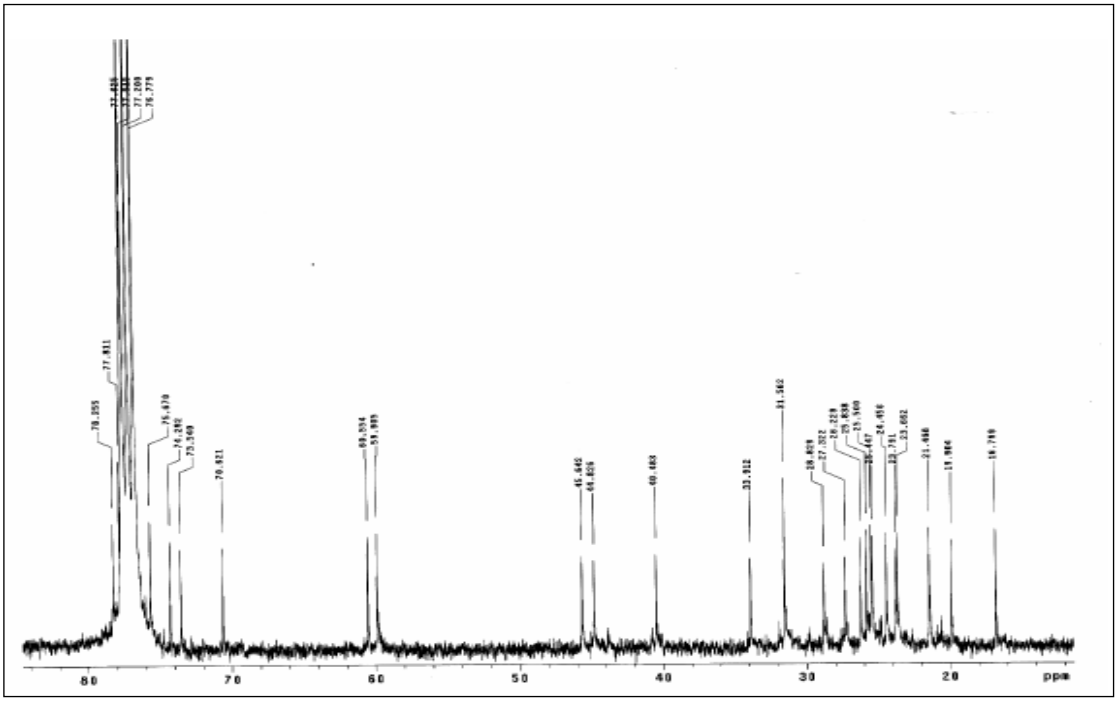

^{13}C NMR spectrum (75 MHz) of armatol J in $CDCl_3$

APPENDIX 1.5

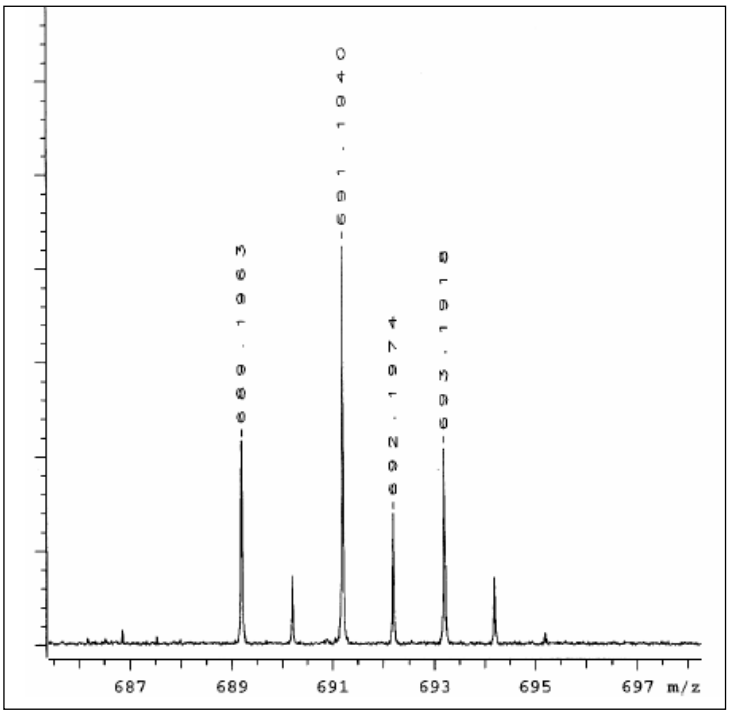

Partial mass spectrum of armatol G

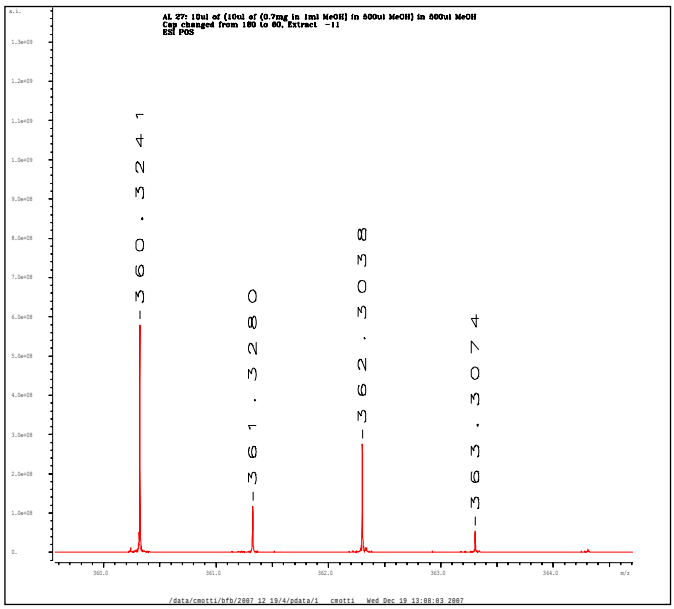

Partial mass spectrum of intricatetraol

APPENDIX 1. 6

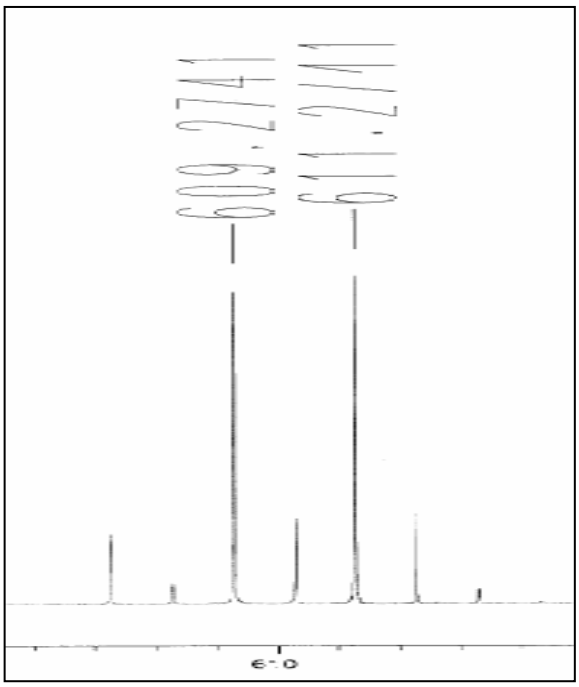

Partial mass spectrum of aplysiol C

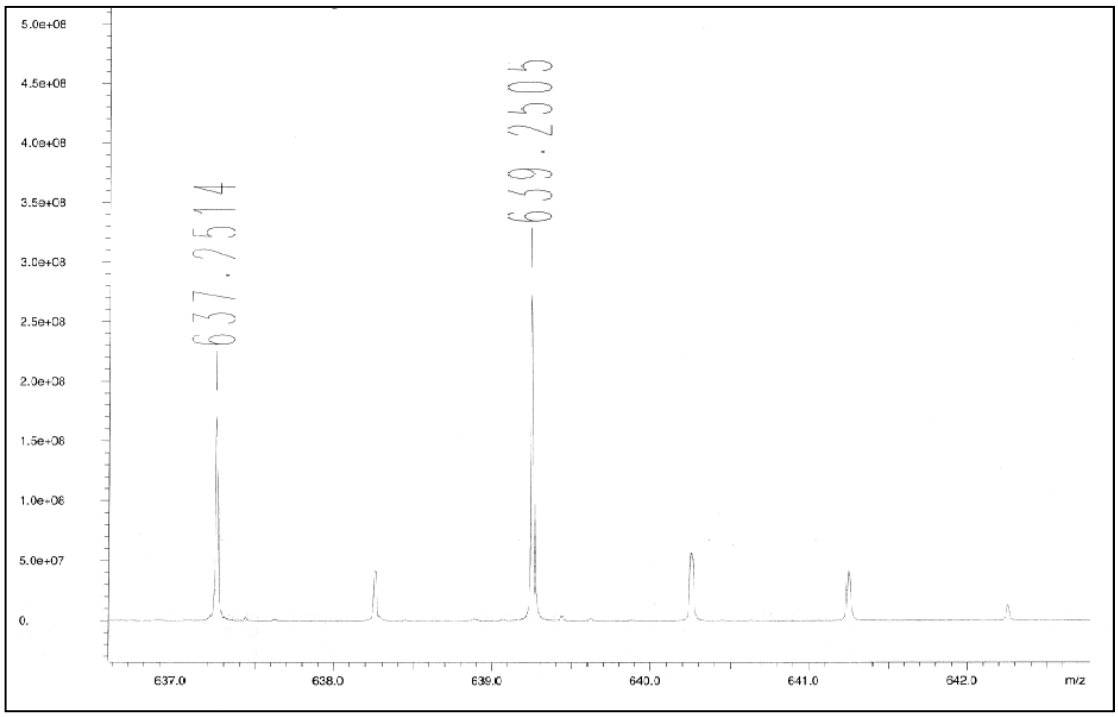

Partial mass spectrum of aplysiol E

APPENDIX 1. 7

^{1}H NMR spectra of armatol H and acetylated armatol G.